

POLITECNICO DI TORINO

Master's Degree in Mechanical Engineering



Master's Thesis

Development of automotive battery pack integrating structural, thermal and electric characteristics

Academic Supervisor:
Prof. Stefano Carabelli

Candidate:
Arman Kianirad

Academic Year: 2020 - 2021

Abstract

As the automotive industry goes through developing a new generation of fully electric or hybrid vehicles with a native electric platform, electrification of older generations of ICE cars as a retro-modification method might also be appealing to certain costumers, as it is not only more environmentally sustainable in terms of reutilizing the older vehicles and avoiding manufacturing, scrappage and new-car development cost, but it is also a more cost-effective solution for popularizing the electric mobility. The aim of this work is to develop a modular lithium-ion battery pack for an electrified classic Fiat model, based on the customer requests while applying the industry standards on the overall architecture of the pack as well as verifying the safety aspect of the design. Firstly, the various design approaches and configurations for energy storage systems currently used in electric vehicles are discussed. Then, based on the set of parameters like dimension and placement of the battery package a design approach that could integrate structural, thermal and energy capacity requisites was devised. The design was carried out for each element of the battery system with respect to the requirements enforced by the regulations as well as the potential customer. Then the design was verified by going through individual structural dynamic and static finite element analysis on the load-bearing elements and the module assembly based on the vehicle safety regulations as well as extreme operational loading cases in order to verify the design as well as find the weak points for further optimization. Then, in order to complete the design assessment, the crashworthiness of the battery pack against ground impact was studied, thus concluding the verification process. In the last chapter, there is a conclusion with a summary and a discussion regarding the design procedure as well as further applications of this modular design on other vehicles.

Keywords: Electrification, FEM analysis, vehicle safety standards, modular design, air-cooling, Li-Ion battery pack

Acknowledgement

I would like to take this opportunity to thank first and foremost my thesis advisor, Professor Stefano Carabelli, who have guided me through this project and have always given me the right suggestion with all his expertise in the technical field.

A debt of gratitude is also owed to Mr. Massimo Guidetto, the CEO at Custom 2.0 s.r.l. who have supported this project in the development and prototyping phase.

Also I would like to acknowledge everyone who have supported me through this journey; my friends, fellow colleagues and more importantly my academic tutors and professors, to whom I would forever be indebted.

And last but not least, I would like to thank my beloved family, who have always been supportive through not only this academic journey, but also for the entirety of my life, and have always taught me with their love and dedication and have always been tolerant and loving, despite the hardships.

Table of Contents

Abstract	i
Acknowledgement	ii
List of Figures	vi
List of Tables	xi
1. Introduction.....	1
2. EVs and energy storage system developments	4
2.1. Introduction	4
2.2. Electric mobility	4
2.3. Energy storage systems for EV application.....	7
2.4. Battery choice and cell configuration	8
2.5. The choice of battery chemistry	11
2.6. ICE based electric platforms and electric conversion	13
2.7. Dedicated EV platforms and future of automotive battery technology.....	16
3. Battery pack design and assembly	23
3.1. Introduction	23
3.2. Module configuration	27
3.2.1. Battery cell specification.....	27
3.2.2. Modules configuration	28
3.3. Ducted lower cover.....	31
3.4. Frame integration.....	33
3.5. Module installation	35
3.6. Mounts design.....	35
3.6.1. Side mount design and assembly	36
3.6.2. Rear mount design and assembly	37
3.7. Battery pack and mounting assembly	39
4. Design verification and simulation studies	41

4.1.	Introduction	41
4.2.	Batter pack weight assessment	42
4.3.	Mounting clearance and departure angle.....	43
4.3.1.	Suspension clearance.....	43
4.3.2.	Departure angle	44
4.4.	Static simulation cases for module assembly	44
4.4.1.	Simulation setup.....	45
4.4.2.	Module static analysis case 1: Longitudinal motion	49
4.4.3.	Module static analysis case 2: Lateral motion	50
4.4.4.	Module static analysis case 3: Vertical motion (up-down).....	51
4.4.5.	Module static analysis case 4: Vertical motion (down-up).....	52
4.4.6.	Results discussion	53
4.5.	Static simulation cases for mounts	53
4.5.1.	Simulation setup.....	53
4.5.2.	Mounts static analysis case 1: Longitudinal motion	58
4.5.3.	Mounts static analysis case 2: Lateral motion.....	59
4.5.4.	Module static analysis case 3: Vertical motion (up-down).....	60
4.5.5.	Module static analysis case 4: Vertical motion (down-up).....	61
4.5.6.	Results discussion	62
4.6.	Dynamic simulation cases for mounts.....	62
4.6.1.	Simulation setup.....	63
4.6.2.	Frequency analysis	65
4.6.3.	Dynamic case 1: Frontal impact.....	66
4.6.4.	Dynamic case 2: Side impact	69
4.6.5.	Dynamic case 3: Vertical road bump impact	72
4.6.6.	Results discussion	74
4.7.	Ground impact simulation	75
4.7.1.	Simulation setup.....	75

4.7.2. Simulation results.....	79
4.7.3. Results discussion	83
5. Conclusion	84
References.....	87

List of Figures

Figure 1.1: Fully electric and hybrid passenger vehicle global sales by region (left) and by powertrain (right) [1].....	1
Figure 1.2: Development stages for an ICE based EV [2].....	2
Figure 1.3: The cutaway illustration for Audi R8 e-tron, showing the battery placement in the engine bay2	
Figure 2.1: National, provincial, and state targets to fully phase out sales of new ICE cars [6]	5
Figure 2.2: Worldwide map of governmental incentives to encourage electric-vehicle sales and use [7]	6
Figure 2.3: Automakers electric transition forecast [1]	7
Figure 2.4: Components in battery pack integration and interface with vehicle [12].....	7
Figure 2.5: Common cell types for EV application (From left: Pouch Cell, Cylindrical Cell and Prismatic Cell) [14].....	8
Figure 2.6: Overview of battery packs indicating their constructions with (a) cylindrical and (b) prismatic cells [13].	9
Figure 2.7: Overview of different cell types used in automotive battery applications: (left) cylindrical cell, (middle) prismatic cell, (right) pouch cell [13].....	9
Figure 2.8: The progress of battery types in terms of specific energy and energy density between 2009 and 2020 [14].....	10
Figure 2.9: The applications of LIBs in the three main fields including consumer electronics & devices, transportation, and grid energy & industry [16].....	12
Figure 2.10: LIB cost and demand outlook, based on recent developments [1].	13
Figure 2.11: Price and range comparison between native and ICE based EVs [17].....	14
Figure 2.12: Tesla Roadster, based on a modified Lotus Elise platform [19].....	15
Figure 2.13: Schematic view of the positions of the elements installed onto the converted vehicle (EM - electric motor, EMC - electric motor controller, G - gearbox, BAT - batteries) [22].....	16
Figure 2.14: VW's MEB platform and the engineering criterias [24]	17
Figure 2.15. Tesla model S battery pack configuration, based on cylindrical cells.....	18
Figure 2.16: Volkswagen MEB platform battery pack, based on pouch type battery cells.....	18
Figure 2.17: Bosch modular battery pack based on prismatic type cells.....	18
Figure 2.18: The evolution battery pack design and vehicle-battery integration [1].	19
Figure 2.19: (a) Schematic diagram of the BYD Blade cell configuration (dashed lines show potential cut points), (b) BYD Blade battery pack as a structural element of vehicle chassis [25].....	19
Figure 2.20; Laminated structural batteries [27].....	20

Figure 2.21: Volvo S80 prototype with composite body panels as energy storage systems [28].	21
Figure 2.22: a) Integrated aerofoils as inspiration, b) The integrated battery pack, c) The battery pack as a chassis member	22
Figure 3.1: Previous design for battery pack	23
Figure 3.2: Module configuration for previous design	24
Figure 3.3: The battery pack internals as assembled.	24
Figure 3.4: The previous battery pack model with the mounts	25
Figure 3.5: The complex mounting structure for the previous design	26
Figure 3.6: The battery pack mounted under the vehicle.	26
Figure 3.7: BYD battery cell.	28
Figure 3.8: Heat sink scheme.	28
Figure 3.9: Sample module assembly and the module elements	30
Figure 3.10: Fully assembled modules	30
Figure 3.11: Schematic battery cell connections in series or parallel	31
Figure 3.12: Bus bar elements and assembly on the modules.	31
Figure 3.13: Lower cover assembly, integrating ducts for cooling and protection.	32
Figure 3.14: Assembled lower cover with the mounting reinforcements	33
Figure 3.15: Integrated frame and its elements	34
Figure 3.16: Frame placement inside the lower cover	34
Figure 3.17: Module placement and sealing off the battery pack	35
Figure 3.18: Vehicle suspension travel and departure angle maximum and minimum values	36
Figure 3.19: Side mount elements (from the left: bottom mount, bushing, (right side) chassis mount)	37
Figure 3.20: Side mount assembly.	37
Figure 3.21: Completed assembly of the (right) side mount.	37
Figure 3.22: Rear mount elements (from left: rear bar, bushing and the chassis mount)	38
Figure 3.23: Rear mount assembly stages.	38
Figure 3.24: Fully assembled rear mount.	38
Figure 3.25: Battery pack ready for vehicle assembly	39
Figure 3.26: Vehicle chassis scan and the mounting points.	39
Figure 3.27: Battery pack installation	40
Figure 3.28: Fully installed battery pack	40

Figure 4.1: Battery pack and the suspension clearance.....	44
Figure 4.2: Vehicle departure angles at maximum and minimum ride height.....	44
Figure 4.3: Module assembly for static simulation.....	46
Figure 4.4: Loading cases in module simulation models.....	46
Figure 4.5: Discretized module simulation model.....	48
Figure 4.6: Fine discretization on critical componenets	48
Figure 4.7: Stress plot for longitudinal load case.....	49
Figure 4.8: Residual displacement plot for longitudinal case	49
Figure 4.9: Stress plot for lateral load case	50
Figure 4.10: Residual displacement for lateral load case.....	50
Figure 4.11: Stress plot for vertical load case (up-down)	51
Figure 4.12: Residual displacement for vertical load case (up-down).....	51
Figure 4.13: Stress plot for vertical load case (down-up)	52
Figure 4.14: Residual displacement for vertical load case (down-up).....	52
Figure 4.15: Mounting simulation model	54
Figure 4.16: Fixtures for mount simulation model	55
Figure 4.17: Loading cases in mount simulation models.....	56
Figure 4.18: Discretized mount simulation model.....	57
Figure 4.19: Fine discretization on critical componenets	57
Figure 4.20: Stress plot for longitudinal load case.....	58
Figure 4.21: Residual displacement plot for longitudinal case	58
Figure 4.22: Stress plot for lateral load case	59
Figure 4.23: Residual displacement for lateral load case.....	59
Figure 4.24: Stress plot for vertical load case (up-down)	60
Figure 4.25: Residual displacement for vertical load case (up-down).....	60
Figure 4.26: Stress plot for vertical load case (down-up)	61
Figure 4.27: Residual displacement for vertical load case (down-up).....	61
Figure 4.28: Mounts simulation assembly	63
Figure 4.29: Mesh quality sample for dynamic analysis.....	64
Figure 4.30: Velocity changes in the Euro NCAP frontal impact test [30]	66

Figure 4.31: Euro NCAP frontal impact test protocol	66
Figure 4.32: Velocity profile for the frontal impact case	67
Figure 4.33: Frontal impact acceleration response plot	67
Figure 4.34: Frontal impact stress plot.....	68
Figure 4.35: Frontal impact residual displacement plot.....	68
Figure 4.36: Velocity changes in the NCAP side impact test [31]	69
Figure 4.37: Euro NCAP side impact test protocol	69
Figure 4.38: Velocity profile for side impact case	70
Figure 4.39: Side impact acceleration response plot.....	70
Figure 4.40: Side impact stress plot.....	71
Figure 4.41: Side impact residual displacement plot	71
Figure 4.42: Standard trapezoidal speed bump profile [32].....	72
Figure 4.43: Displacement profile for vertical bump impact.....	72
Figure 4.44: Vertical bump impact acceleration response plot.....	73
Figure 4.45: Vertical impact stress plot	73
Figure 4.46: Vertical impact residual displacement plot	74
Figure 4.47: Ground impact mode for present (top) and previous (bottom) designs	75
Figure 4.48: The ground impact full assembly	76
Figure 4.49: Plastic stress-strain curve for steel.....	77
Figure 4.50: Boundary conditions on simulation models	77
Figure 4.51: Velocity field assigned for the impact sphere	77
Figure 4.52: Mesh discretization on past model.....	78
Figure 4.53: Mesh discretization on present model.....	78
Figure 4.54: Past model at 0.0 s	79
Figure 4.55: Past model at 0.002 s	79
Figure 4.56: Past model at 0.004 s	79
Figure 4.57: Past model at 0.006 s	80
Figure 4.58: Past model at 0.008 s	80
Figure 4.59: Past model at 0.01 s	80
Figure 4.60: Present model at 0.0 s	81

Figure 4.61: Present model at 0.002 s.....	81
Figure 4.62: Present model at 0.004 s.....	81
Figure 4.63: Present model at 0.006 s.....	82
Figure 4.64: Present model at 0.008 s.....	82
Figure 4.65: Present model at 0.01 s.....	82

List of Tables

Table 2.1: Summurized list of major car markets with a set deadline for sales of various ICE vehicle [3] .	5
Table 2.2: An overview of common EVs battery configuration (s: series, p: parallel connection) [13] ...	11
Table 2.3: Energy, power, and cycle life for lead acid, NiMH, and lithium ion batteries [11].....	12
Table 3.1: Cell specification	27
Table 3.2: Cell dimensions	27
Table 3.3: The list of module elements.....	29
Table 4.1: List of battery pack elements with weight approximation.....	42
Table 4.2: Weight comparison between the previous and proposed design	43
Table 4.3: Mesh details	47
Table 4.4: Material sepecifications for mount simulation srudy.....	54
Table 4.5: Mesh details	56
Table 4.6: Mesh properties for dynamic analysis	64
Table 4.7: List of frequencies for the natural modes	65
Table 4.8: Mass participation for the first 10 modes	65
Table 4.9: Ground impact material properties	76
Table 5.1: Summary of design features and specification	84

1. Introduction

As the awareness for climate change and the need for a sustainable alternative power source for personal mobility purposes increase, there is a substantial increase in demand for fully electric or plug-in hybrid vehicles among major car markets, including the United States, China, United Kingdom and a majority of European countries. Ever since the 2016 Paris agreement on climate change was enacted, it became clear that in order to achieve the emission targets for passenger vehicles, the development for electric vehicles should be accelerated. This has resulted in a competition between major car makers, as they not only need to meet the states regulations, but also have to maintain their market share, since the public has shifted their demand from fossil fueled cars to fully electric or hybrid alternatives (Figure 1.1).

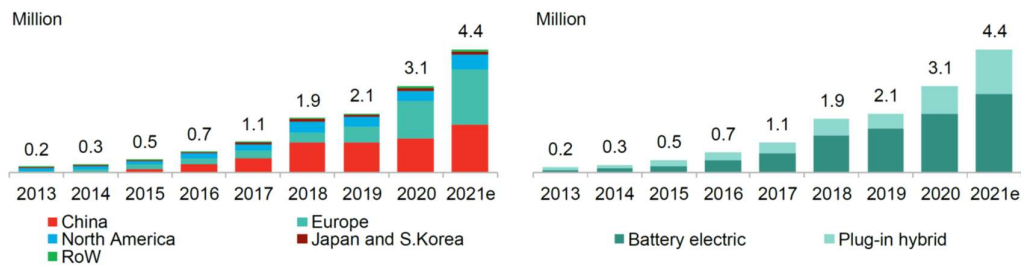


Figure 1.1: Fully electric and hybrid passenger vehicle global sales by region (left) and by powertrain (right) [1].

The phase-out of internal combustion engines (ICE) and the shift towards battery powered vehicles in the new car market, has also caused a secondary movement in the used car market, which is electric vehicle conversion. Electric conversion has long been adapted by established car makers in the early stages shift towards full EV¹ mobility in order to not fall behind the start-up electric car makers and also to meet Corporate Average Fuel Economy (CAFE) targets. The general idea behind electric conversion is to replace the engine, drivetrain (including transmission, axles, etc.) and the fuel tank with a number of electric motors and a battery storage system, referred to as the battery pack. Depending on the scale of conversion, vehicle's chassis and suspension may also be modified and other elements, such as axles or dedicated cooling systems might be needed. In Figure 1.2 the development stages for an EV conversion is illustrated.

¹ EV: Electric Vehicle

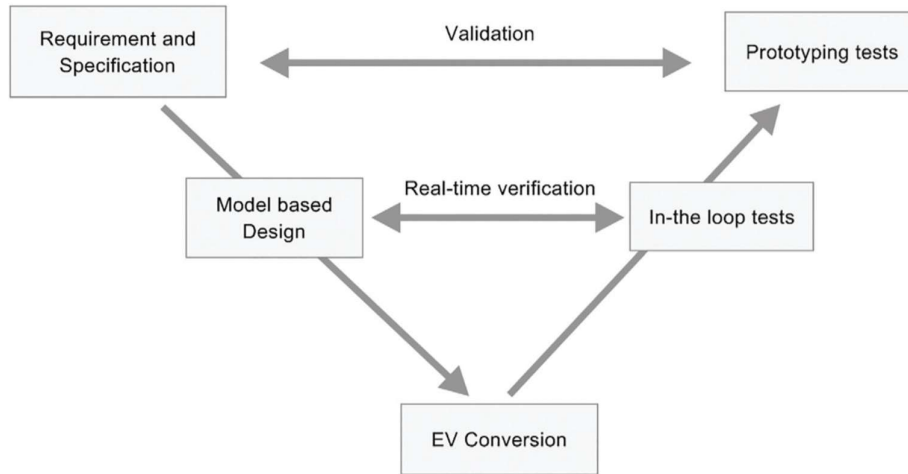


Figure 1.2: Development stages for an ICE based EV [2]

Arguably, the key elements for such project is the battery pack. Depending on the donor vehicle underpinnings, the battery pack is placed where the engine or fuel tank used to be, in order to maximize the space utilization as well as matching the same weight distribution as the original vehicle. This will minimize the need for further modification on suspension as well as developing structural mounting points to carry the loads.



Figure 1.3: The cutaway illustration for Audi R8 e-tron, showing the battery placement in the engine bay

In this thesis, the goal is to design a battery pack system that satisfies the requirements from safety, structural and thermal perspective. As part of the electric conversion of a first generation Fiat Panda, a suitable battery configuration was necessary. The design had to maximize space optimization while providing the cooling power that was demanded by a previous thermal management study. The design was carried out in

SolidWorks™ CAD software and based on the battery placement in the rear section of vehicle's underbody, the mounting structure was devised. The approach towards the battery pack configuration was based on the modular platforms that are applied in the industry. However, the pack should also integrate functionalities such as conductive air-cooling capacity, protection from the environment and ease of disassembly.

In order to verify whether or not the design satisfies the requirements, based on each criteria the design is analyzed and compared to the previous works if necessary. First the overall mass and the battery pack dimensions with respect to vehicle dynamics and geometry are assessed. Then the battery pack and the mounting assembly were analyzed through a number of structural static and dynamic simulation cases. These studies were based on electric vehicle conversion legislation and also the industry standard tests in order to verify vehicle safety, as well as battery system's integrity in the common loading scenarios and extreme impact cases. Through SolidWorks™ simulation tool and based on the requirements, the static and dynamic loads were defined. Primarily, the modules and mounts were studied through the static cases in longitudinal, lateral and vertical directions. Then for the dynamic analysis, the mounts were studied with velocity and displacement input loads representing frontal and side impact in case of an accident, as well as vertical impact due to road bumps. By plotting the stress and residual displacement for all the simulation cases as well as the response diagram for the battery pack center of gravity in dynamic cases, the results were discussed and the models were examined for the weak points.

In the last step in order to verify the design, the protection capability of the design was assessed with respect to the previous works. In this simulation study, using Abaqus™ Explicit FEM software, a case of ground impact scenario was modelled, using an impact sphere and the two representative battery pack lower covers from the previous and the present design. The results of this study is discussed at the end and the battery pack protection claim was confirmed.

It should be mentioned that, although this design process had a specific purpose and was for a particular case of battery system retrofitting project, but the methods that are applied here can be implemented for further projects with similar requisites, since the battery configuration follows a modular design and overall, the design process addresses the standard requirements for safe vehicle operation.

2. EVs and energy storage system developments

2.1. Introduction

In this chapter, the reasoning behind the current move towards electric mobility is discussed. First, the challenges that the automakers face in general coming from both the state regulations as well as the competition in the market. Then the energy storage solutions for such mean of transport, both in terms of choice of material and cell type and also packaging and configuration from the cells to the complete package is discussed. Lastly, the advantages and disadvantages of different design approaches for a battery system by various manufacturers are presented. The goal is to have a clear understanding of the challenges for developing an energy storage system, as well as the solutions that the industry has come up with so far.

2.2. Electric mobility

As the automotive industry faces its biggest challenge in decades, which is the “phase-out of the fossil fuel vehicles”, electro-mobility has become the sole solution to the transportation needs of the masses [3]. With the signing of the Paris agreement in 2016 and United Nations Framework Convention on Climate Change (UFCCC), the state parties which includes all the members of the European Union, United States, China and other major car markets in the world, proposed their plans to reduce the impact of the fossil fuel powered cars in order to meet the greenhouse gases and CO₂ targets set by the agreement as well as addressing the health issues caused by the pollution particulates [4].

The ban on fossil fueled vehicles as well as implementation of zero-emission vehicles sales was proposed by most of the governments, as part of their national climate plans [5]. The map of proposed bans as well as the set deadlines for major car markets to prohibit the sale of ICE cars are demonstrated in Figure 2.1 and Table 2.1 respectively.

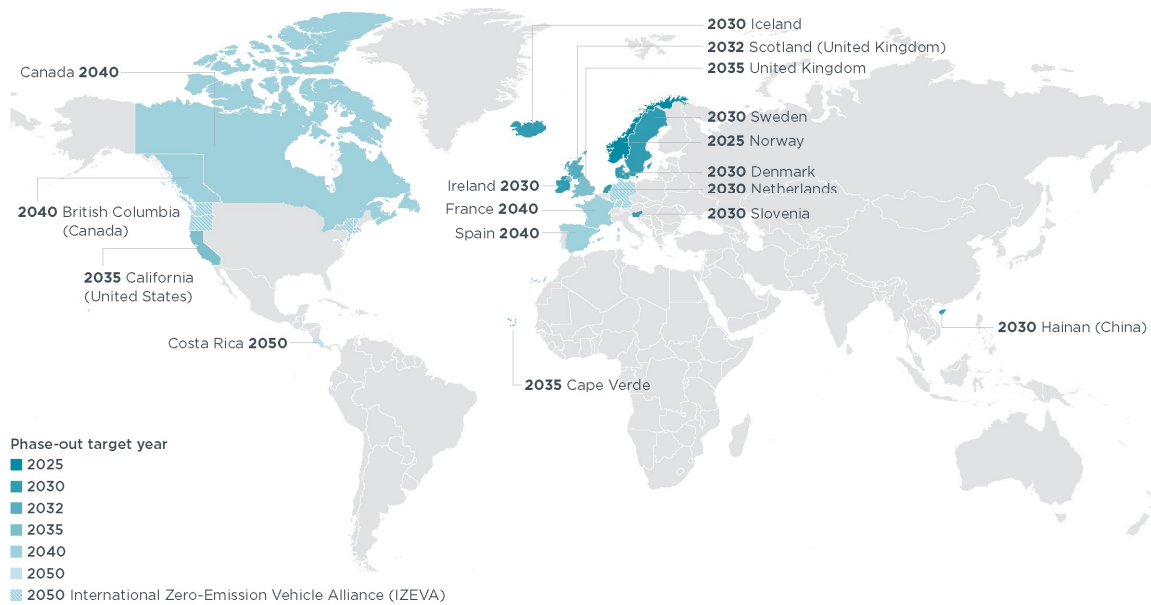


Figure 2.1: National, provincial, and state targets to fully phase out sales of new ICE cars [6]

Table 2.1: Summurized list of major car markets with a set deadline for sales of various ICE vehicle [3]

Country	Start year	Scope
United States	2035 (California)	All emitting vehicles
China	2030 (Hainan Province)	Diesel and petrol
United Kingdom	2040	Diesel and petrol
Germany	2030	All emitting cars
Netherlands	2030	Diesel and petrol
Italy	2024 (Rome), 2030 (Milan)	Diesel cars

In addition to the prohibition on sales of fossil fueled vehicle, governments have also applied incentive methods in order to ramp up the popularity of the electric vehicles (Figure 2.2).

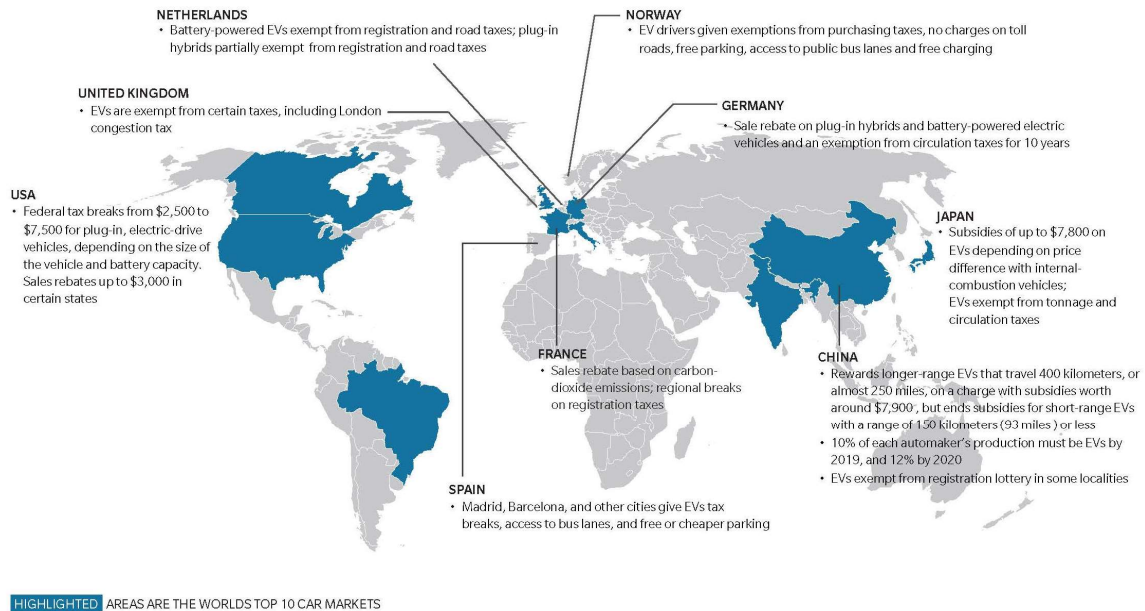


Figure 2.2: Worldwide map of governmental incentives to encourage electric-vehicle sales and use [7]

Following the governmental plans and incentives, established manufacturers of ICE powered cars have also joined the movement and have released detailed plans and statements regarding their new generation of zero-emission product line-up. General Motors who was one of the first companies to release a long-range all-electric vehicle in 2016, plans to completely phase out combustion engines by 2035 [8]. Volvo Cars who have already started the transition toward an all-electric car maker since 2019, by launching every vehicle equipped with an electric motor, has stated their entire vehicle line-up will be fully electric by 2030 [9]. Volkswagen, who is the key car manufacturer in Europe, have also stated that their final generation of combustion engines will be developed by 2026 and they will completely shift their focus on electric vehicle [10]. Looking at the Figure 2.3 below, it is clear that the future of personal mobility is going to be fully electric.

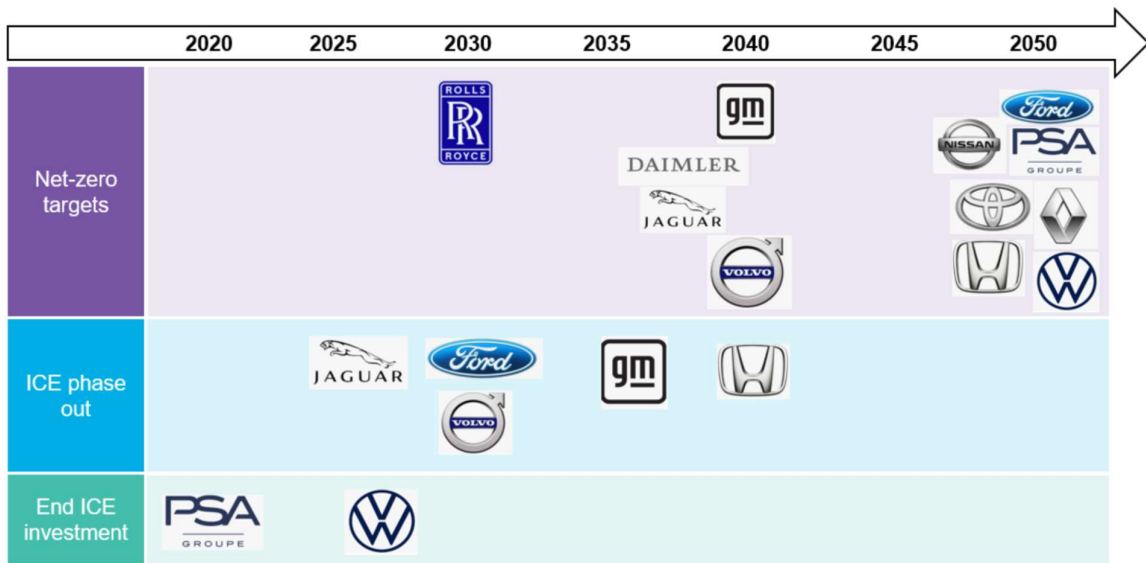


Figure 2.3: Automakers electric transition forecast [1]

2.3. Energy storage systems for EV application

The battery pack is an integral part of an EV conversion. The energy storage system for an EV determines the range, recharging time and the final cost. Some of the main factors when considering a battery type for the pack are power density, energy density, weight, volume, cycle life and temperature range [11]. In Figure 2.4, the various factors for choosing the right energy storage system (ESS) with respect to vehicle design requirements is demonstrated.

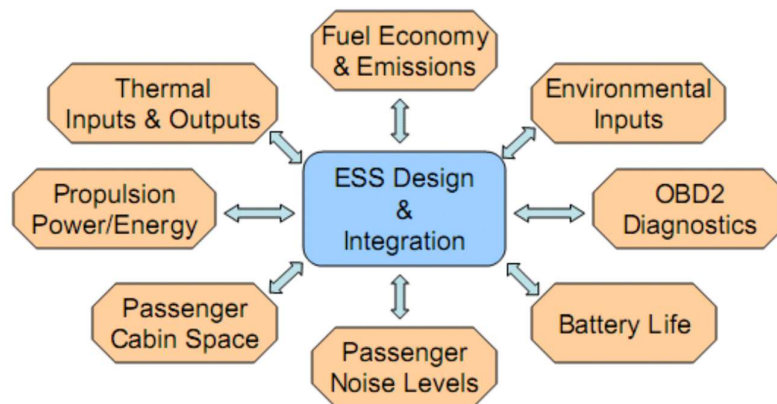


Figure 2.4: Components in battery pack integration and interface with vehicle [12]

When designing the battery pack, the main factors to be considered are

- Cell to cell interconnection
- Cell, module and electronic assembly
- Pack protection against shock and vibration
- The attachment point regarding the pack and vehicle assembly [12].

In the next chapters we will consider each of these elements when we design the pack in order to optimize the assembly and pack configuration.

2.4. Battery choice and cell configuration

Battery packs in automotive applications are commonly designed and manufactured in modular configuration, in which, depending on the cell type and size (Figure 2.7) and depending on the desired voltage and amperage to be comply with the motor, the cells can be clustered differently (Figure 2.6). In Figure 2.6 (a) an example of pack configuration with larger cells is shown, and in Figure 2.6 (b) an alternative assembly with higher number of smaller cells (connected in parallel to maximize the capacity) is demonstrated. The choice to have higher number of cells in parallel or series (or mixed) depends on the required capacity and amperage or power supply [13]. A “cell” refers to the electrochemical unit that acts as the building brick for the modules. Each module consists a number of cells that are interconnected in a way to provide a voltage of up to 50V. The modules then are connected together to create the pack. The pack is then located in the vehicle and acts as a sub-system that interacts with the rest of EV elements [12].



Figure 2.5: Common cell types for EV application (From left: Pouch Cell, Cylindrical Cell and Prismatic Cell) [14]

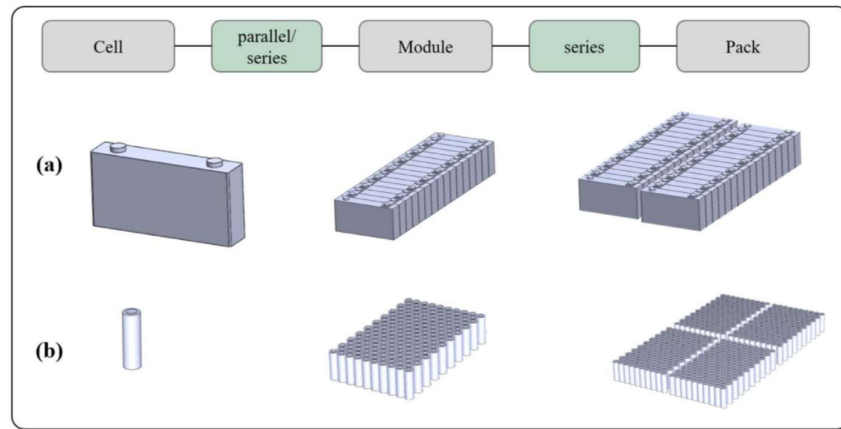


Figure 2.6: Overview of battery packs indicating their constructions with (a) cylindrical and (b) prismatic cells [13].

There are 3 types of cell design for automotive application: Pouch, Cylindrical and Prismatic cells (Figure 2.5). EV manufacturers choose either of these cell types based on the packing density, their space management strategy and weight of the pack [14]. For example, BMW and Nissan chose prismatic cells for their i3 and Leaf models, while Tesla chooses cylindrical cells for their vehicles. Each cell type has its benefit; while prismatic cells offer less complexity which can be beneficial for battery management system (BMS), cylindrical cells offer higher flexibility in terms of pack design, as well as better reliability in case of an open wire failure [13].

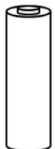
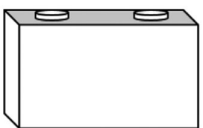

Cylindrical cell	Prismatic cell	Pouch cell
		
<ul style="list-style-type: none"> • Small size (e.g. 18650 type (ø 18 mm, height 650 mm)) • Hard casing • Low individual cell capacity • Build in safety features • Comparably cheap 	<ul style="list-style-type: none"> • Hard casing • Large size • High individual cell capacity 	<ul style="list-style-type: none"> • Soft casing • Large size • High individual cell capacity • Geometrical deformation during (dis-)charging

Figure 2.7: Overview of different cell types used in automotive battery applications: (left) cylindrical cell, (middle) prismatic cell, (right) pouch cell [13].

Löbberding et al. have analyzed 25 EV examples from 10 manufacturers, with a start-of-production (SOP) between 2010 to 2019. They have taken into account their specific energy, energy density, cell type and cell size. Figure 2.8 Shows the progress of cylindrical vs. pouch and prismatic battery cell types in terms of specific energy (Wh.kg⁻¹)

¹⁾ and energy density (Wh. L⁻¹). The cylindrical cells represent Tesla battery elements, while non-Tesla vehicles are represented by prismatic or pouch cell types.

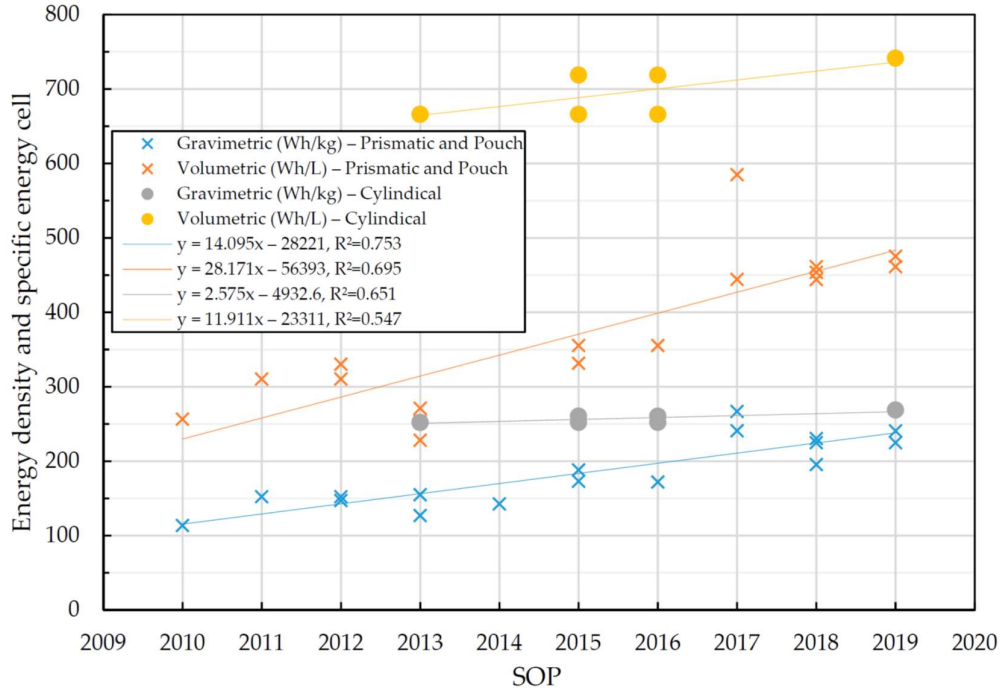


Figure 2.8: The progress of battery types in terms of specific energy and energy density between 2009 and 2020 [14]

Overall, both groups have improved their volumetric energy density, while non-Tesla manufacturers have caught up in terms of specific energy.

On the module level, the cell type can affect the number of parallel or series connections. For example, BMW i3, which has a prismatic Samsung battery cell, has a 96 cell battery pack with a “12s8s” configuration. This means that each module consists of 12, 60 Ah cells in series, and overall there are 8 modules, connected in series. On the other hand, the Tesla Roadster battery pack contains 6831 laptop style Lithium-Ion cylindrical cells, arranged in 11 sheets and connected in parallel. Each sheet contains 9 bricks and each brick is made of 69 cells, connected in series [13]. Zwicker et al. have compiled further examples of battery pack configurations of various EVs, shown in Table 2.2.

Table 2.2: An overview of common EVs battery configuration (s: series, p: parallel connection) [13]

Vehicle	Tesla Model S 85 kW	Tesla Roadster	BMW i3	Nissan Leaf	Chevrolet Bolt EV - Second generation	Volkswagen MEB – (I.D. family models)
Modules	16	11	8	58	7	Up to 12
Cells per module	404	621	12	4	24 & 32	24
Cell configuration	74P6S16S	69p9s11s	1p12s8s	2p2s48s	96s2p	–
Total no. of cells	7104	6831	96	192	192	Up to 288
Cell Type	Cylindrical 18,650	Cylindrical 18,650	Prismatic	Pouch	Pouch (12.7 by 17.7-cm)	Prismatic or Pouch
Cell manufacturer	Panasonic	–	Samsung SDI	AESC	LG Chem	–

2.5. The choice of battery chemistry

Currently, Lithium-Ion batteries dominate the major markets of electronic devices (Figure 2.9). From personal laptops and smartphones to power tools and electric toothbrush. Lithium-Ion batteries were first developed by John Bannister Goodenough, but it was Akira Yoshino who first commercialized Li-Ion batteries at Asai Kasei Corporation in Japan. On 1991, Sony Corporation applied their technology to power world's first cellphones [15]. Since then, owing to their electrical and mechanical properties like high energy density, long cycle life and lack of memory effect, Li-Ion batteries have become the battery of choice for electronic devices, among a variety of commercialized battery types (Table 2.3) including lead-acid, Ni-Cd and Ni-MH [16].

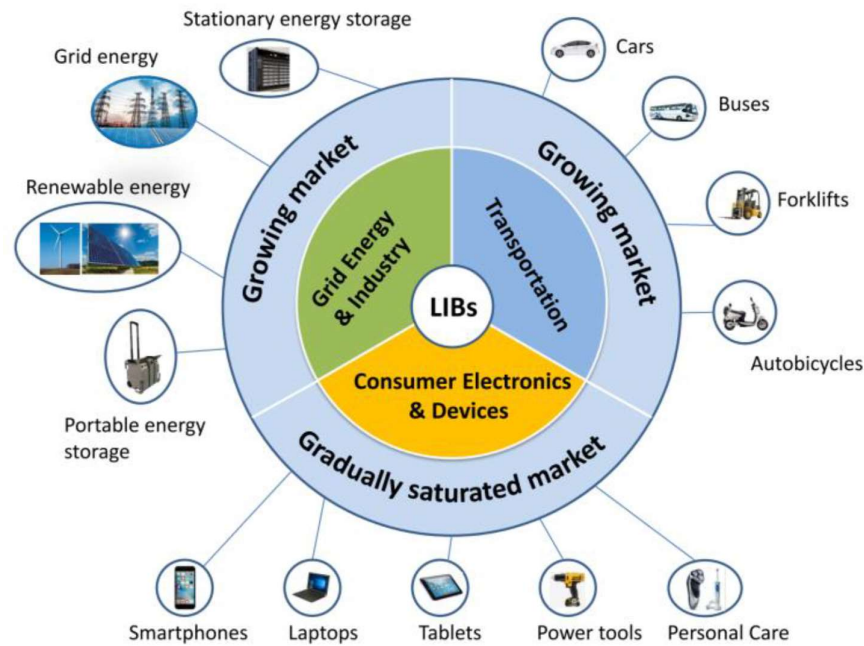


Figure 2.9: The applications of LIBs in the three main fields including consumer electronics & devices, transportation, and grid energy & industry [16].

Table 2.3: Energy, power, and cycle life for lead acid, NiMH, and lithium ion batteries [11].

Battery Type	Lead Acid	NiMH	Lithium-Ion
Energy density (Wh/kg)	30–40	50–80	100–150
Power density (W/kg)	120–200	250–1000	1000–1500
Cycle life	200–300	300–500	500–1000

Regarding the automotive battery requirements such as energy density and energy cost, LIB²s are particularly favorable. Mainly due to the latest target set by United States Department of Energy (DOE) for the year 2022, which mandates a minimum of 300 miles per charge as well as battery cost of \$125/kWh [16]. These mandated requirements, as well as manufacturing progress for LIB cells in recent years made them the battery of choice for EV purposes too. Ever since Tesla opted for Li-Ion batteries for their Tesla

² LIB: Lithium Ion Battery

Roadster back in 2008, the rest of car makers have followed this decision [11]. In Figure 2.10, the outlook for battery pack price per kWh, as well as LIB market size for each EV segment are demonstrated.

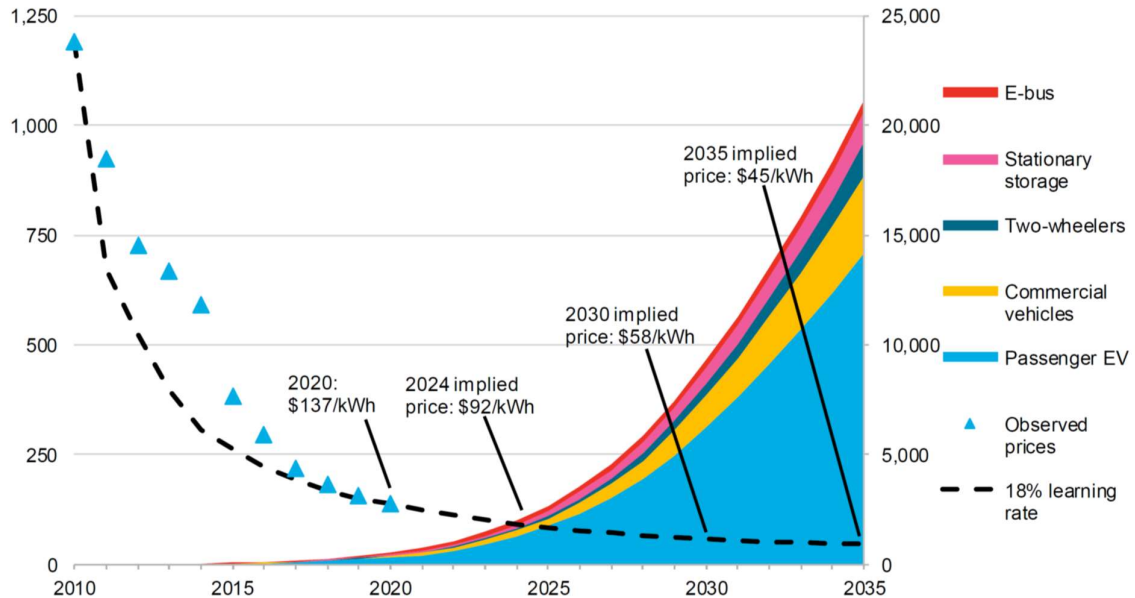


Figure 2.10: LIB cost and demand outlook, based on recent developments [1].

2.6. ICE based electric platforms and electric conversion

Earlier electric cars were mostly based on combustion engine platforms. For smaller start-up companies like Tesla, developing the first commercial product, the Roadster back in 2008, based on an ICE platform seemed reasonable, since they didn't have the resources or technical expertise to develop a bespoke platform from the ground up. For the more established manufacturers however, the reason for choosing one of their models that's already in production was mostly to speed up their EV development and fill up their electric portfolio, in order to keep up with the competition. But mostly, choosing this type of EV design is a matter of development cost and hence, the final price (Figure 2.11). The advantages of this method that result in lowering the final price of the EV are:

- Lowering the development cost
- Avoiding the need for retooling the production line
- Platform sharing between ICE and electric models

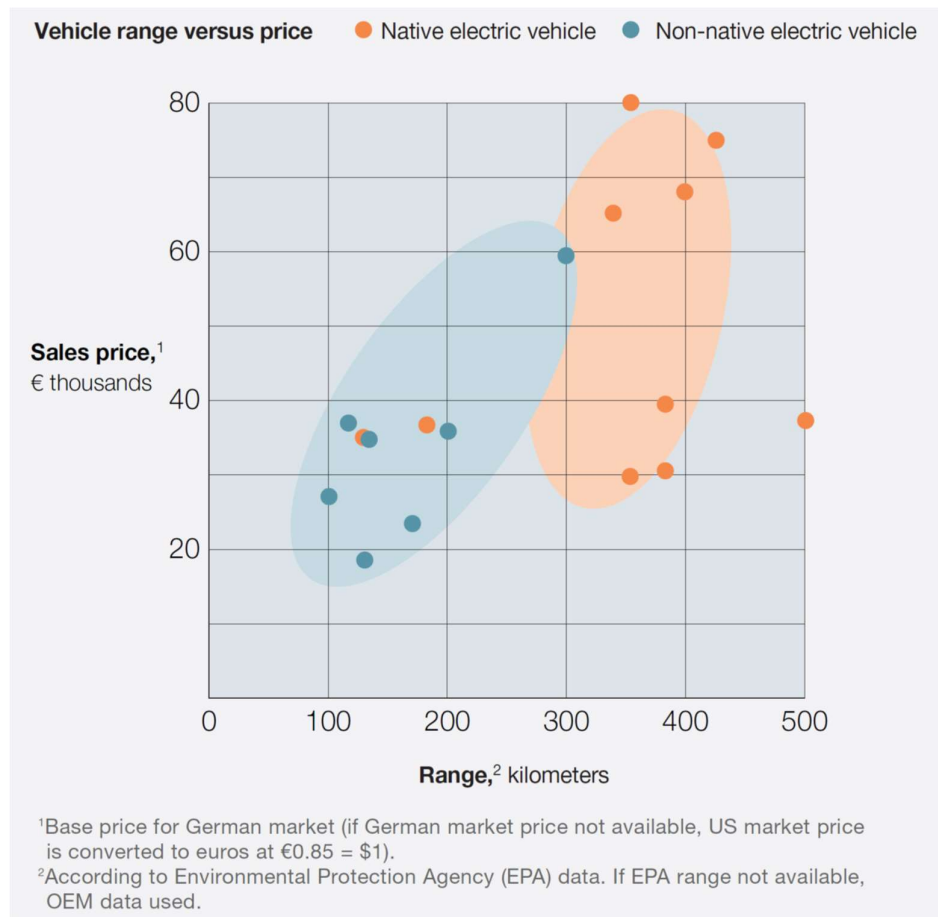


Figure 2.11: Price and range comparison between native and ICE based EVs [17].

Looking at Figure 2.11, we can see that the biggest disadvantage of ICE based EVs is range. Since the electric vehicle replaces the engine and drivetrain for battery packs and motors, the only placement option are the voids left by the engine, fuel tank and drivetrain. This results in limited space for battery placement, and a less efficient use of space. Moreover, the inherent benefits of a dedicated EV platform like modularity as well as practicality is compromised. In order to keep their product competitive in terms of battery capacity and range, car makers tend to modify the base platform and that also results in a heavier vehicle. As Elon Musk has stated in an interview regarding using Lotus Elise platform as the base for their Roadster model (Figure 2.12), by the time the electric elements are mounted, the weight of the vehicle was increased for about 30% and that forced the engineers to mostly redesign the vehicle [18].

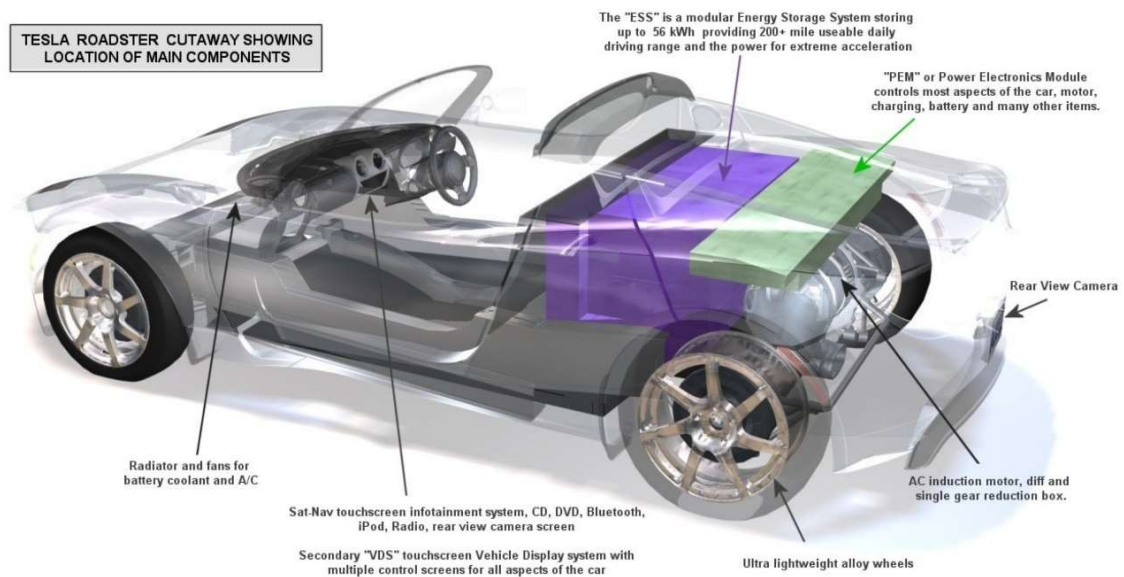


Figure 2.12: Tesla Roadster, based on a modified Lotus Elise platform [19]

The climate crisis and the need for a more sustainable mean of personal transport has also resulted in a secondary movement in the second-hand and classic car markets: electric vehicle conversion. Electric conversion of second-hand cars is not only a hobby for classic car enthusiasts, but it also addresses the shortfall in new EV availability for the masses [20]. While the auto industry puts all its effort to meet the stringent regulations regarding emissions, the electric conversion can be an alternative to not only bring the costs of EV ownership down, but also reduce the cost of vehicle development and manufacturing, as well as the scrappage or vehicle dumping cost regarding the older cars on the road [21].

To sum up, the benefits of electric vehicle conversion are:

- Used vehicle recycling and reducing the environmental impact of vehicle ownership, by avoiding the scrappage and new vehicle manufacturing
- Reducing the cost of personal EV ownership
- Reducing the donor vehicle's need for regular maintenance, by reducing the drivetrain complication as well as the hazards in case of self-diagnostic by the user
- Extending the road-worthiness of the vehicle in case of the classic or collector used cars

The basic principal of this conversion is to replace the powertrain and the drivetrain of the car with one or more electric motors plus a battery pack. The vehicle's chassis and suspension components might be modified or altered, depending on the motor

configuration, battery pack weight, size and placement and vehicles weight distribution after conversion. In Figure 2.13, the placement of each element in an EV conversion is shown. The key to an optimized conversion is to have the minimum difference for total mass as well as mass distribution before and after the conversion [22].

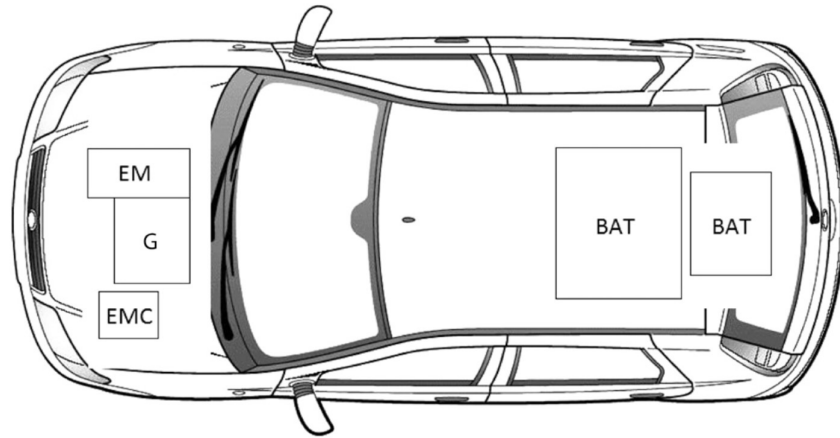


Figure 2.13: Schematic view of the positions of the elements installed onto the converted vehicle (EM - electric motor, EMC - electric motor controller, G - gearbox, BAT - batteries) [22].

The electric motor(s) chosen for this application are either brushed DC, permanent magnet synchronous motor or AC induction type [23]. Choosing the right motor is mostly a matter of performance, intended use and efficiency, as well as the motor maintenance, controller complexity and compatibility with the battery pack. Having the right combination of batteries and motors will determine range, vehicle speed and total cost of the conversion [21].

2.7. Dedicated EV platforms and future of automotive battery technology

While the earlier EVs were based on ICE platforms, more recent vehicles like VW ID.3 and Tesla model S have an EV platform designed from the ground up. The latest generation of BEV³s are designed with their battery pack and motors integration in mind.

A great benefit of having a dedicated electric platform is the flexibility. A dedicated EV platform is made of a battery pack that is mounted on the floor bed of the chassis, while the motors are placed where there used to be the axles on the equivalent ICE vehicle. This architecture enables the engineers to have maximum flexibility when it comes to platform sharing between different body segments and classes, since it is only a matter

³ BEV: Battery Electric Vehicle

of changing the chassis length or ride height and hence increasing or decreasing the size of the battery pack. It also enables them to have the desired traction configuration (RWD or AWD) and perfect weight distribution (Figure 2.14).

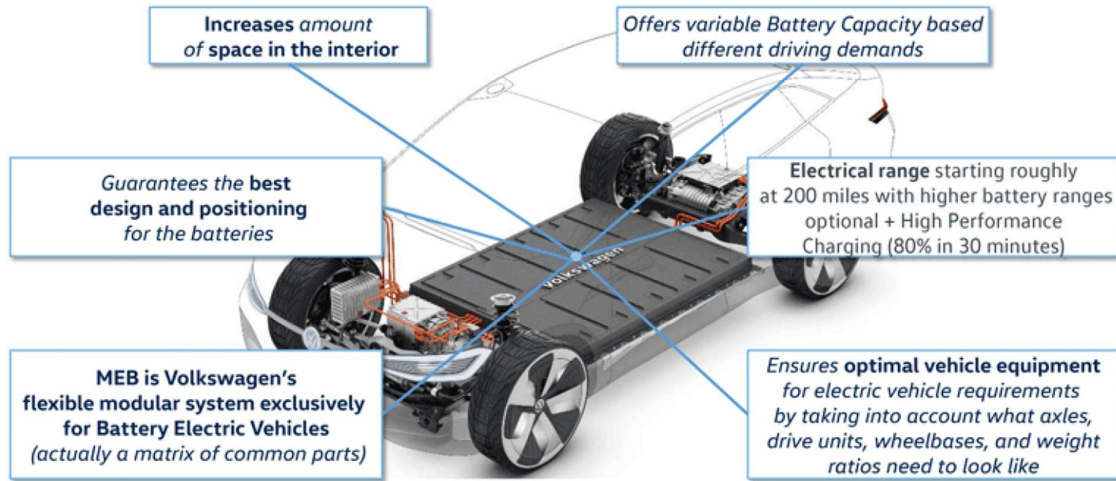


Figure 2.14: VW's MEB platform and the engineering criterias [24]

In the case of Volkswagen MEB platform, the modular design allows engineers to maximize the interior space, while positioning the batteries at the optimum location so that the center of gravity is as low as possible, thus the vehicle dynamics is favorable [24]. This platform has enabled VW to produce a variety of models in different segments, with minimum engineering cost, as it benefits the manufacturer in terms of the economy of scale [1].

Having a dedicated BEV platform is a further development of having a modular design in mind. The key to this design is the modular architecture for the battery pack, whether we choose cylindrical, pouch style or prismatic cells. Here there are some examples of each modular design, currently used by OEMs⁴.

⁴ OEM: Original Equipment Manufacturer

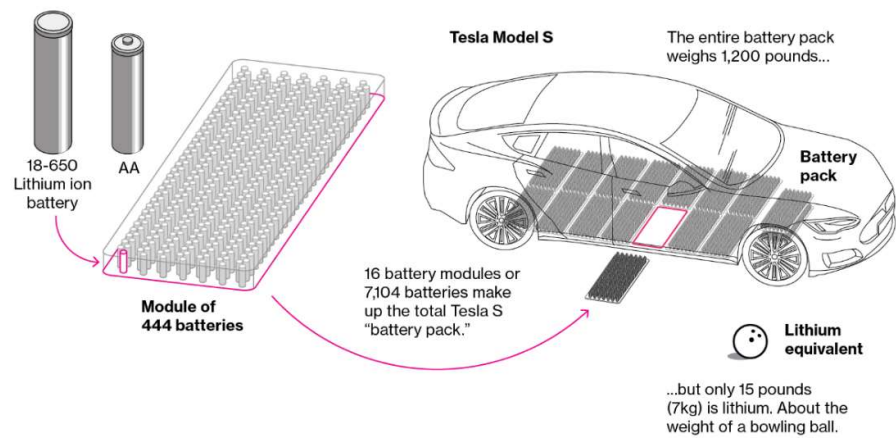


Figure 2.15. Tesla model S battery pack configuration, based on cylindrical cells

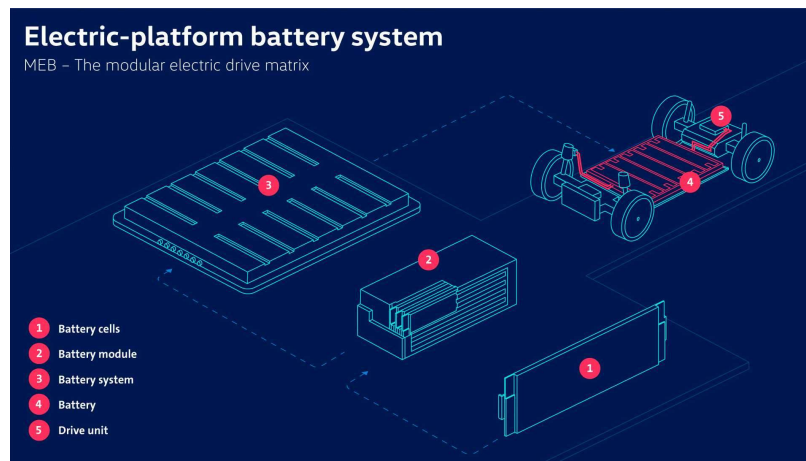


Figure 2.16: Volkswagen MEB platform battery pack, based on pouch type battery cells

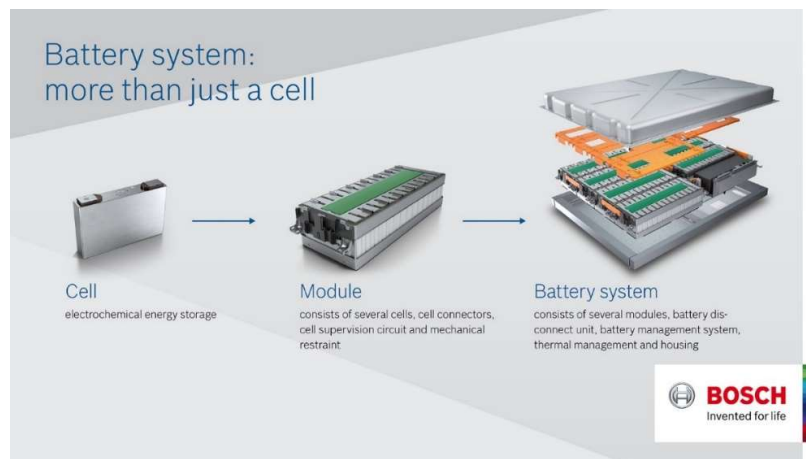


Figure 2.17: Bosch modular battery pack based on prismatic type cells

As more car companies adopt a fully electric platform for their vehicles, some of them are developing designs that integrate the battery into the vehicles architecture. The designs that are currently suggested are the BYD blade battery, which is referred to as 3rd generation battery pack design, and the structural battery packs, which is referred to as 4th generation design and is currently under development by Tesla [1].

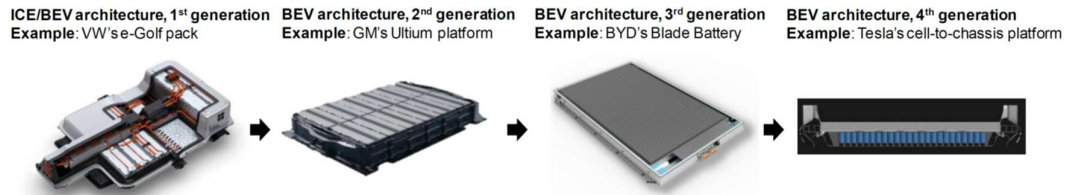


Figure 2.18: The evolution battery pack design and vehicle-battery integration [1].

In the design proposed by BYD that follows CTP (Cell-to-Pack) approach, the cells are design as long and thin members called “blades”, which are stashed in a way so that the need for modules are eliminated. Moreover, they act as structural member of the vehicle and allow for maximum space utilization, as well as higher specific energy. Also BYD suggest that their design allows for a more standardized disassembly procedure and a universal fixing for various vehicle application [25].

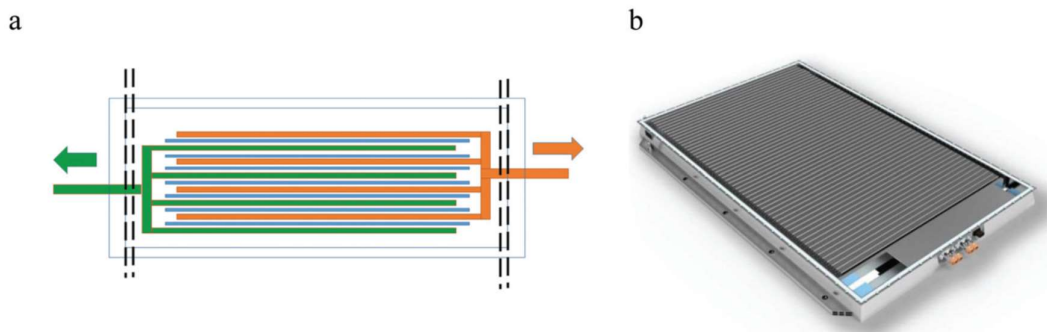


Figure 2.19: (a) Schematic diagram of the BYD Blade cell configuration (dashed lines show potential cut points), (b) BYD Blade battery pack as a structural element of vehicle chassis [25].

For further integration between the energy storage system and the vehicle structural elements, there is the CTC (Cell-to-Chassis) approach, which loses both the modules and pack configuration for a so called “structural battery” design. These batteries, which are also referred to as “massless”, can lower the mass of the vehicle by combining the load bearing parts with power storage elements in the storage system. Structural batteries were first developed by US military in mid-2000s. By having a multi-purpose material that combines the structural and energy storage functions, it was possible to reduce the mass and volume that’s dedicated to carrying power sources [26].

In the design that was developed by Dr. Wetzel et al. at the U.S. Army Research Laboratory (ARL), the composite battery consists of a metal mesh with a cathode coating, a carbon fiber weave that acts as the anode, a LiFePO_4 or Aluminum fiber weave that represents the cathode, a glass weave as the separator and solid polymer as both the electrolyte and the binder (Figure 2.20) [27].

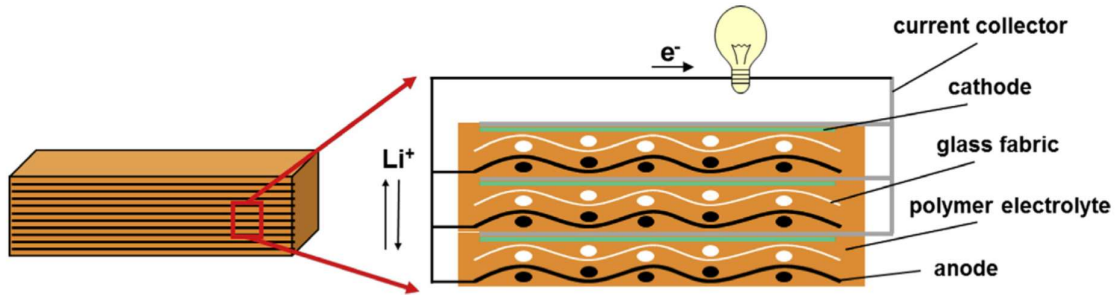


Figure 2.20; Laminated structural batteries [27]

In 2013 Volvo has developed a prototype based on this methodology. They replaced some of the vehicles body panels with the ones made for structural energy storage. The composite contained a carbon fiber weave as the anode, a polymer liquid electrolyte with ionic Nano-particles, on top of a LiFePO_4 coated foil acting as the cathode [27]. The battery system was able to store the regenerative energy recuperated from the brakes, as well as by being plugged-in for charge. Adopting these composite panels in place of the original ones, resulted in 50% weight reduction in panels weight as well.

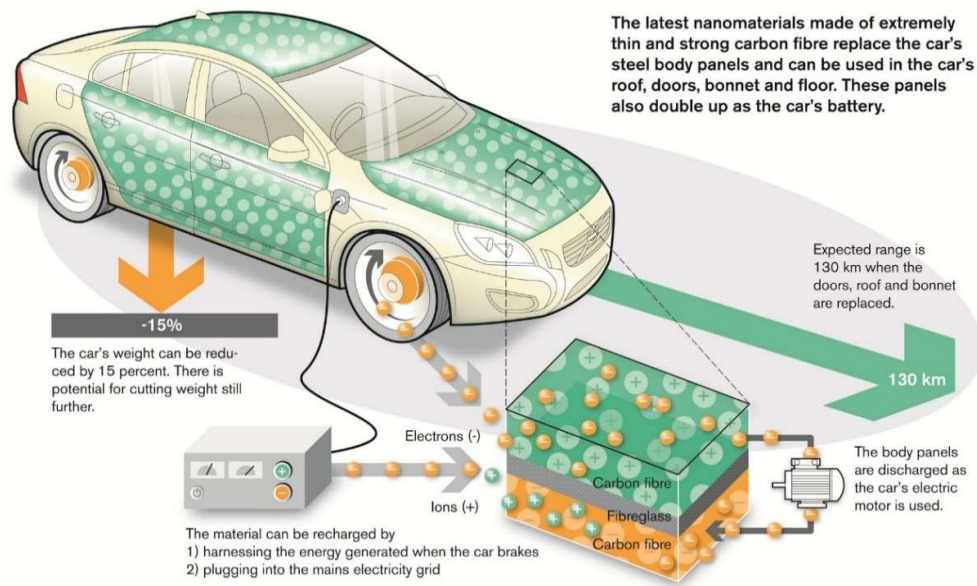


Figure 2.21: Volvo S80 prototype with composite body panels as energy storage systems [28].

This design is still maturing for EV application, but Tesla have applied a similar approach to incorporate the battery cells as a load bearing member of the chassis. Their concept, which takes inspiration from the integrated fuel tank in an airplane wing (Figure 2.22 (a)), uses a sandwich structure with cylindrical cells that act as load carrying beams, cased inside a honey comb (Figure 2.22 (b)). In this design, instead of focusing on alternative multi-functional materials, the weight and volume reduction targets are met via “shape optimization” [27]. In Figure 2.22 (c), we can see the battery pack acting as the central section of the vehicle chassis.

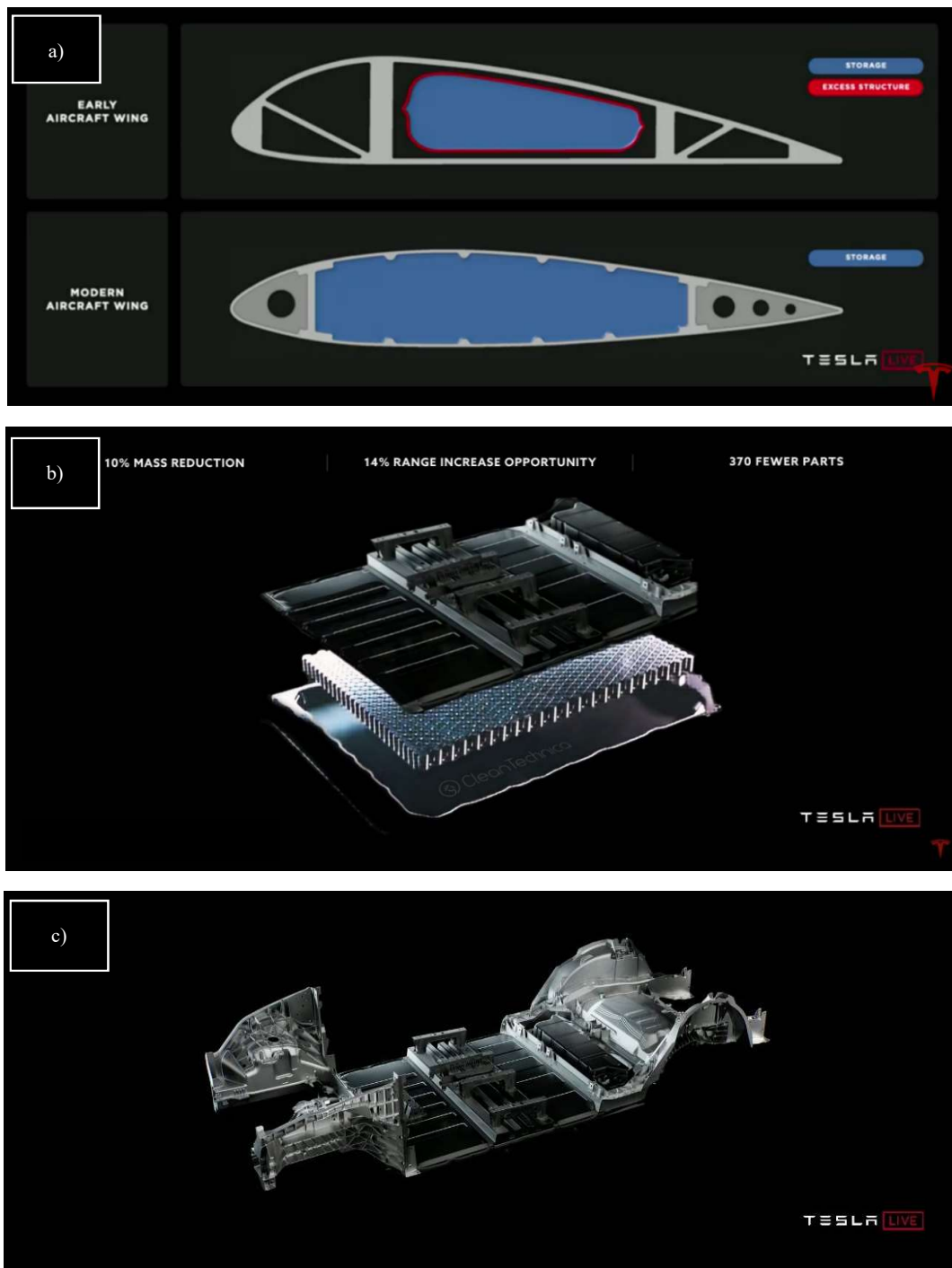


Figure 2.22: a) Integrated aerofoils as inspiration, b) The integrated battery pack, c) The battery pack as a chassis member

3. Battery pack design and assembly

3.1. Introduction

In this chapter, based on the previous works for a battery pack design for Fiat Panda electric conversion application, a new design, configuration and assembly is proposed. First, the battery cell specification is discussed. Then, based on the design requirements from the client, a modular cell configuration consisting of 56 cells and 10.2 kWh capacity is proposed. The battery pack itself is then designed, based on the thermal and structural characteristics that are demanded. The design should integrate the cooling capacity as well as the pack protection with the pack structure, thus minimizing the number of parts and hence avoiding a weight increase with respect to the previous design (Figure 3.1).

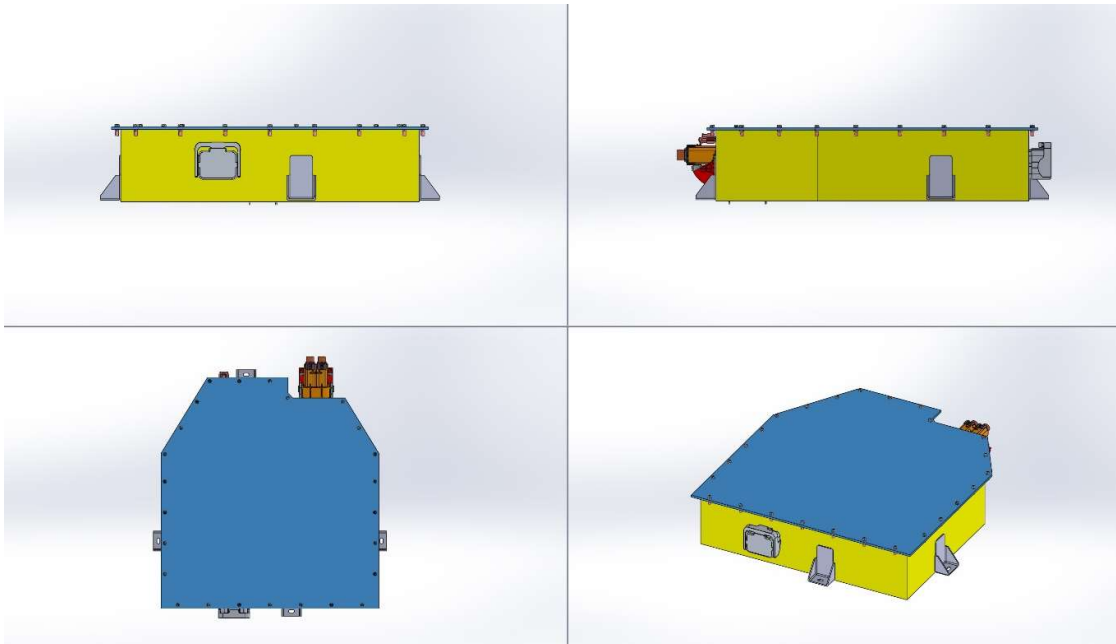


Figure 3.1: Previous design for battery pack

Inside the pack, the cells are divided in 3 modules, with a 28s2p configuration⁵ (Figure 3.2 and Figure 3.3). In the new design, the cell connections should be respected in order to match the electric drivetrain and avoid a complete reconfiguration of motors and transmission.

⁵ 28 pair of parallel cells, connected in series

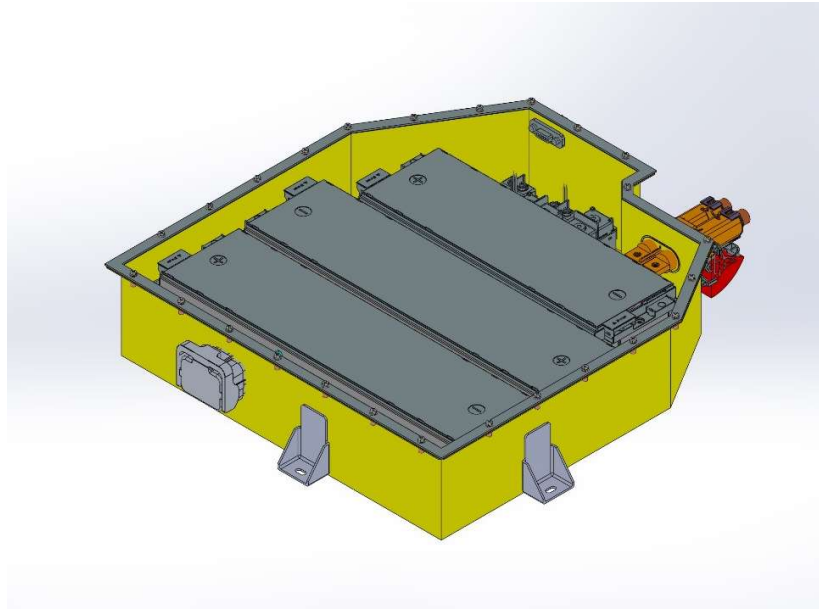


Figure 3.2: Module configuration for previous design

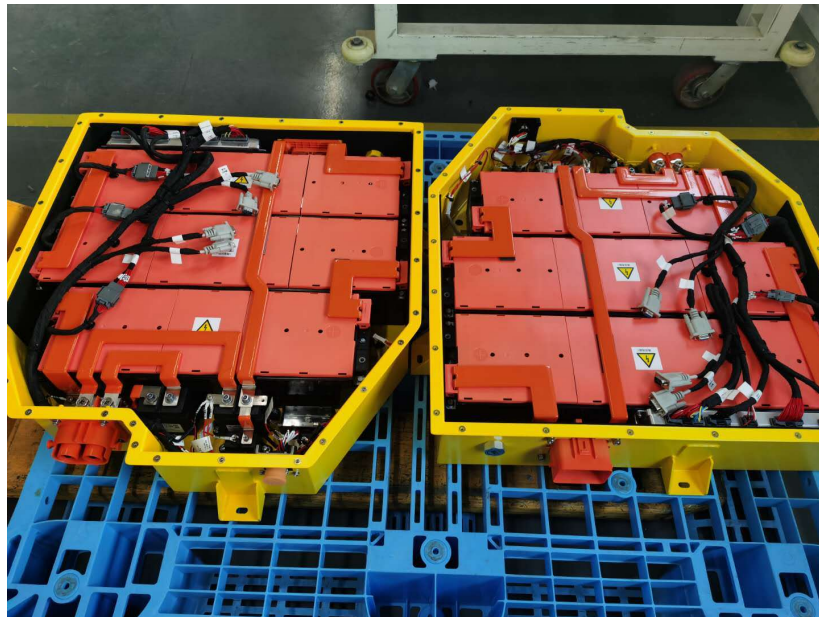


Figure 3.3: The battery pack internals as assembled

With respect to previous works, the main constraints for the battery pack design are:

- Battery pack dimensions
- Battery pack capacity
- Battery pack placement on the vehicle

The proposed design should however include other features, such as:

- (Indirect) air-cooling
- Protection from normal use
- Modularity and ease of manufacturing

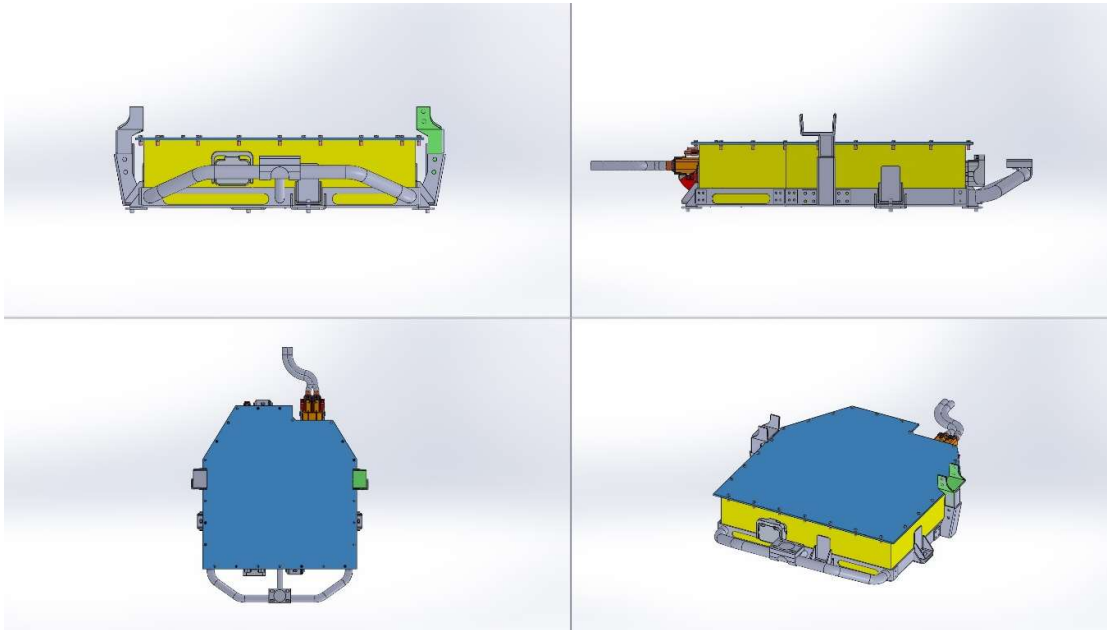


Figure 3.4: The previous battery pack model with the mounts

After the design for the battery was conceived, a new mounting system was also devised. The mounting elements had to respect the vehicle mount locations, however they should also minimize the complexity and reduce assembly effort with respect to the previous design (Figure 3.5).

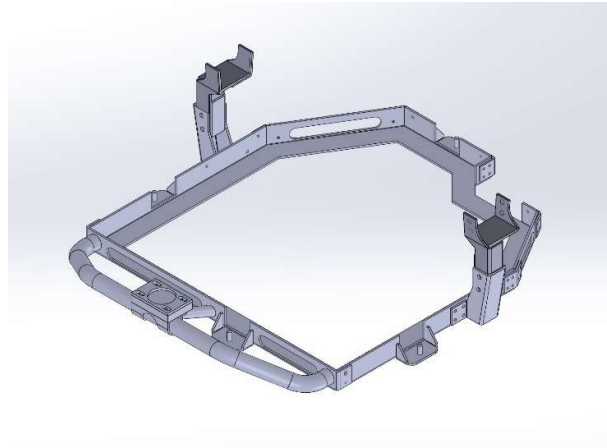


Figure 3.5: The complex mounting structure for the previous design

In Figure 3.6 the previous battery pack assembly is shown as it is mounted under the vehicle

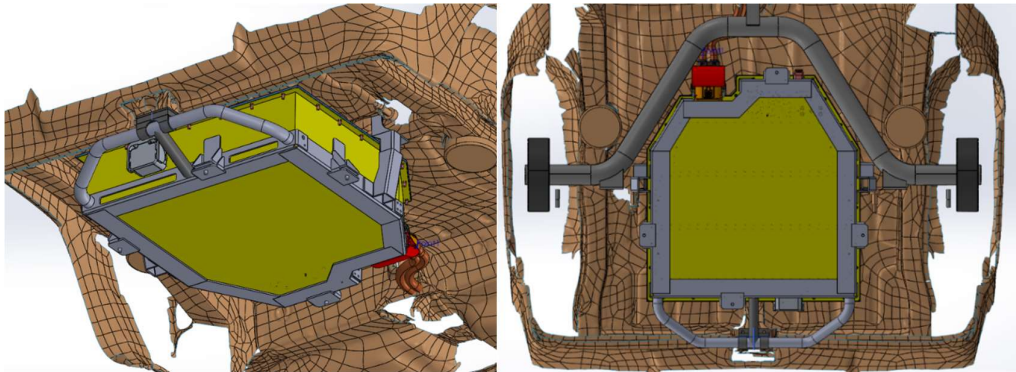


Figure 3.6: The battery pack mounted under the vehicle

In summary, the main requirements for the battery pack and the mountings are:

- Minimum battery capacity of 56 cells (10.8 kWh capacity in total)
- Maximum thermal conductivity between the cells and outside environment
- Integrated protective frame and mountings
- Bottom side protection of the pack against impact
- Mountings should sustain impact loads in case of accident in lateral and longitudinal directions, and dynamic loads in vertical direction due to uneven road surface
- Ease of assembly and disassembly and minimizing the mounting elements

Based on the requirements and in order to verify the design, a number of simulation studies are devised, which will be covered in Chapter 4.

3.2. Module configuration

3.2.1. Battery cell specification

The cells chosen for this application are CE32BNCD-50Ah Lithium Ion cells from BYD and they were chosen based on their thermal capacity as well as energy density. In Table 3.1 the cell specification is listed while in Table 3.2 and Figure 3.7 the cell dimension is demonstrated.

Table 3.1: Cell specification

Voltage of one cell	3.6 V
Rated capacity of one cell	50 Ah
Charge/Discharge rate	50 A
Run- time	1 hour
Num. elements in series	28
Num. series in parallel	2
Total cells	56
Voltage of storage	101 V
Current of storage	100 A
Total Energy stored	10.08 kWh
Cell weight	0.85 kg
Total weight	47.6 kg

Table 3.2: Cell dimensions

Length	Thickness	Height (with terminals)	Height (w/o terminals)
148 mm	26.5 mm	91 mm	98.4 mm

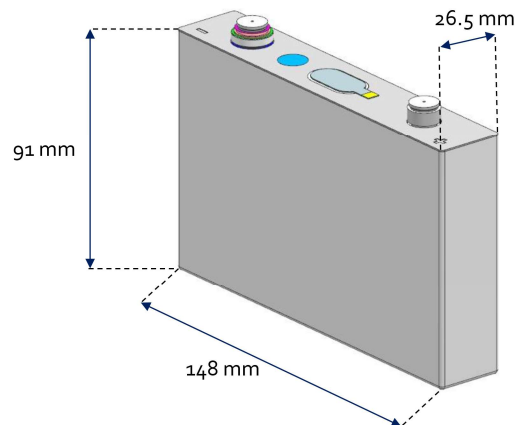


Figure 3.7: BYD battery cell

3.2.2. Modules configuration

The module design is based on the idea of “indirect cooling”. In order to maximize the thermal energy transmission between the cell and the outside environment, the bottom side of the cells should be directly in contact with the floor of the battery pack. In this way, despite the fact that there is no direct ventilation to regulate the cell temperature, the thermal conduction between the cell and the battery pack floor will provide the necessary cooling power. This approach is based on the heat sink design used in electronic devices, as it is demonstrated in Figure 3.8.

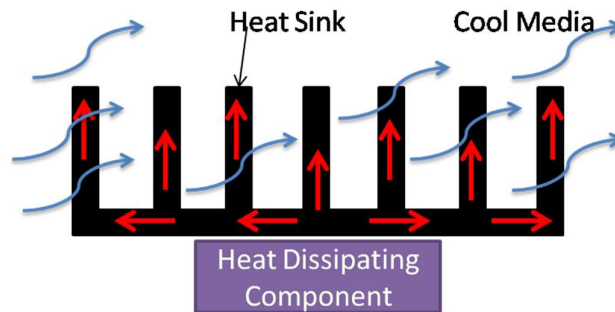


Figure 3.8: Heat sink scheme

In order to achieve the cooling target as well as having a structurally sound module, the design was carried by devising the elements listed in Table 3.3.

Table 3.3: The list of module elements

Element	Number per Module/cell	Number in Total	Material	Notes
Battery cell	Module A: 16 Module B & C: 20	56	-	Weight: 0.85 kg
Module holders	2 per module	6	304 Steel	Thickness: 2 mm
Compression pads	Module A: 17 Module B & C: 21	59	Neoprene rubber	Thickness: 1 mm
Threaded rod	2 per module	6	304 Steel	Length: Module A: 465 mm Module B & C: 575 mm Total weight:
Holder nut	8 per module	24	304 Steel	-
Bus bar panel	One per module	3	Plastic with copper connectors	-

Cells are kept together by the friction force of rubber plates and the pre-load by rod nuts. The rubber pads maximize the friction between the cells in order to avoid relative displacement, while acting as electric insulation. They also provide minor damping effect in case of impact. The threaded rod and the holders are also preloaded in order to provide the normal force on the pads and keep the cells tightly in contact. The Figure 3.9 shows an exploded view of a 2 cell sample and the module elements while in the Figure 3.10 the fully assembled modules are demonstrated.

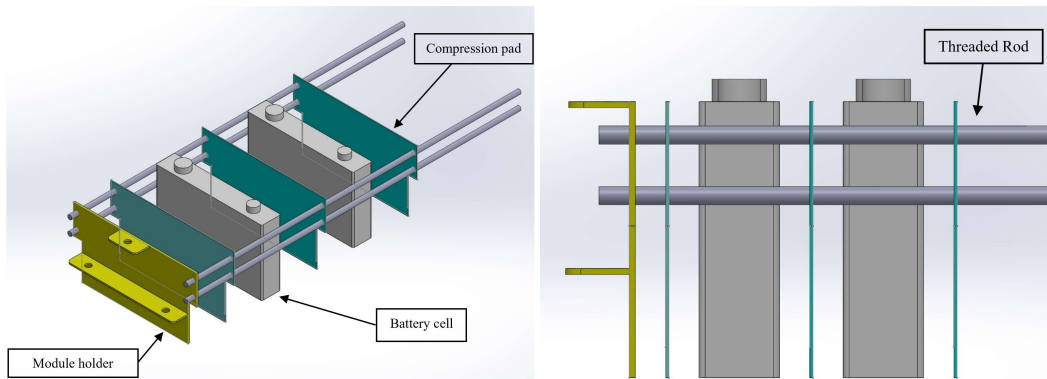


Figure 3.9: Sample module assembly and the module elements

Below, all the modules are demonstrated in isometric and side view after completion of the assembly.

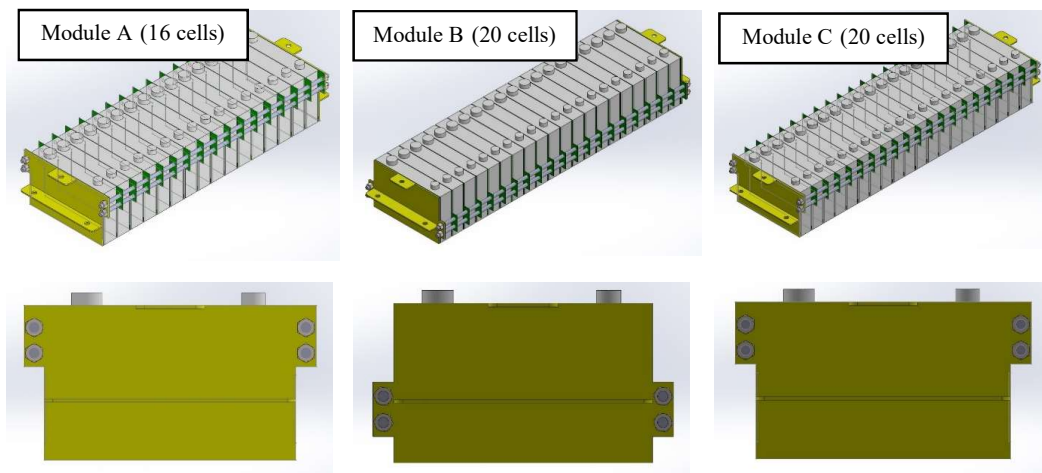


Figure 3.10: Fully assembled modules

In order to have the correct orientation for the cell terminals and also for the modules, the schematic connections and bus bars are demonstrated in Figure 3.11, where we see the correct cell configuration and also the diagram for parallel or series connection between the cells, in order to provide the amperage required. The “red rectangles” represent the bus bar connections in each module while the “red lines” represent the connections between the modules and at the final terminals.

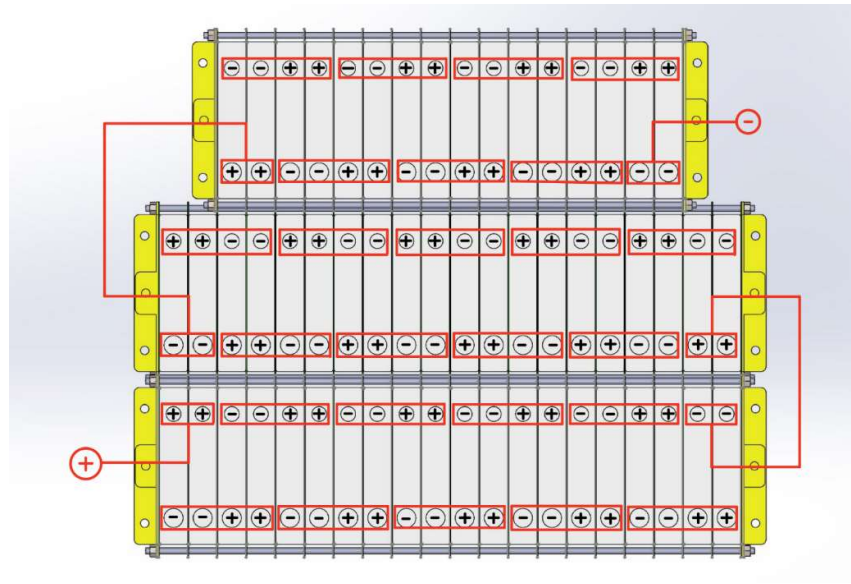


Figure 3.11: Schematic battery cell connections in series or parallel

The last element to be considered as module element is the bus bar panel. The bus panel houses the bus bar connectors and also provides the terminals (Figure 3.12 a) in order to connect the modules together and also the outlet ports for BMS (Figure 3.12 b). Figure 3.12 also demonstrates an exploded view of the module A before assembling the bus bar panel. After the addition of bus bar panel on module A, it is ready to be mounted onto the frame and connect to the circuit.

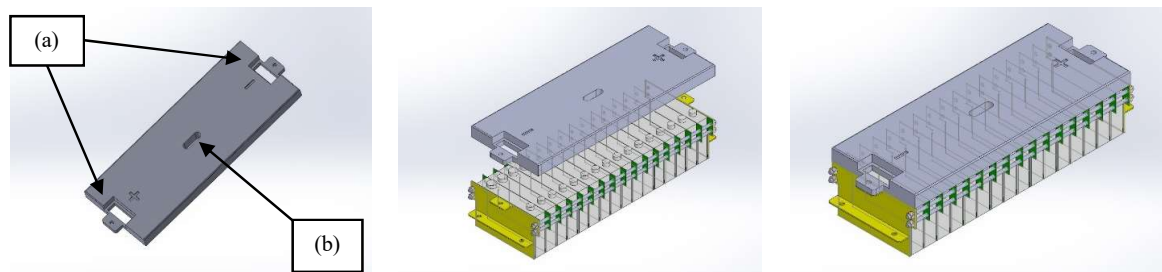


Figure 3.12: Bus bar elements and assembly on the modules

3.3. Ducted lower cover

The main housing element of the battery pack is the lower cover assembly. The cover not only provides the cooling conduction for the cells, but also integrates the duct as protective elements as well. The lower cover assembly consists of 3 elements:

- The cover itself which houses the cells and battery internal elements
- The cooling ducts which also help absorbing energy in case of impact from below

- The shield which completes the cooling pathways and also provides the protection from below

All these elements are welded together in order to guarantee the structural integrity as well as high thermal conductivity. In Figure 3.13 the lower cover elements are demonstrated.

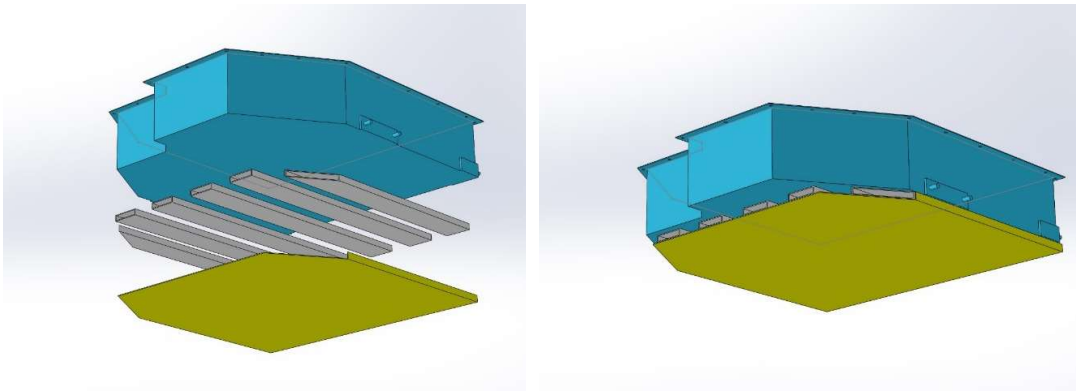


Figure 3.13: Lower cover assembly, integrating ducts for cooling and protection

The lower cover provides the following characteristics as requested:

- Maximum available surface in order to cool down the battery cells from the bottom, by applying a ducted design on the bottom side
- Protection in case of impact from the bottom, without an additional structures
- Mounting reinforcement and welded M8 bolt threads in order to connect the side mounts (and the rear mounts).

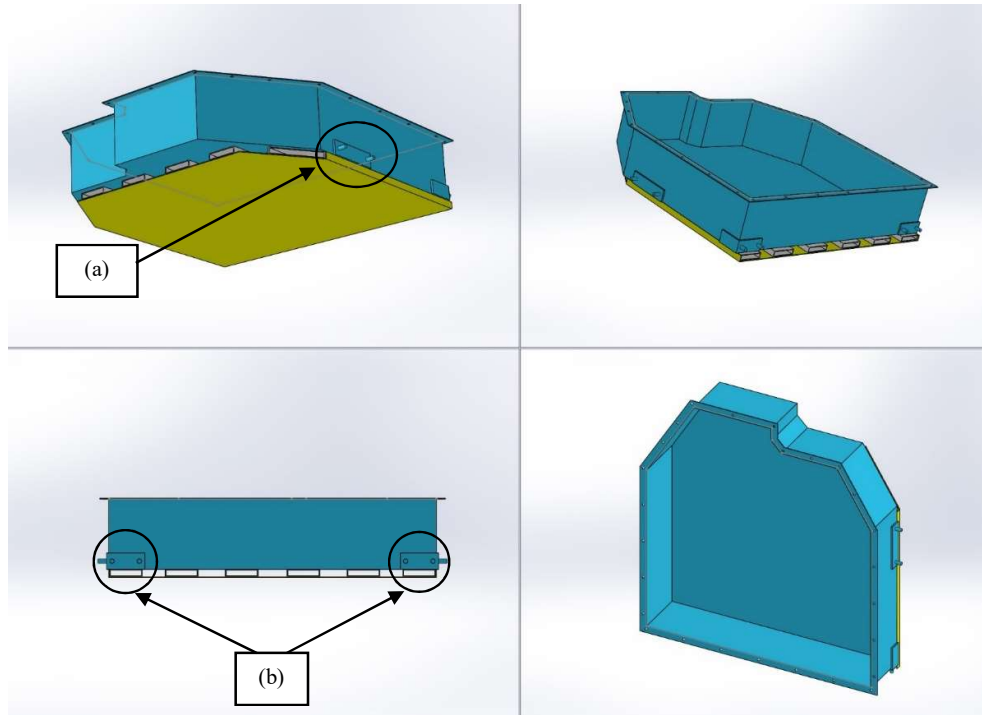


Figure 3.14: Assembled lower cover with the mounting reinforcements

3.4. Frame integration

In order to transmit the static loads such as the weight of the battery as well as the dynamic loads to the mounts during normal operation, a structural element should be foreseen in order to be integrated inside the battery pack. In the previous design such structure didn't exist. Instead there was a steel frame that surrounded the lower cover and held the pack by connecting to the mounts. The main disadvantages of such structure were complexity as well as limiting the surface area on the bottom side of the pack and hence, limiting the heat dissipation capacity.

For our application, the frame consists of longitudinal and transversal sections, with reinforcements on the surfaces where the modules are attached. The steel frame is made up of rectangular (15*10) transversal tubes and (30*10) longitudinal tubes and is reinforced in places where the modules will be mounted (Figure 3.15 a). The transverse beams as well as the 4mm plate at the front of the frame (Figure 3.15 b) provides the structural integrity as well as constraining the longitudinal movement of the modules. For module A attachment, the mounting plate is welded to a 4mm thick steel plates welded on the frame. For modules B and C attachment, the frame is cut and reinforced with wider rectangular section (30*20) (Figure 3.15 c). There are also bolt holes for the mounts, and the M8 nuts are welded under the thick steel plates in order to mount the

modules (Figure 3.15 d). Also the frame is reinforced with 4mm steel plates where the modules are mounted (Figure 3.15 e).

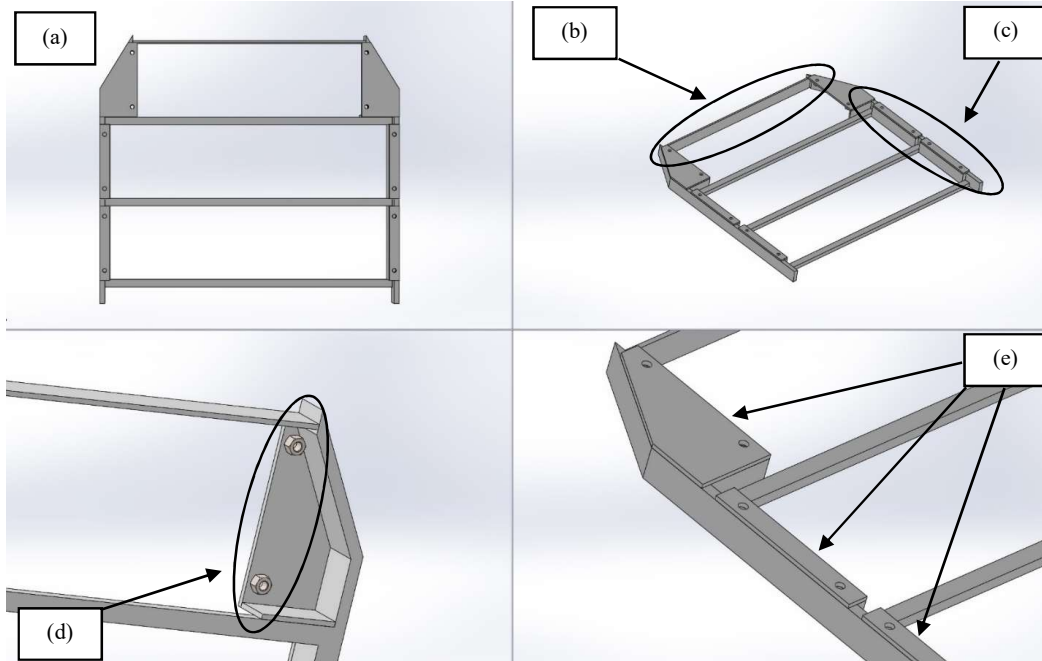


Figure 3.15: Integrated frame and its elements

After the construction, the frame is then placed inside the lower cover and is welded. The frame is designed in a way to carry the loads from the mounting points and also the battery modules. While the longitudinal beams carry most of the static and dynamic loads from the modules to the mounts and vice versa, the transversal beams are there to limit the cell movements in case of an impact, where the modules pre-loading is not sufficient.

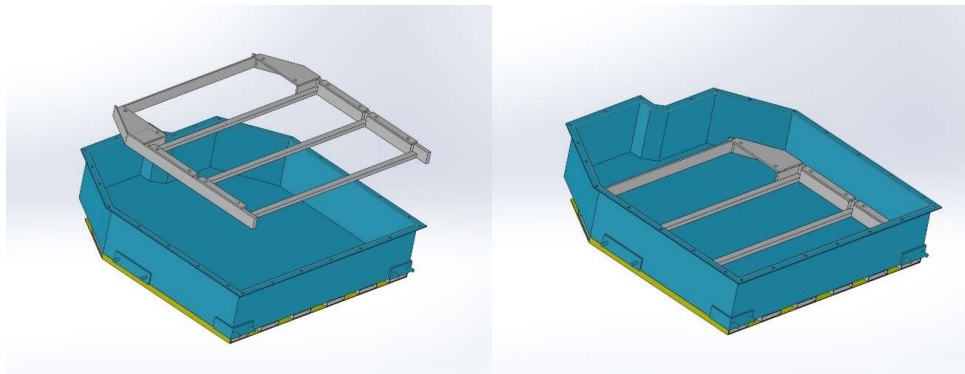


Figure 3.16: Frame placement inside the lower cover

3.5. Module installation

The last step to complete the battery pack assembly is module installation. The modules are then connected together and the auxiliaries such as the safety switch and the relays are added to complete the electric circuit. Following the correct configuration for the modules, they are attached to the frame by 2 M8 bolt screws on each side. In order to protect the inner components of the pack, a rubber seal is applied before closing the pack. The seal is there to make sure the battery pack is IP67 compliant in terms water resistance. The top cover and the seal are mounted using 26 M6 bolt screws. After sealing off the battery pack, it is ready to be connects to the mounts and then to the vehicle.

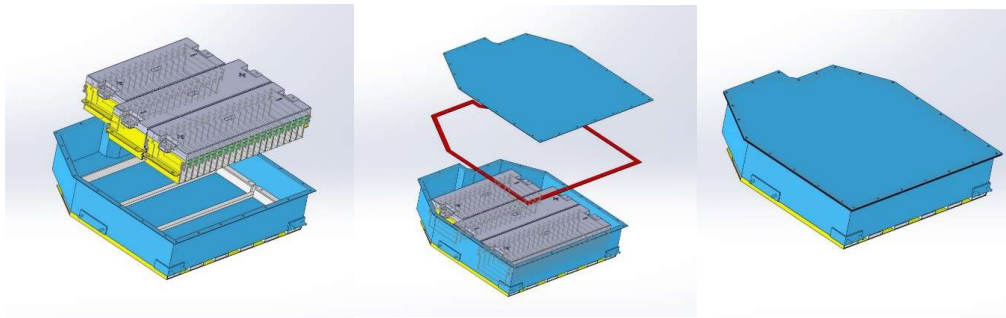


Figure 3.17: Module placement and sealing off the battery pack

3.6. Mounts design

The mounts are designed to carry the static and dynamic loads while minimizing the vibrations transmitted to the battery pack internals. The design was carried out with respect to the mounting points and underbody dimensions of the vehicle plus the angle of departure in the rear. There are 3 mounts, each one consists of three elements:

- The chassis mount
- The battery pack mount
- The bushings

The mounts are designed in order to maximize the ease of assembly and disassembly. Based on the requirements, the design was carried out in SolidWorks CAD software. Based on the vehicle underbody configuration, the design should respect some constraints

- Rear axle suspension elements
- Mounting points on the chassis
- Rear departure angle

The departure angle is particularly important because we need to make sure the battery pack and the mounts do not get hit before the vehicles load bearing elements (like the rear bumper or the tires) in case of rear-ending or hitting the curbs. The departure angle should be considered both in case of maximum suspension travel and full compression.

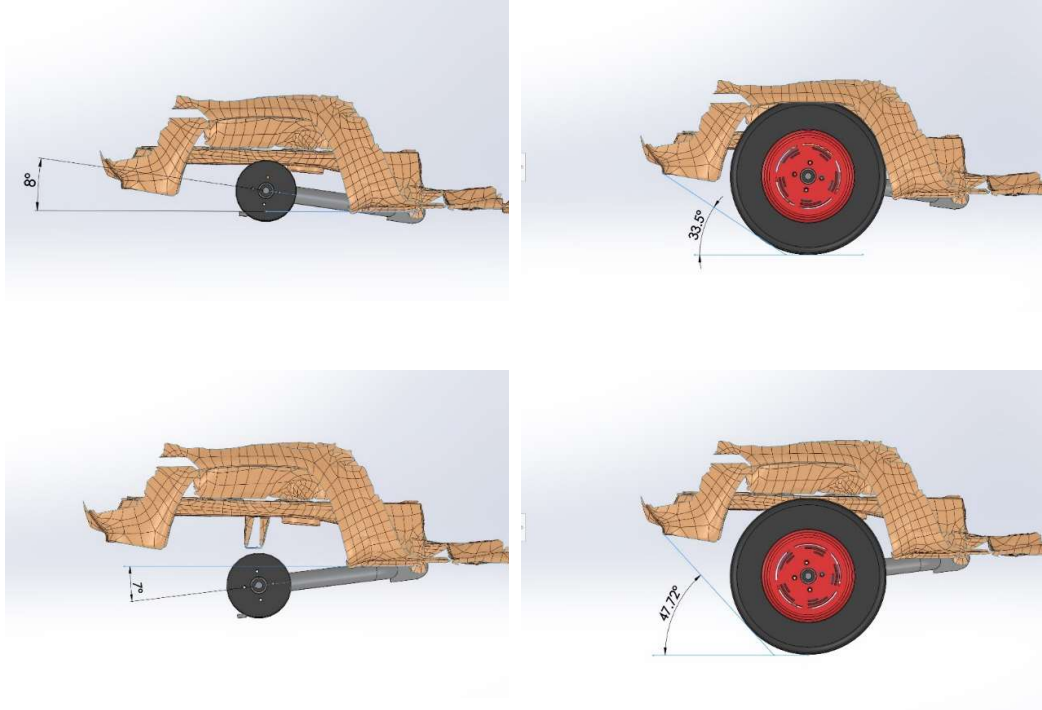


Figure 3.18: Vehicle suspension travel and departure angle maximum and minimum values

3.6.1. Side mount design and assembly

The two side mounts are the main load bearing elements in the mount design. Based on the previous mounting placement on the battery pack, the mounts are located on the trajectory that passes through the battery pack center of gravity. Thus minimizing the torque caused by the off-center.

Unlike the previous design however, the new side mounts directly attach to the battery pack via the reinforcement plates. Moreover, there are elastic rubber elements in the form of bushing to minimize the vibration transmission and add to the safety of the battery pack operation.

In Figure 3.19 the mounting elements for the right side mount is shown. The two side mounts are identical bar the upper chassis elements, which are symmetrical. In Figure 3.20 and Figure 3.21 the final assembly of the mount are shown.



Figure 3.19: Side mount elements (from the left: bottom mount, bushing, (right side) chassis mount)

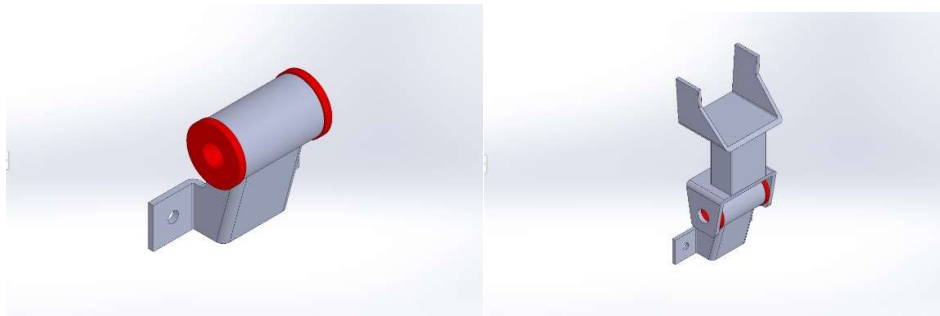


Figure 3.20: Side mount assembly

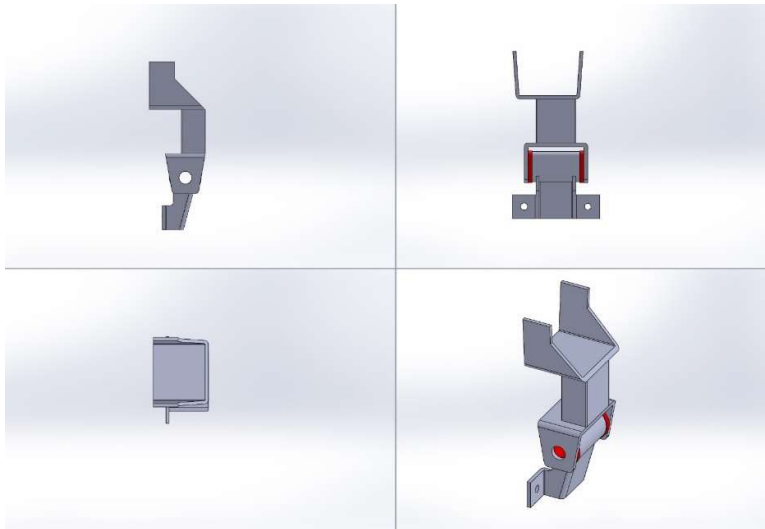


Figure 3.21: Completed assembly of the (right) side mount

3.6.2. Rear mount design and assembly

The rear mount main task is to stabilize and fully constrain the battery pack movement against loading scenarios, since for three-dimensional body, it is necessary to have 3 constraining elements to limit the transitional and rotational movements in 6 directions.

The rear mount are also positioned on the extension of center of gravity trajectory and it should also provide the ease of assembly and disassembly (Figure 3.22).

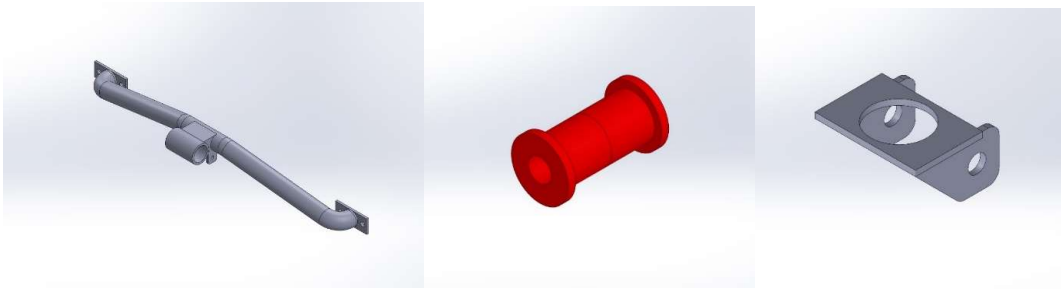


Figure 3.22: Rear mount elements (from left: rear bar, bushing and the chassis mount)

In order to protect the back-end of the pack from rear ending and impact, a protective shield was added (right picture). In Figure 3.23 and Figure 3.24 the assembly stages of the rear mount are demonstrated.



Figure 3.23: Rear mount assembly stages

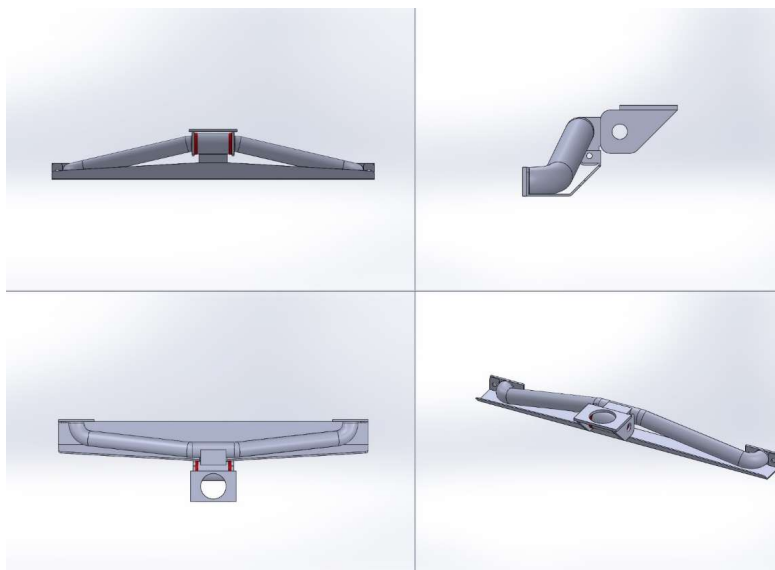


Figure 3.24: Fully assembled rear mount

3.7. Battery pack and mounting assembly

The last step before completion of battery pack installation is battery pack mounting under the vehicle. As it was mentioned before, each mount consists of a pack mounted element and a chassis mounted element. In Figure 3.25 the battery pack with the pack mounted elements are shown. On the vehicle chassis however, there are three chassis mounts located on the vehicle transversal beam at the rear (Figure 3.26 a) as well as the rear tow bar attachment point (Figure 3.26 b). In this setup the vehicle is raised and the battery pack is ready to be bolted to the chassis mount.

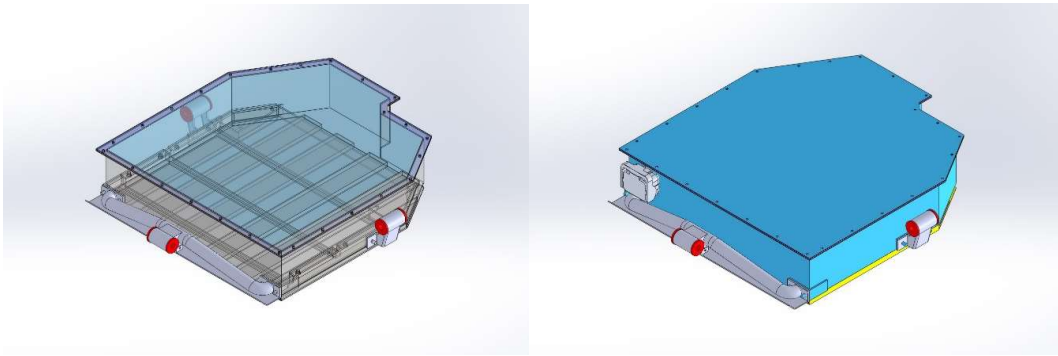


Figure 3.25: Battery pack ready for vehicle assembly

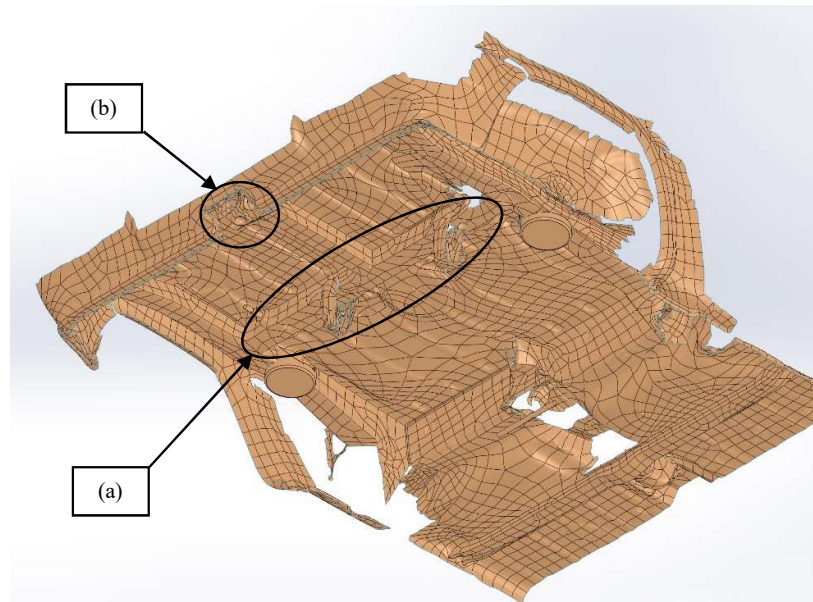


Figure 3.26: Vehicle chassis scan and the mounting points

The chassis mounts are welded to the chassis structures, while the pack is then attached to the chassis mounts by the use of 3 M16 bolts. This allows a quick and easy assembly procedure and removes the need for special tooling in case of maintenance.

In Figure 3.27 and Figure 3.28 the assembly stages as well as fully installed battery pack are shown.

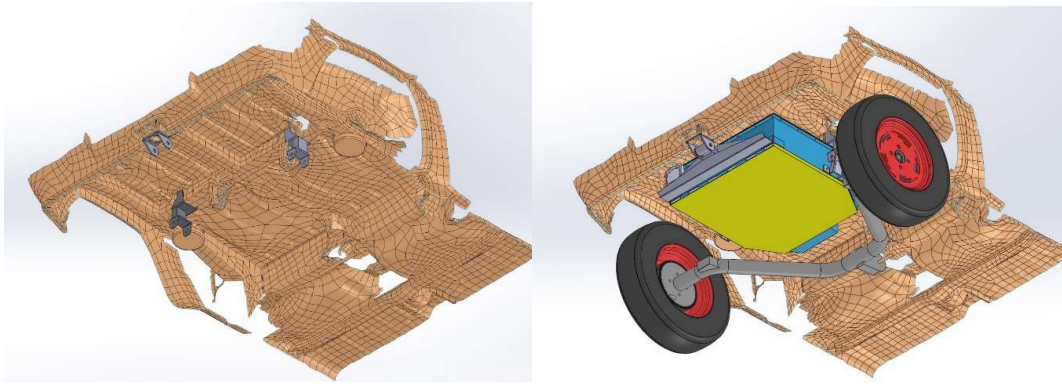


Figure 3.27: Battery pack installation

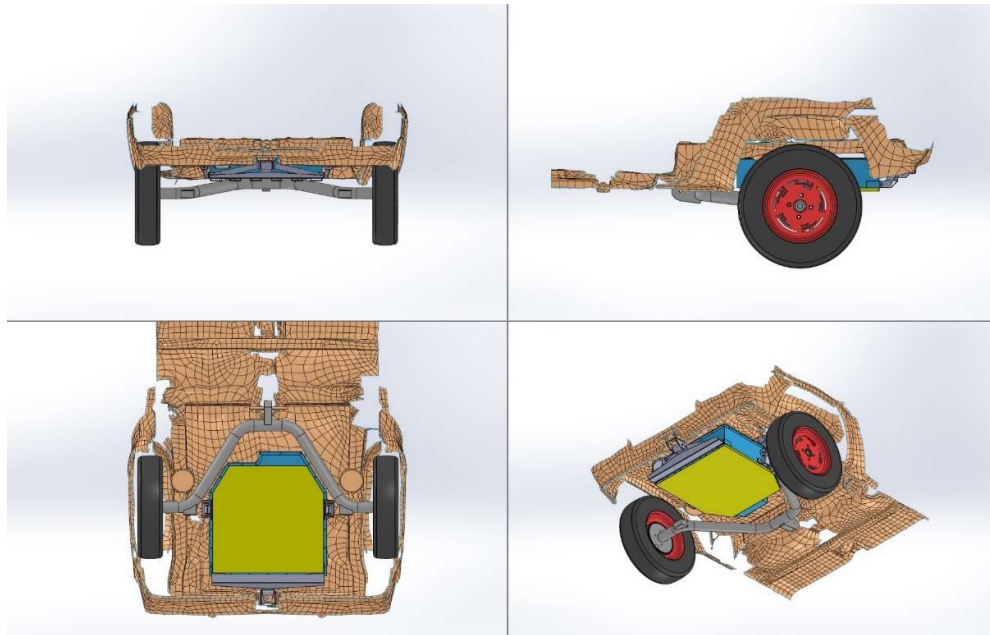


Figure 3.28: Fully installed battery pack

4. Design verification and simulation studies

4.1. Introduction

In this chapter, we verify the design with respect to the main requirements for the battery pack and the mounting assembly, as well as the previous design as the reference. The verification process has a number of criteria:

- Keeping the weight in check
- Maintaining the vehicle departure angle
- Mounts ability to withstand the static and dynamic loads
- Battery pack bottom side protection

The first design target was to add all the cooling and structural feature without over complicating the design and thus, avoiding weight increase. So in the first step, there is a weight assessment on all of the battery pack and mounting elements that were discussed previously. Then, the mentioned design is compared against the old battery pack specifications as a reference point.

Next, the design is assessed with respect to the requirement regarding vehicle suspension geometry and the departure angles. The main objective of this section is to verify that the battery pack is well-protected against day-to-day diving use and abuse and the pack and mounting structure do not get in the way of other vehicle sub-systems, such as suspension geometry or alter vehicle specification such as floor height or angle of attack/departure.

For the last two criteria, the battery pack and the mounts were simulated using FEM tools in Solidworks™ and Abaqus Explicit™. First we focus on the inside and on the module assembly. Here we only considered the main load bearing elements and neglect the presence of lower and top cover assembly. Regarding the study cases for module assembly, by defining a gravitational field based on standard regulation demanded by the key target market, we are able to simulate the different loading cases. Then we apply the static loads on the mounts. Then a simplified assembly that only considers the mounting structure was studied. It was assumed that the mounts carry the weight of the pack considering a safety factor, since we neglected some of the pack internal elements in our design. Then in the next section, the same model goes through a series of dynamic simulation studies. The dynamic cases include frontal impact, side impact and vertical impact due to road bump. The main objective of these studies are to examine the mounting structure and find out the weak points during extreme loading scenarios. Moreover, based on the response plots in the dynamic mounting studies, the maximum impact acceleration in 3 directions are obtained. At the end we examine the critical points and discuss the results.

In the last section, we verify the battery pack capability to absorb impact from the bottom, by studying the battery pack bottom cover behavior based on real ground impact from stones on the road surface. In this section the lower cover assembly as well as the integrated frame are put against the ones from the previous design and are examined in an impact test with sphere from the bottom side, representing road debris. Then the results from the two simulation cases are discussed and compared with each other.

4.2. Batter pack weight assessment

The weights of the designed parts were estimated using the SolidWorks mass properties using the dimensions of the parts and the assigned material density. There is a safety factor considered in the end, in order to account for the auxiliary electronic elements inside the pack that we didn't take into account in our model. Table 4.1 lists all the pack elements in terms of number and overall weight.

Table 4.1: List of battery pack elements with weight approximation

Element	Material	Element's weight (grams)	Total number	Total weight (grams)	
Battery cell	-	850	56	47600	
Holders	304 Steel	288	6	1728	
Compression pads	Neoprene rubber	18.5	59	1091.5	
Rods	304 Steel	105.2	12	1262.4	
Nuts	Cast steel	3.25	24	78	
Bus bar panel	ABS plastic	1785	3	5355	
Frame	304 Steel	4120	1	4120	
Seal	Neoprene rubber	135	1	135	
Lower cover assembly	304 Steel	18330.97	1	18330.97	
Top cover	304 Steel	4630	1	4630	
				Total weight	84330.87
				Total +10% (auxiliaries)	92763.957
					84.33 kg
					92.76 kg

Table 4.2: Weight comparison between the previous and proposed design

	Previous design	Proposed design
Active elements (battery cells)	47.6 kg	47.6 kg
Battery pack auxiliaries	22.4 kg	45.4 kg
Mounting elements	30 kg	5 kg
Overall weight	100 kg	98 kg

Comparing the proposed design and the previous design in terms of active elements and overall weight (Table 4.2), since the cell specifications and overall number of cell is constant, the active portion of the weight is unchanged. Moreover, we can see the overall weight is maintained, while the battery pack itself is heavier since the frame and other structural elements are integrated in the pack rather than being part of the mounting elements. However, in the previous design, despite the lower weight of pack itself, due to the lack of inner structural elements, the mounting structure and the frame around the package make up for the rest of weight. It should be mentioned that the auxiliaries inside the battery pack, such as the connectors, the BMS⁶ and the relays, are assumed to be similar between the two designs.

4.3. Mounting clearance and departure angle

4.3.1. Suspension clearance

One of the main design criteria that is already discussed is avoiding changes in other vehicle sub-systems, including the suspension. As a result, the battery pack and the mounts should respect the suspension geometry and there should be sufficient tolerances between the battery pack and the suspension at any ride height. These tolerances also allow for an easier access to chassis mount for pack installation.

In Figure 4.1, the aforementioned tolerances at the most critical value, which is at maximum suspension compression is demonstrated.

⁶ BMS: Battery Management System

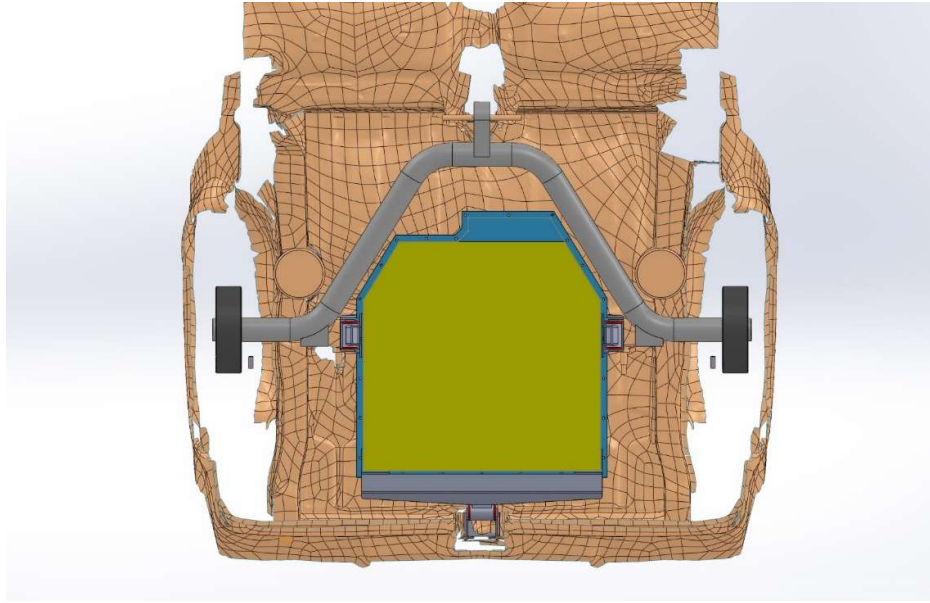


Figure 4.1: Battery pack and the suspension clearance

4.3.2. Departure angle

Another vehicle dynamic specification that should be respected was the departure angle. Maintaining the departure angle at minimum and maximum suspension travel also guarantees battery pack protection against rear end impact or curb hitting while parking, as it is illustrated in Figure 4.2 for the two extremes of vehicle ride height.

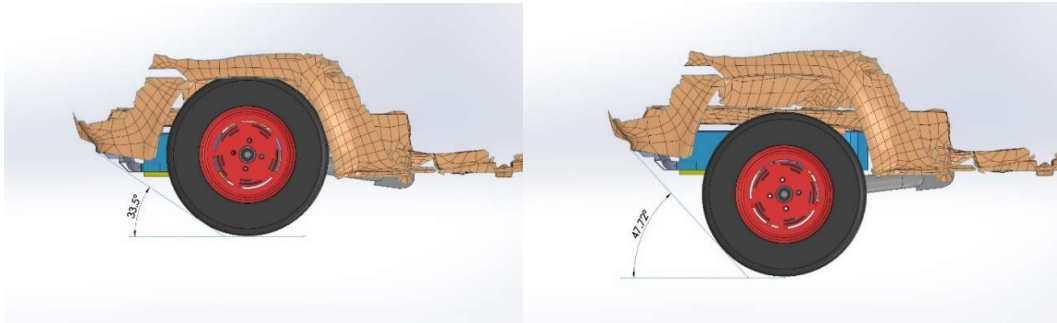


Figure 4.2: Vehicle departure angles at maximum and minimum ride height

4.4. Static simulation cases for module assembly

As part of the design verification process, the electric vehicle conversion has to meet the requirements and legislation demanded by the authorities in the sale market. One of the main target markets of the vehicle is France and it was necessary to meet the design regulation set by the French National Automobile Federation (FNA) [29]. Regarding the

structural integrity of the battery pack, the decree states that the battery pack and the mountings should withstand:

- 2g acceleration in longitudinal direction
- 1g acceleration in lateral direction
- 2g acceleration in vertical direction from top to bottom
- 1g acceleration in vertical direction from bottom to top

Based on these criteria, 4 static simulation cases were devised using SolidWorks simulation tool. The objective for this simulation study is to verify whether the module assembly can withstand the forces acting on the battery pack. For the sake of simplicity, in this section we focus on the modules and battery pack internal only, including the frame and the 3 modules. This representative model matches the original in terms of overall dimension, design, mass value and the center of gravity.

4.4.1. Simulation setup

The frame is made of 304 steel and is considered as a remote mass, since it is not part of the study. Regarding the modules themselves, the bus bar panels on the top are made of ABS plastic and also considered as remote mass since they are not part of load bearing structure. For the battery cells, since it is a composite structure, a material similar to 1060 aluminum was assigned; but with a costume density since the mass value of the cell is already given. The rods were kept as it was in the original model. However, nuts are excluded from the study, however by defining the correct bonding connection we maintain the physical constraints provided by the nuts. For reference, the list of the original modules elements are shown in Table 3.3.

In terms of constraints, we also apply the appropriate fixtures on the bolt holes on the module holders and choose Global Contact in order to simulate the friction forces and effect of pre-load and normal forces on the cells. In Figure 4.3 the final simulation model is demonstrated.

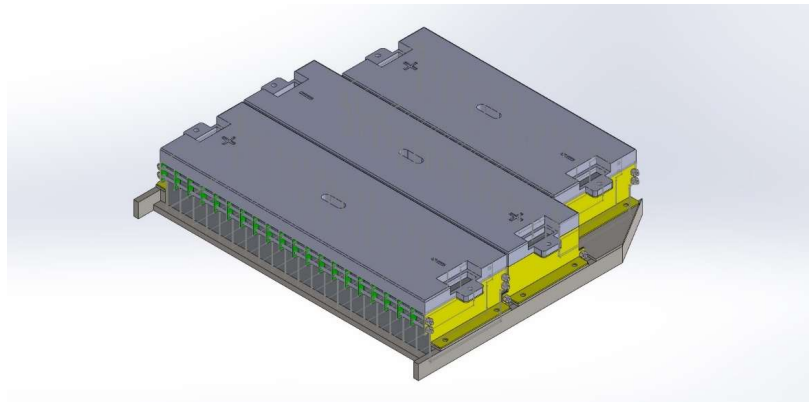


Figure 4.3: Module assembly for static simulation

In Figure 4.4 the loading cases as well as fixtures are shown:

- a) Longitudinal load case
- b) Lateral load case
- c) Up-down vertical load case
- d) Down-up vertical load case

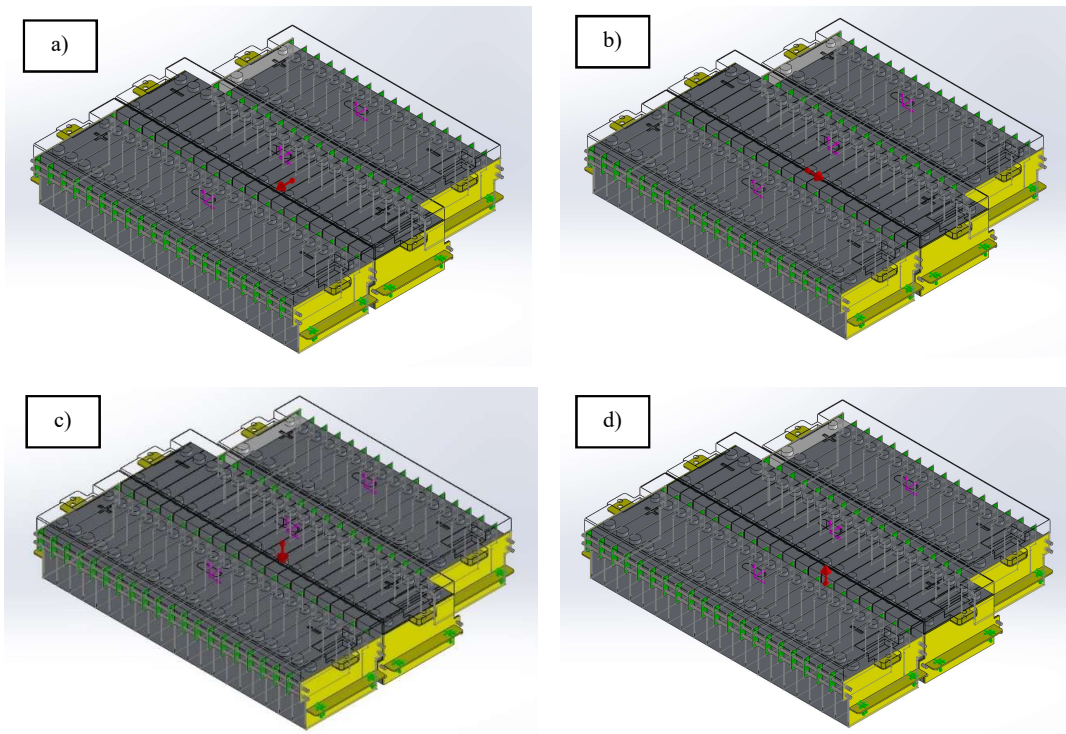


Figure 4.4: Loading cases in module simulation models

In terms of discretization, since the model has different material assigned and has a variety of fillet, holes and thicknesses, the curvature based mesh was chosen. Also by applying the highest quality mesh and assigning the smallest elements dimension in the model as the minimum elements size there was no need for secondary mesh controls to apply finer mesh size on the more critical geometries (Figure 4.5 and Figure 4.6).

Table 4.3: Mesh details

Mesh type	Solid Mesh
Mesher Used	Curvature-based mesh
Jacobian points	4 Points
Maximum element size	41.4595 mm
Minimum element size	1.91342 mm
Mesh Quality Plot	High
Remesh failed parts with incompatible mesh	On
Total Nodes	753190
Total Elements	460042
Maximum Aspect Ratio	67.991
% of elements with Aspect Ratio < 3	84.5
% of elements with Aspect Ratio > 10	3.37

After this step, the studies are submitted for analysis. The results of each case is demonstrated in the following sections.

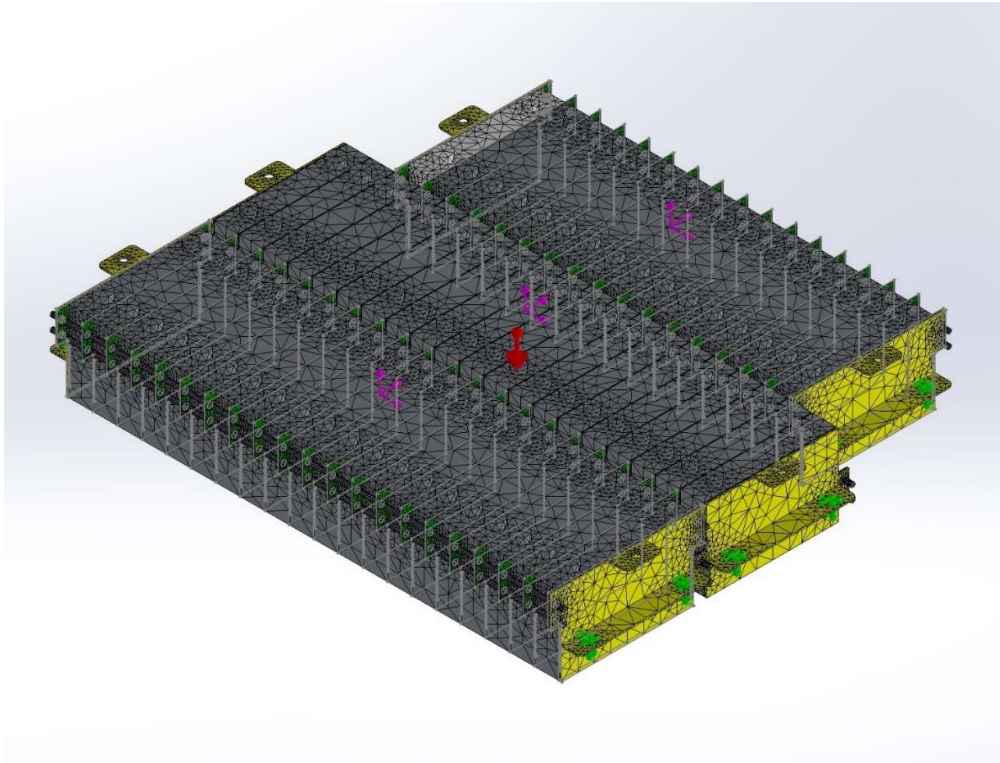


Figure 4.5: Discretized module simulation model

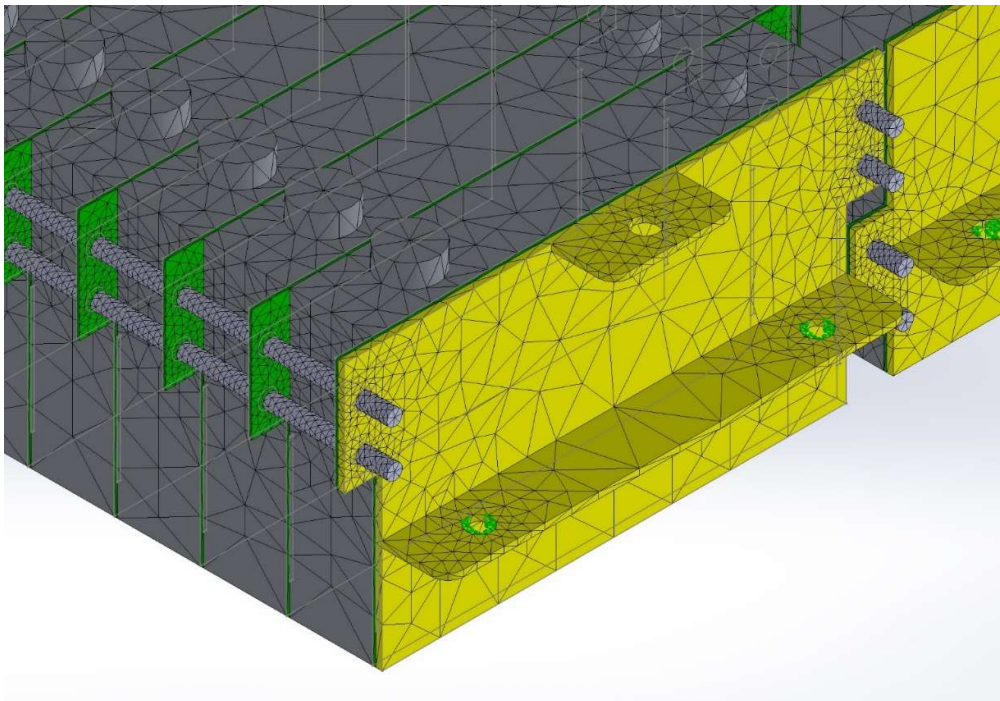


Figure 4.6: Fine discretization on critical components

4.4.2. Module static analysis case 1: Longitudinal motion

- Stress plot

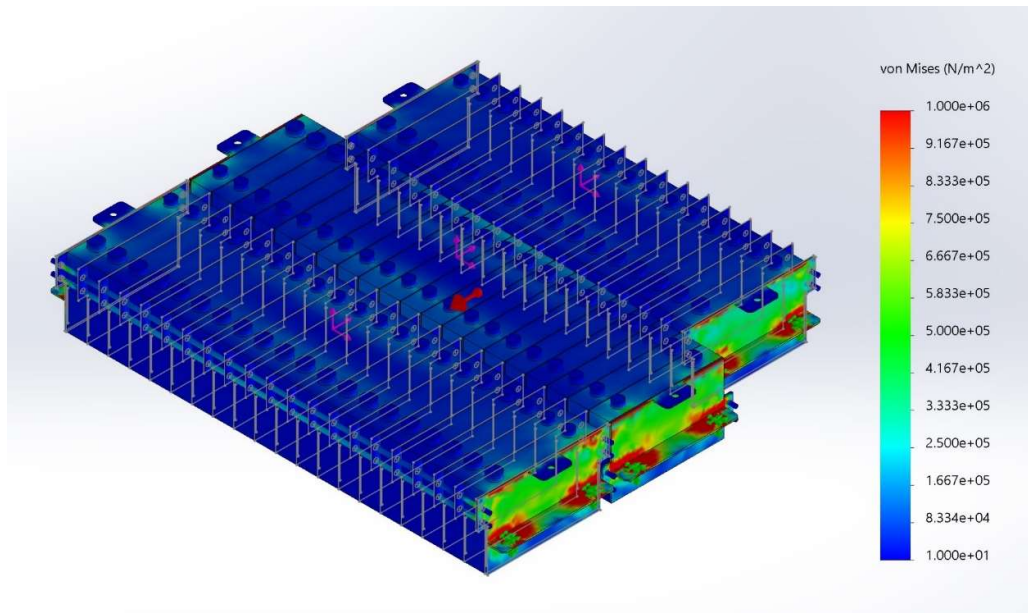


Figure 4.7: Stress plot for longitudinal load case

- Residual displacement plot

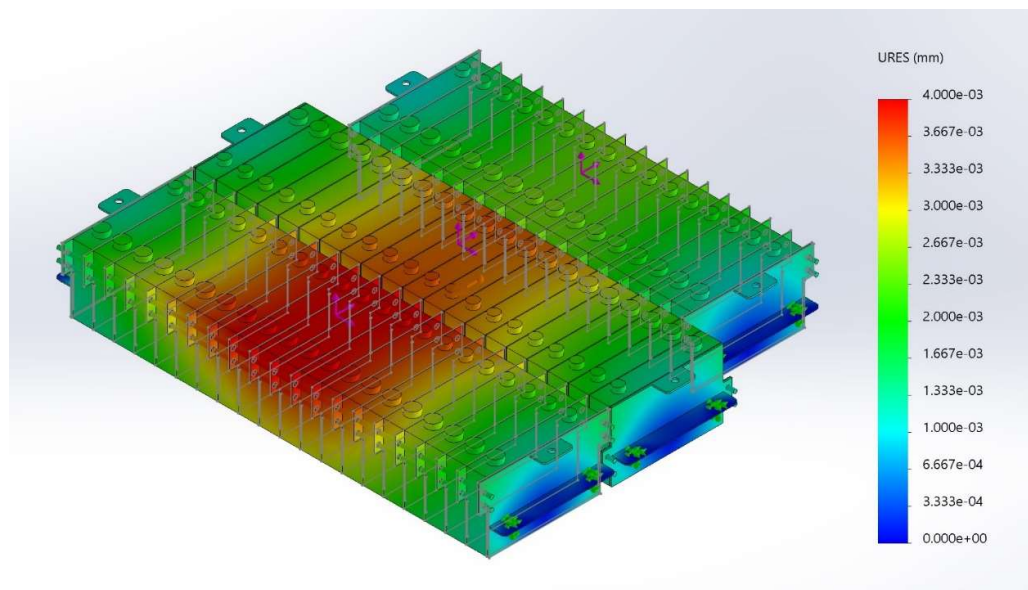


Figure 4.8: Residual displacement plot for longitudinal case

4.4.3. Module static analysis case 2: Lateral motion

- Stress plot

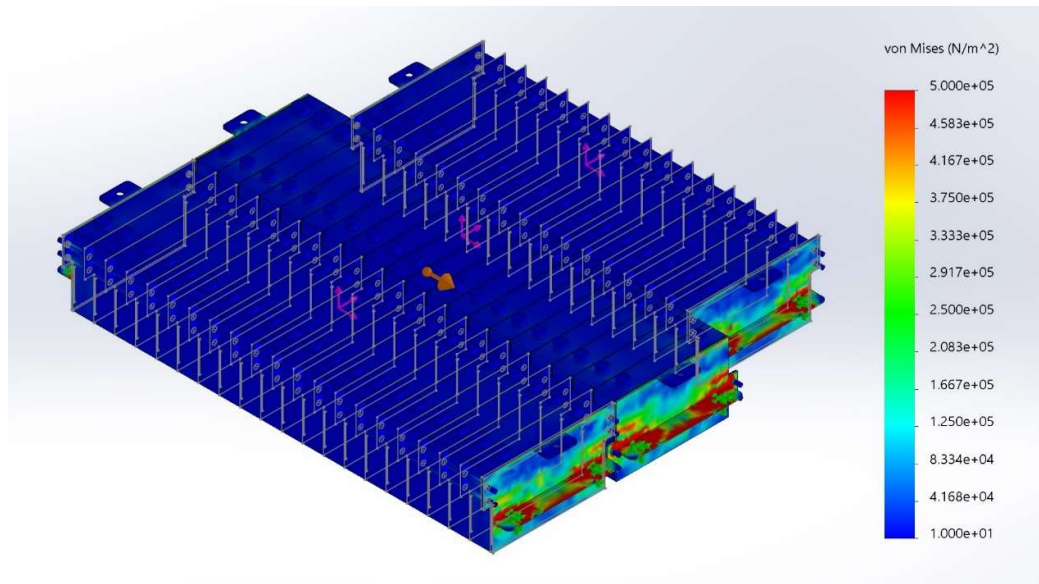


Figure 4.9: Stress plot for lateral load case

- Residual displacement plot

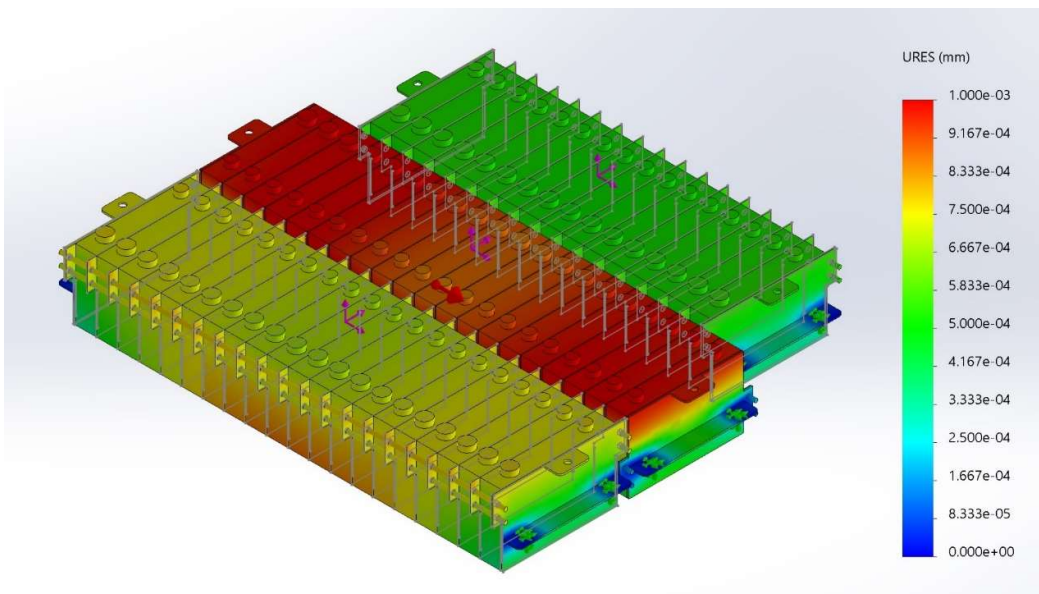


Figure 4.10: Residual displacement for lateral load case

4.4.4. Module static analysis case 3: Vertical motion (up-down)

- Stress plot

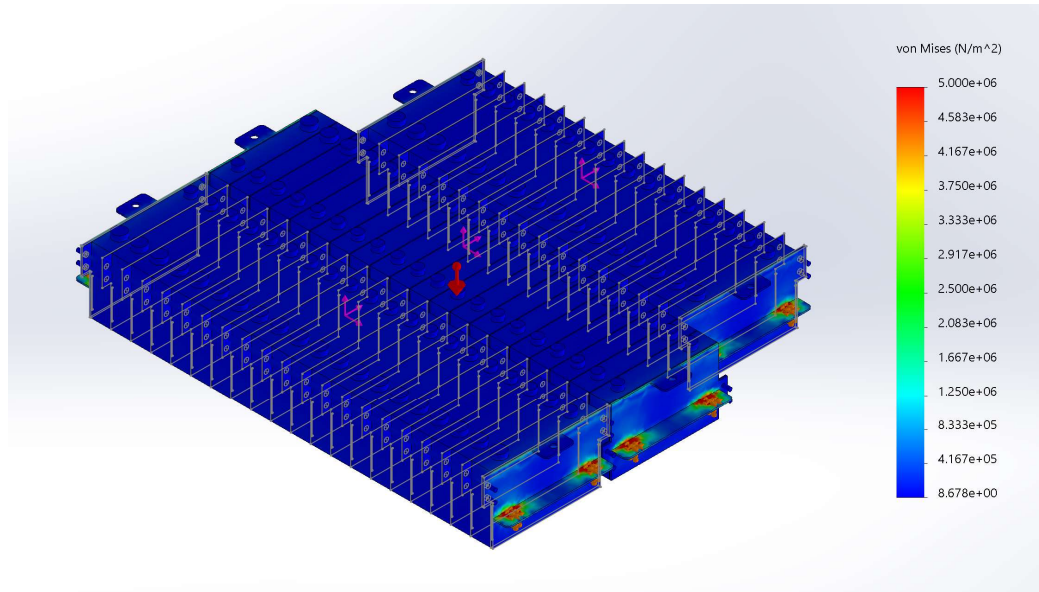


Figure 4.11: Stress plot for vertical load case (up-down)

- Residual displacement plot

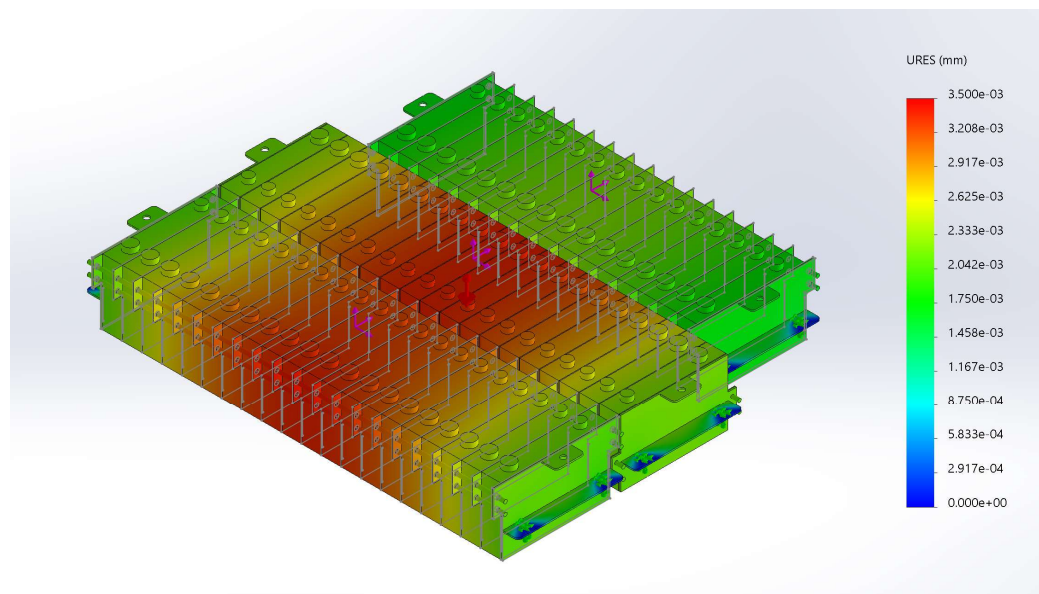


Figure 4.12: Residual displacement for vertical load case (up-down)

4.4.5. Module static analysis case 4: Vertical motion (down-up)

- Stress plot

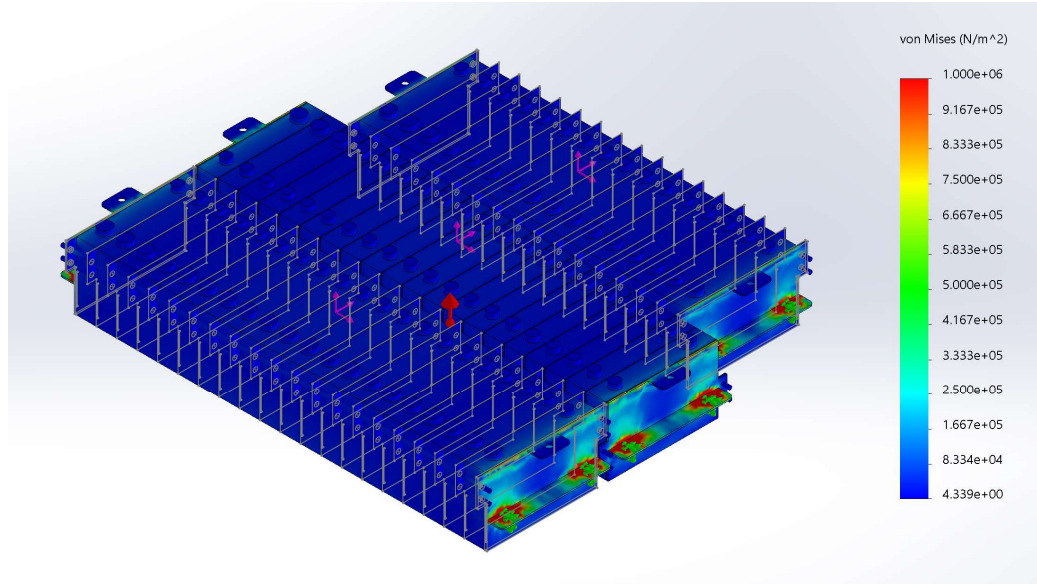


Figure 4.13: Stress plot for vertical load case (down-up)

- Residual displacement plot

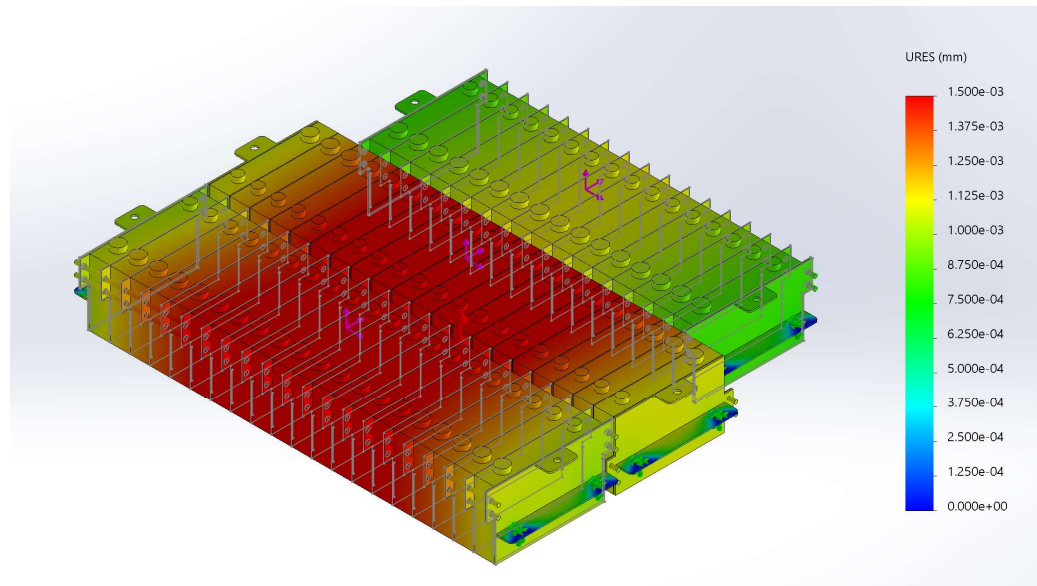


Figure 4.14: Residual displacement for vertical load case (down-up)

4.4.6. Results discussion

Regarding the modules assembly, in the stress analysis we should keep in mind that since the model is made up different materials the safety thresholds will be different depending on the elements maximum yield stress values. However, the maximum values recorded for stress is at the side holders (notably near the bolt holes) are at least 2 orders of magnitude below the yield value for the 304 steel used in those elements (Figure 4.7, Figure 4.9, Figure 4.11, Figure 4.13)

Regarding the residual displacement, the maximum values are recorded on module B and C. However, the maximum residual displacements for the module assembly are also at the micron level and in general, it stays below the minimum threshold.

We should also keep in mind that in these studies we have neglected the effect of having the battery cells supported by the pack floor from the bottom, since it is not the main load bearing element. Moreover, we should guarantee that the fastening elements of the model (bolts and nuts) are tight adequately torqued

4.5. Static simulation cases for mounts

The objective for these simulation studies is to verify whether the mounts can withstand the forces acting on the battery pack, based on the aforementioned legislation [29]. In order to reduce the computational cost, we simplify the model accordingly, by only considering the main load bearing elements and neglect the presence of inner battery pack elements and module assembly (Figure 4.15). We assume the mounts carry the weight of the pack considering a safety factor, since we neglected some of the pack internal elements in our design and for reference the values stated in Table 3.3 are used in order approximate the battery pack mass. This representative model matches the original in terms of overall dimension, design, mass value and the center of gravity.

Using SolidWorks simulation tool a gravitational field for each case was defined, representing the different loading cases. In the end we examine the critical points and discuss the results

4.5.1. Simulation setup

First, we define the material properties of the study. The assigned material for the battery pack is a costume steel based on AISI 304. The density values for the material was overwritten in order for the model pack to match the overall mass values for the original battery pack. Then the model pack is considered as a remote mass, since the mass value and center of gravity concerns our study and the mechanical behavior are not part of the study. For the bushing elements the material assigned from the SolidWorks library, was rubber. The material properties of these studies is listed in Table 4.4.

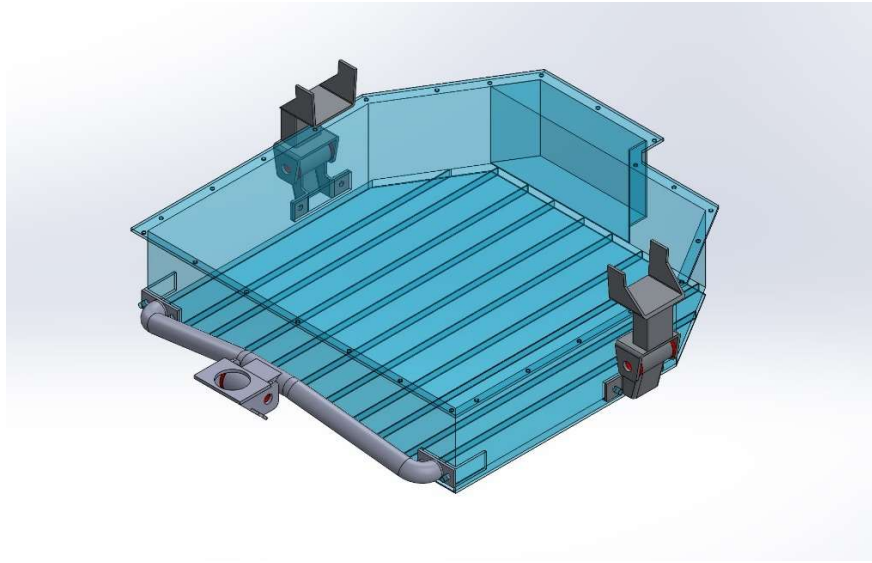


Figure 4.15: Mounting simulation model

Table 4.4: Material specifications for mount simulation study

	AISI 304 Steel	Rubber	Unit
Elastic Modulus	1.90E+11	6100000	N/m ²
Poisson's Ratio	0.29	0.49	--
Shear Modulus	7.50E+10	2900000	N/m ²
Mass Density	8000	1000	kg/m ³
Tensile Strength	5.17E+08	13787100	N/m ²
Yield Strength	2.07E+08	9237370	N/m ²
Thermal Expansion Coefficient	1.80E-05	0.00067	1/K
Thermal Conductivity	16	0.14	W/(m·K)
Material Damping Ratio	0.01	0.05	--

In terms of constraints, we also apply the appropriate fixtures on the chassis mount top surfaces (Figure 4.16). This represents the welding joint between the top mounts and the vehicle chassis. In terms of material contact in the model, a global friction coefficient of 0.05 was chosen in order to simulate the friction forces and effect of tightening loads from the nuts and bolts.

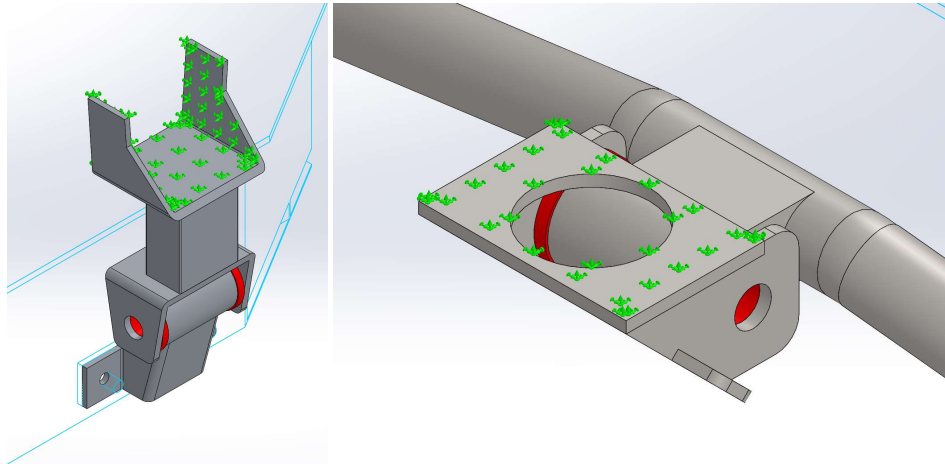


Figure 4.16: Fixtures for mount simulation model

Following the same simulation procedure as the module study cases, loading cases are:

- a) 2g for longitudinal load case
- b) 1g for lateral load case
- c) 2g for up-down vertical load case
- d) 1g for down-up vertical load case

In Figure 4.17, each of the loading cases are demonstrated.

In terms of discretization, since the model has different material assigned and has a variety of fillet, holes and thicknesses, the curvature based mesh was chosen. Also by applying the highest quality mesh and assigning the smallest elements dimension in the model as the minimum elements size there was no need for secondary mesh controls to apply finer mesh size on the more critical geometries (Figure 4.5 and Figure 4.6).

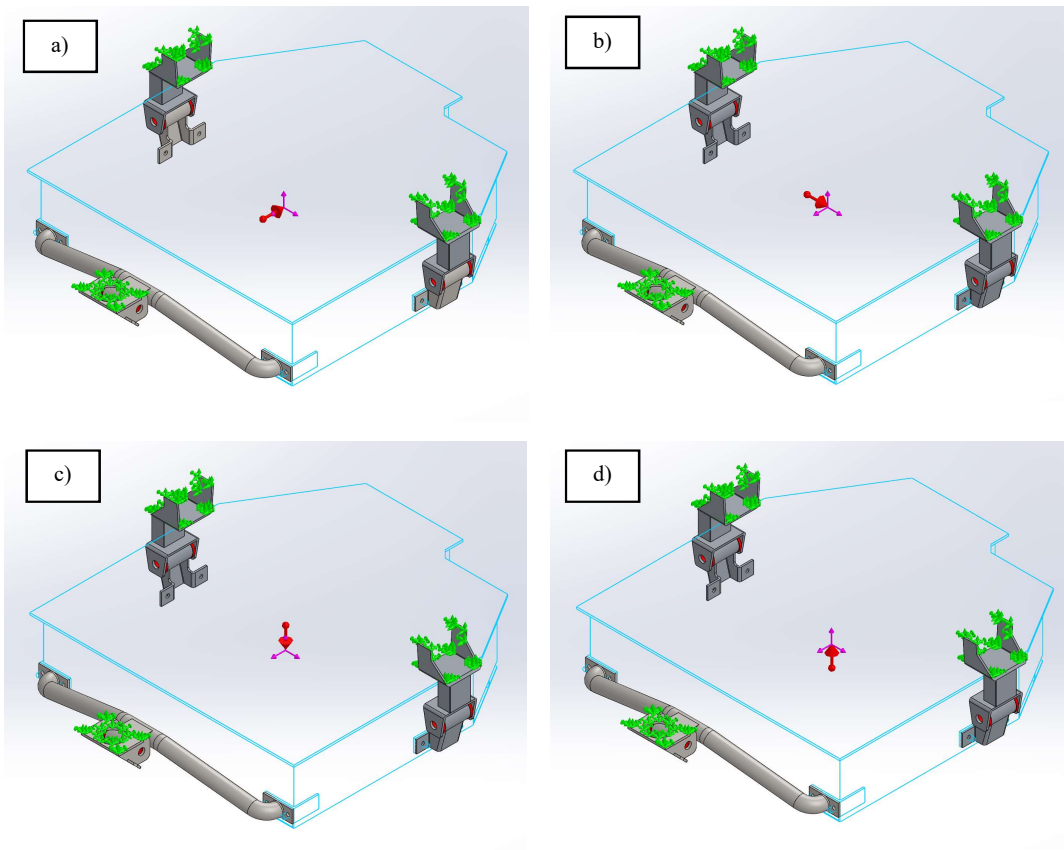


Figure 4.17: Loading cases in mount simulation models

Table 4.5: Mesh details

Mesh type	Solid Mesh
Mesher Used	Curvature-based mesh
Jacobian points	4 Points
Maximum element size	12.0499 mm
Minimum element size	0.765367 mm
Mesh Quality Plot	High
Total Nodes	123712
Total Elements	68730
Maximum Aspect Ratio	153.09
% of elements with Aspect Ratio < 3	76.5
% of elements with Aspect Ratio > 10	2.81

After this step, the studies are submitted for analysis. The results of each case is demonstrated in the following sections.

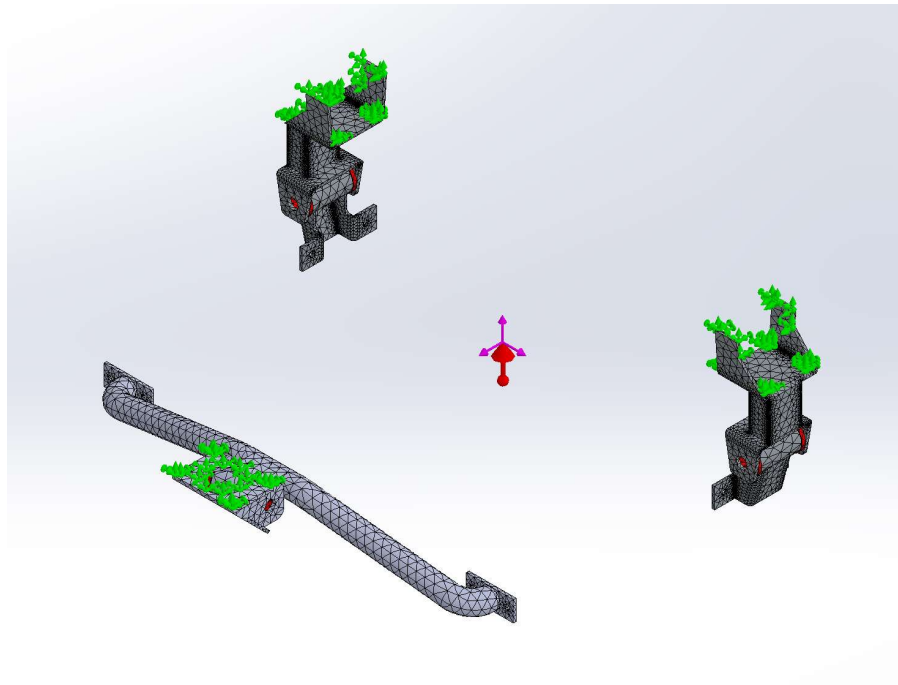


Figure 4.18: Discretized mount simulation model

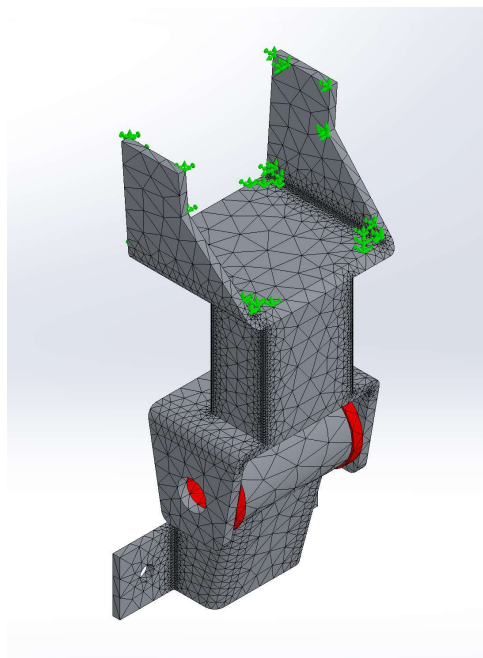


Figure 4.19: Fine discretization on critical components

4.5.2. Mounts static analysis case 1: Longitudinal motion

- Stress plot

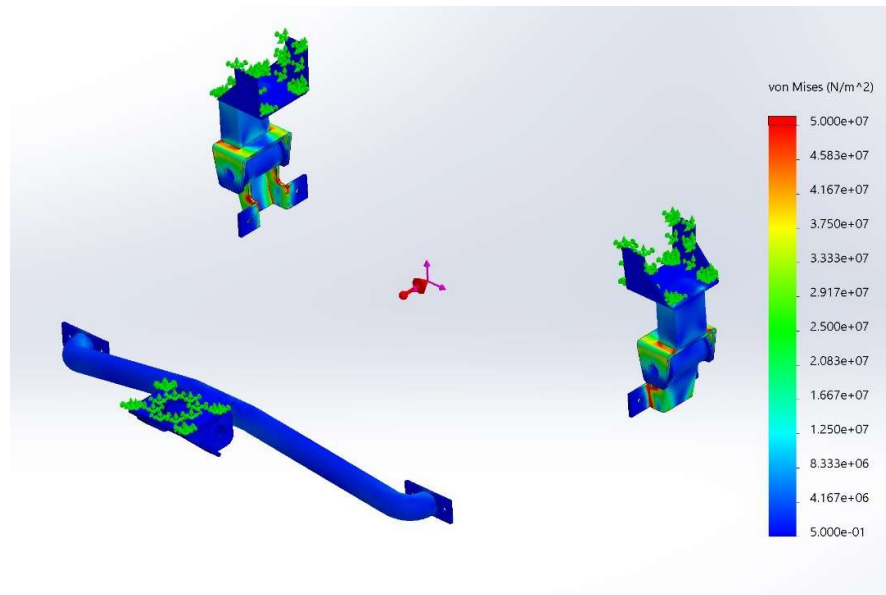


Figure 4.20: Stress plot for longitudinal load case

- Residual displacement plot

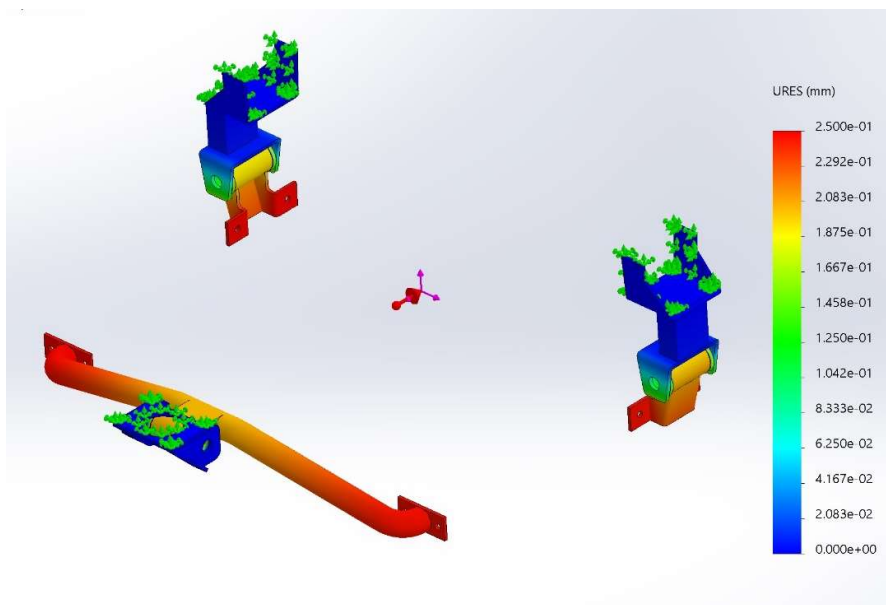


Figure 4.21: Residual displacement plot for longitudinal case

4.5.3. Mounts static analysis case 2: Lateral motion

- Stress plot

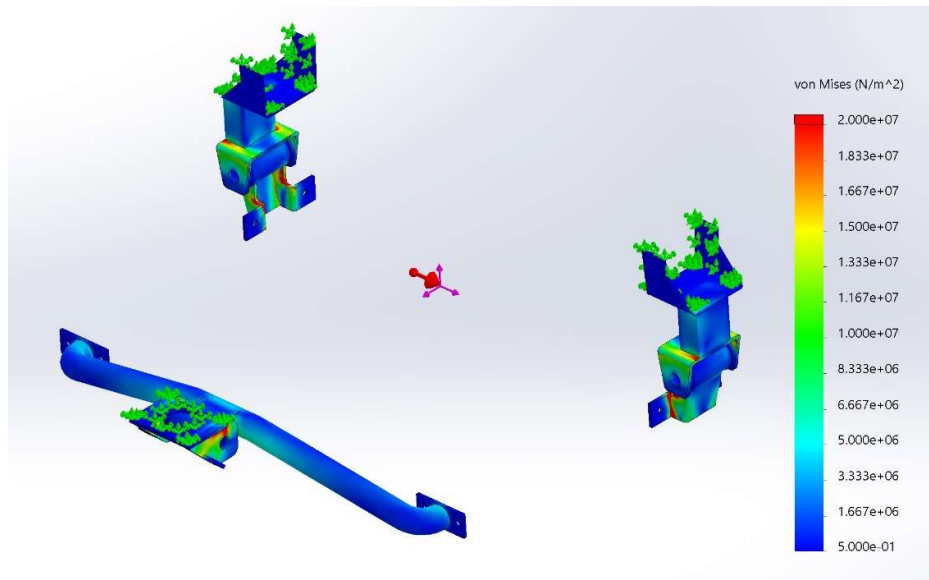


Figure 4.22: Stress plot for lateral load case

- Residual displacement plot

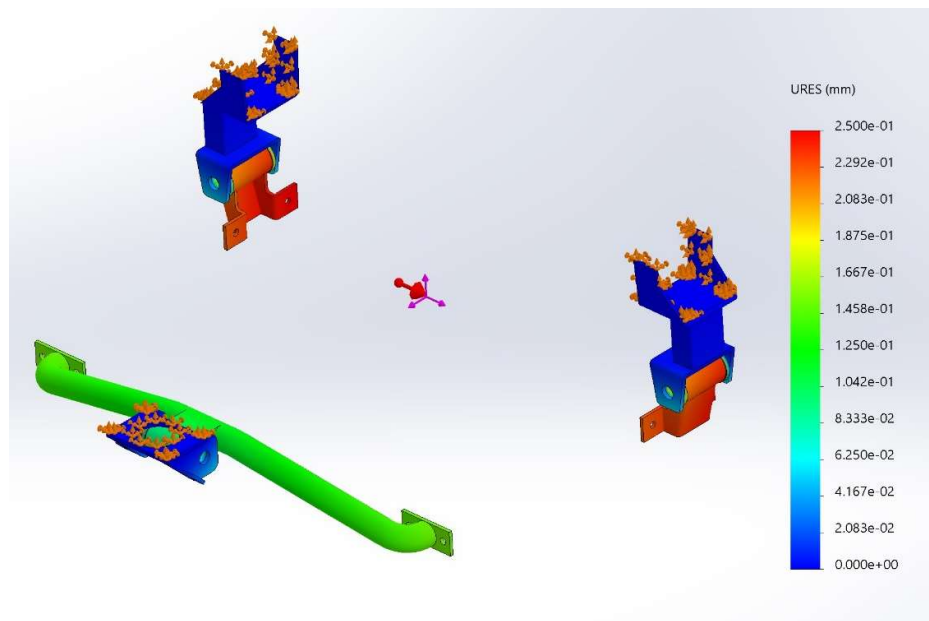


Figure 4.23: Residual displacement for lateral load case

4.5.4. Module static analysis case 3: Vertical motion (up-down)

- Stress plot

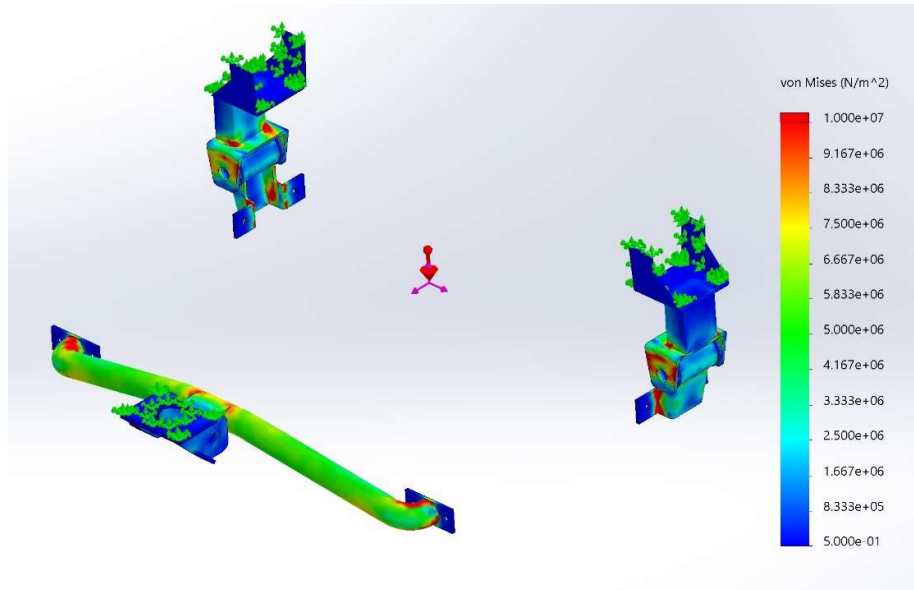


Figure 4.24: Stress plot for vertical load case (up-down)

- Residual displacement plot

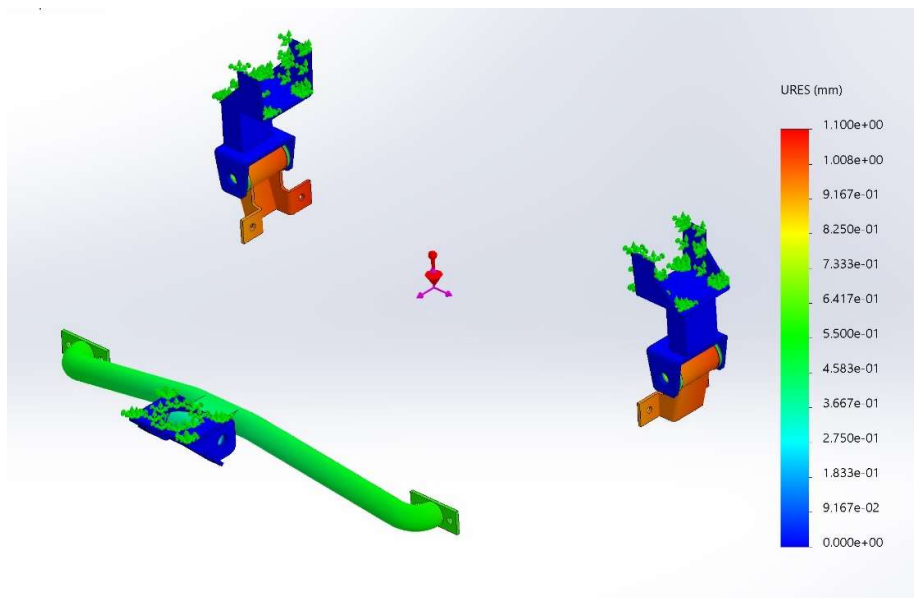


Figure 4.25: Residual displacement for vertical load case (up-down)

4.5.5. Module static analysis case 4: Vertical motion (down-up)

- Stress plot

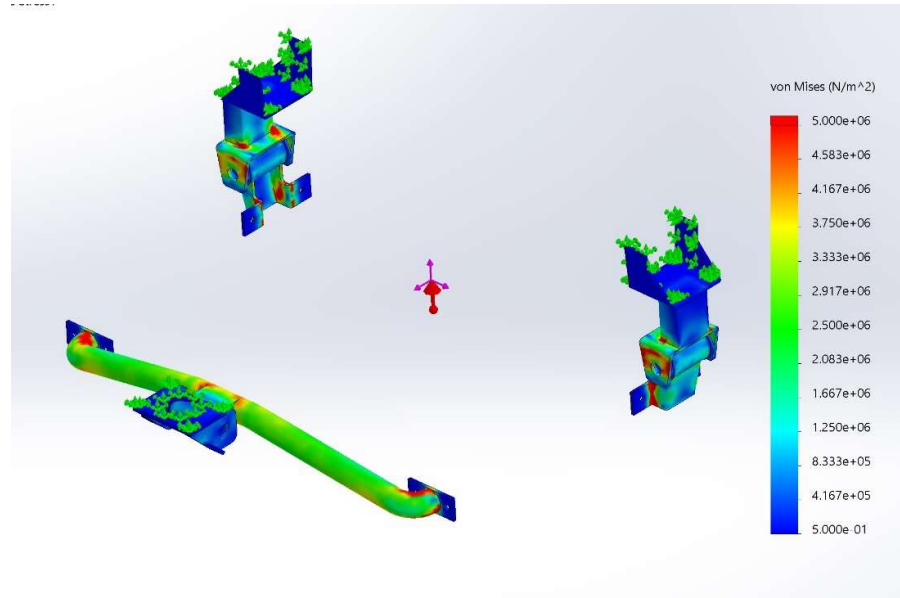


Figure 4.26: Stress plot for vertical load case (down-up)

- Residual displacement plot

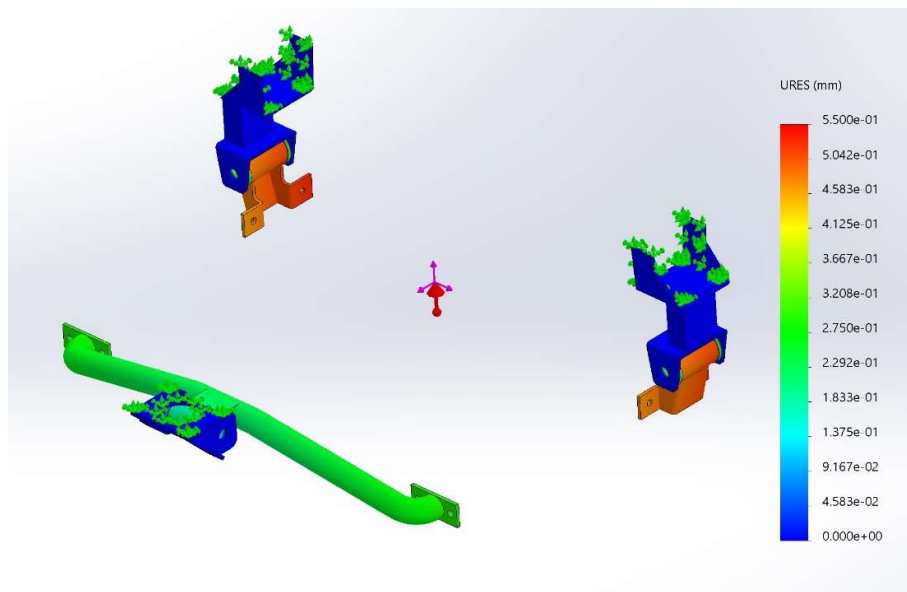


Figure 4.27: Residual displacement for vertical load case (down-up)

4.5.6. Results discussion

Regarding the stress analysis on mounting assembly in longitudinal direction, the maximum stress values is recorded only in the corner edges of the side mounts assembly, while in the rear mounting assembly, the stress values are at least one order of magnitude smaller. In lateral study, the maximum stress values can be seen both on the edges of the side mount assembly and near the bolt hole for the rear chassis mount. In the vertical study cases however, although there are still some critical zones in the side mounts, but the rear assembly has an overall higher recorded stress value, where it reaches its maximum value near the connection edges between the rear bar and the bushing mount, as well as in the bends.

Overall, the maximum recorded value for the von-mises stress in these static analysis is at least one order below the yields value for the steel material.

Regarding the residual displacements, the maximum values are always recorded in the mounting plate that connects the side mounts to the battery pack. While in the chassis mounts, the residual displacements stay below 10^{-5} m, which is negligible.

In the case of lateral and longitudinal cases, the bottom portion of the side mount assembly reaches displacement values in the order 0.1 mm, while in the vertical up to bottom motion study, the maximum values are one order of magnitude higher. Since the gradient is almost constant along the bottom mountings, the displacement is due the compliance of the bushing in the side mounts.

4.6. Dynamic simulation cases for mounts

In this chapter the dynamic behavior of the mounting structure for the battery pack is studied, using the simulation tool in SolidWorks software. As it was the case with the static analysis, only the main load bearing elements and neglect the presence of lower and top cover assembly are considered for the simulation. In summary, the mounts are designed to:

- Carry the static loads according to the standard legislations
- Deal with the dynamic loads due to road bumps
- The dynamic loads due to frontal and side impact

The focus of these dynamic simulation studies are the last two loading cases above, which are based on day-to-day operation scenarios, as well as the extreme crash tests.

The objective for this simulation study is to verify whether the mounts can withstand the forces acting on the battery pack

In order to maintain our focus on the mounting elements, we will consider a simplified version of the assembly (Figure 4.28). This representative pack model matches the original in terms of overall dimension, design, mass value and the center of gravity.

Furthermore, there is a response plot sensor at the battery pack center of gravity in order to record the accelerations in 3 coordinate directions. This is an extra step for examining the behavior of the pack in extreme impact cases that was demanded for further development stages of the vehicle.

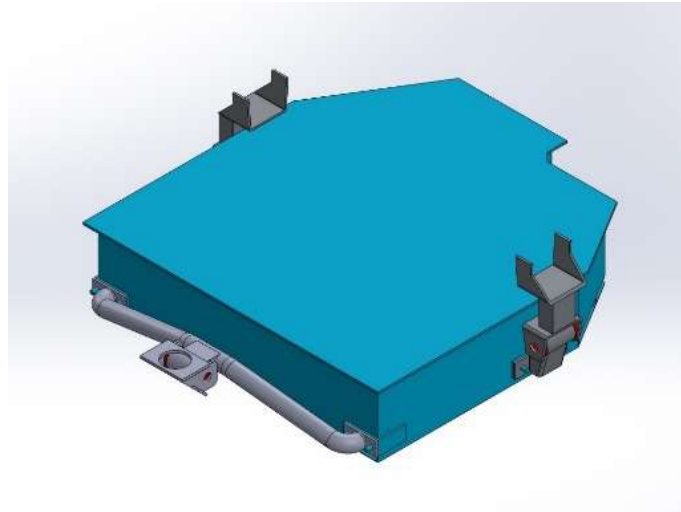


Figure 4.28: Mounts simulation assembly

4.6.1. Simulation setup

As it was the case in the static section, the weights of the designed parts was estimated using the SolidWorks mass properties (Table 4.1). After setting up the materials, the battery pack itself was assigned as remote mass, so that only the mass and center of gravity of the pack is taken into account. The fixtures were assigned as in the case of the static analysis (Figure 4.16) and the model was ready to mesh. The mesh was chosen based on the default settings (Table 4.6).

In the next sections, each of the dynamic simulation cases are discussed and the results are presented in terms of stress plots, residual displacement plots and acceleration response plots.

Table 4.6: Mesh properties for dynamic analysis

Mesh type	Solid Mesh
Mesher Used:	Blended curvature-based mesh
Jacobian points	4
Element Size	1~5 mm
Mesh Quality	High
Total Nodes	169314
Total Elements	94027
Maximum Aspect Ratio	17.02
% of elements with Aspect Ratio < 3	95%
% of elements with Aspect Ratio > 10	0.0138%

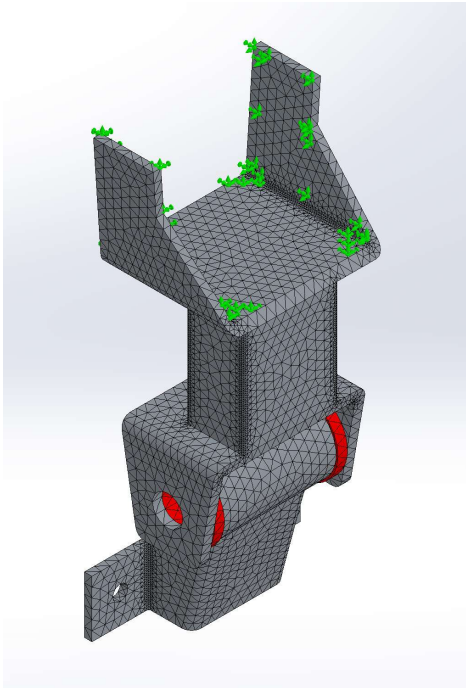


Figure 4.29: Mesh quality sample for dynamic analysis

4.6.2. Frequency analysis

Before we initiate the dynamic test, the frequency analysis was necessary. For the purpose of the dynamic tests, the first 10 modes were studied since the mass participation was sufficiently high. The frequencies for the first 10 modes, as well as the mass participation for each mode in X, Y and Z direction are listed in Table 4.7 and Table 4.8 respectively.

Table 4.7: List of frequencies for the natural modes

Mode No.	Frequency(Rad/sec)	Frequency(Hertz)	Period(Seconds)
1	134.97	21.482	0.046551
2	184.98	29.44	0.033967
3	194.03	30.88	0.032383
4	240.03	38.202	0.026177
5	248.67	39.577	0.025267
6	473.08	75.293	0.013281
7	1971.9	313.83	0.003186
8	4308.3	685.68	0.001458
9	6774.6	1078.2	0.000927
10	7009.4	1115.6	0.000896

Table 4.8: Mass participation for the first 10 modes

Mode No.	Freq (Hertz)	X direction	Y direction	Z direction
1	21.482	9.02E-08	0.78841	2.88E-05
2	29.44	0.88507	0.000158	0.00011
3	30.88	0.000724	0.18886	0.004146
4	38.202	1.75E-05	2.23E-05	4.27E-05
5	39.577	8.69E-05	0.001127	0.97517
6	75.293	0.093532	3.29E-07	1.18E-05
7	313.83	3.22E-08	0.000316	0.000322
8	685.68	8.73E-10	2.47E-05	9.55E-06
9	1078.2	4.56E-05	8.61E-11	6.43E-12
10	1115.6	4.02E-06	3.09E-12	5.24E-12
		Sum X = 0.97948	Sum Y = 0.97892	Sum Z = 0.97984

4.6.3. Dynamic case 1: Frontal impact

In the event of a frontal impact, the mounts should be able to withstand the dynamic loads. Moreover, the peak loads might multiply when it's transmitted to the battery pack center of gravity. In order to verify these arguments, based on the industry standard Euro NCAP Frontal impact testing (Figure 4.30 and Figure 4.31), a dynamic velocity load change is defined in Figure 4.32. The initial impact velocity is set at 64 km/h which translates to 17.8 m/s and it gradually reduces to zero in 0.1s.

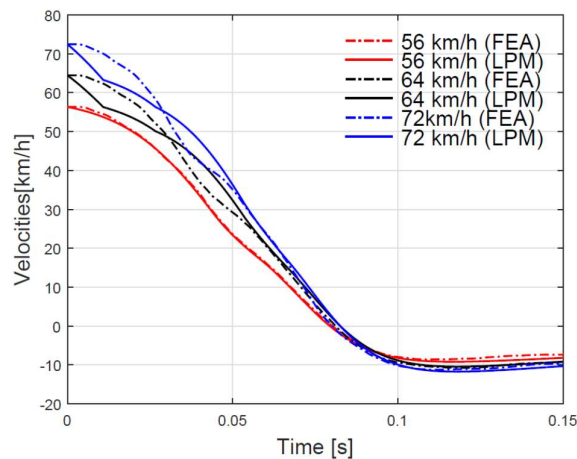


Figure 4.30: Velocity changes in the Euro NCAP frontal impact test [30]

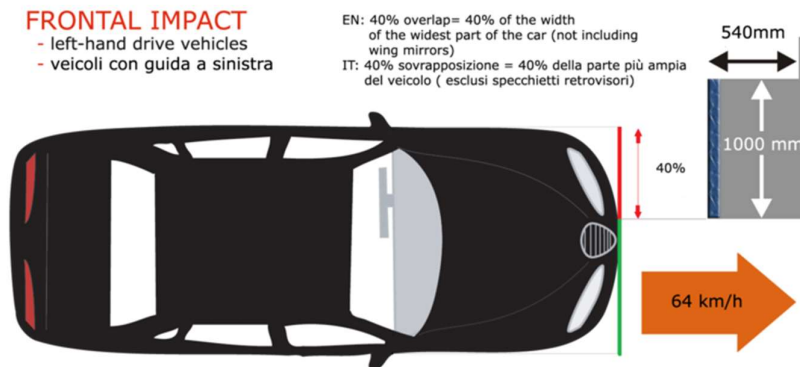


Figure 4.31: Euro NCAP frontal impact test protocol

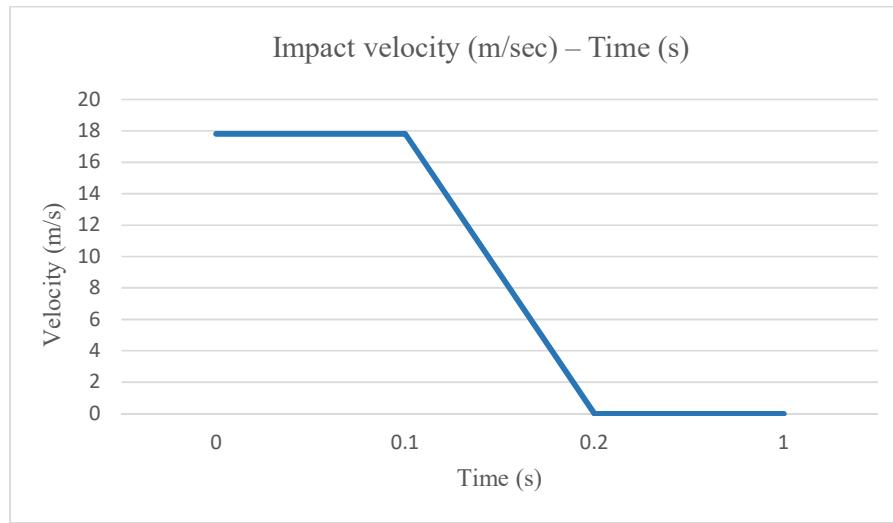


Figure 4.32: Velocity profile for the frontal impact case

The followings are the results of the study:

- Battery pack acceleration response plot

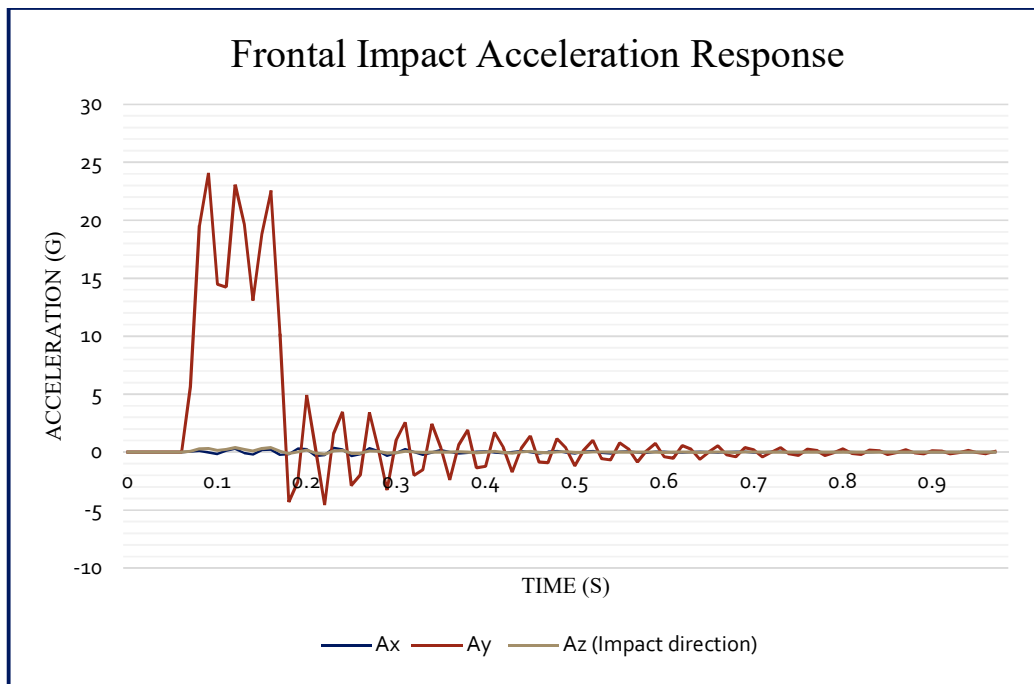


Figure 4.33: Frontal impact acceleration response plot

- The stress plot (at the maximum values)

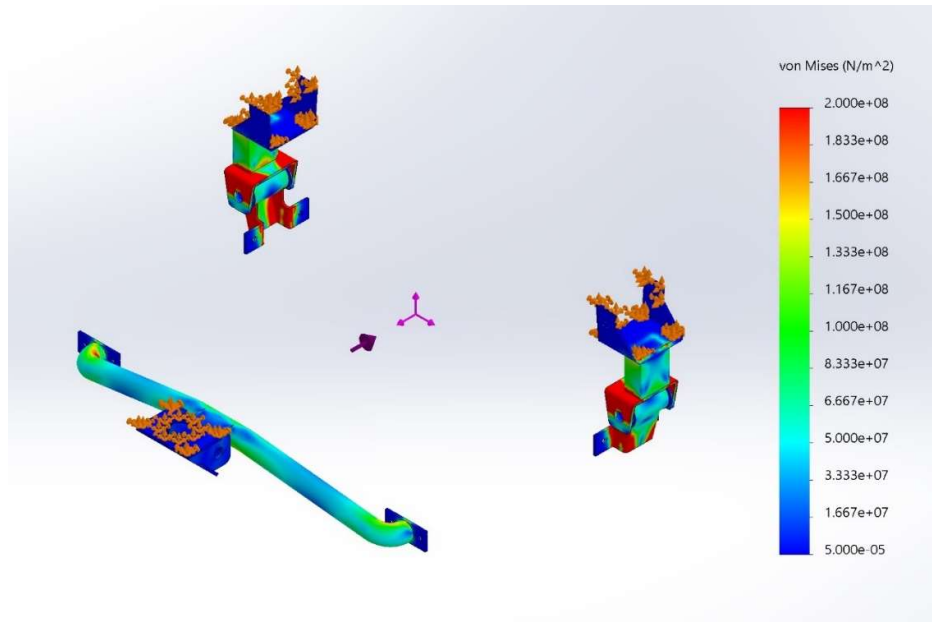


Figure 4.34: Frontal impact stress plot

- The residual displacement plot

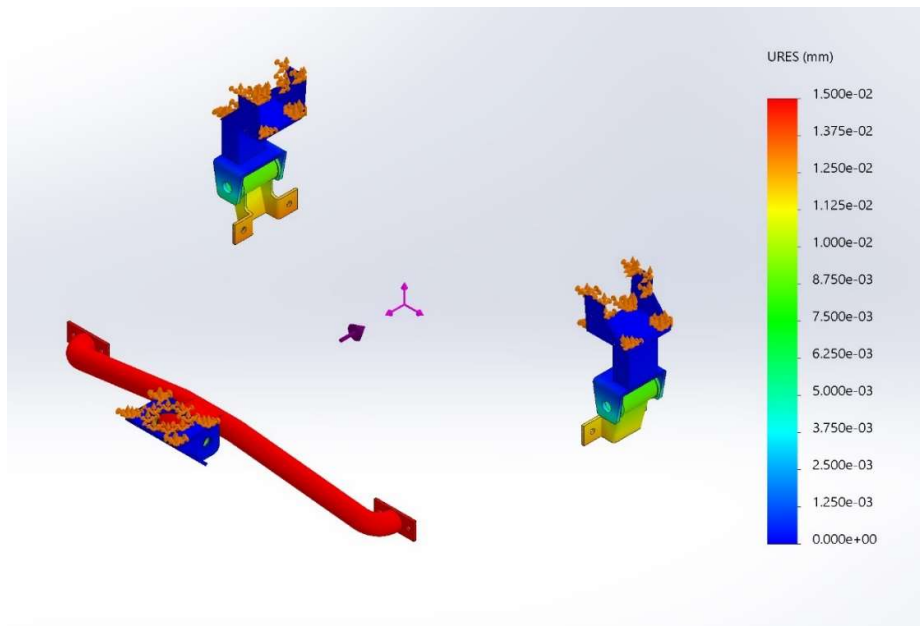


Figure 4.35: Frontal impact residual displacement plot

4.6.4. Dynamic case 2: Side impact

In the event of a side impact, the mounts should be able to withstand the dynamic loads. Moreover, the peak loads might multiply in the when it's transmitted to the battery pack center of gravity.

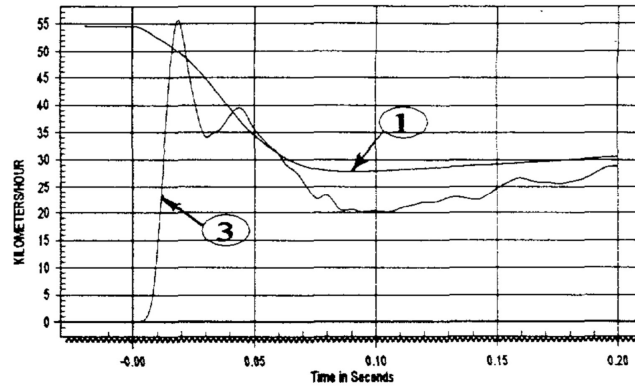


Figure 4.36: Velocity changes in the NCAP side impact test [31]

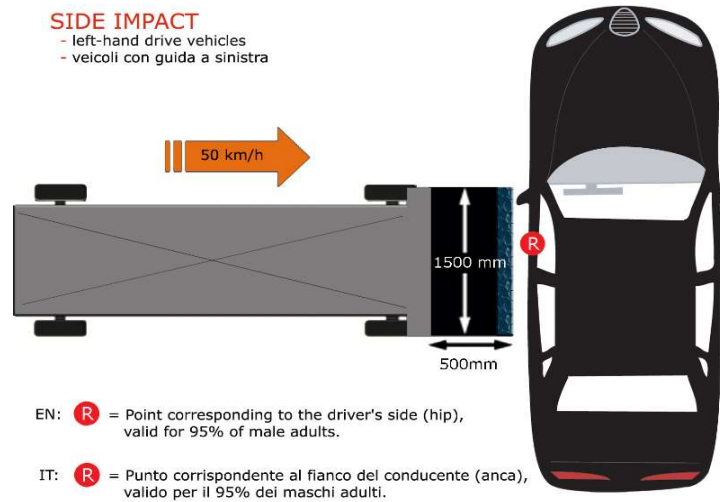


Figure 4.37: Euro NCAP side impact test protocol⁷

In order to verify these arguments, based on the industry standard Euro NCAP Side impact testing (Figure 4.36 and Figure 4.37), a dynamic velocity load change is defined

⁷ In recent testing protocols, the side impact initial speed is increased to 60 km/h

in Figure 4.38, where the initial vehicle speed is set at 60 km/h (16.7 m/s) and it gradually decreases to zero in 0.1s.

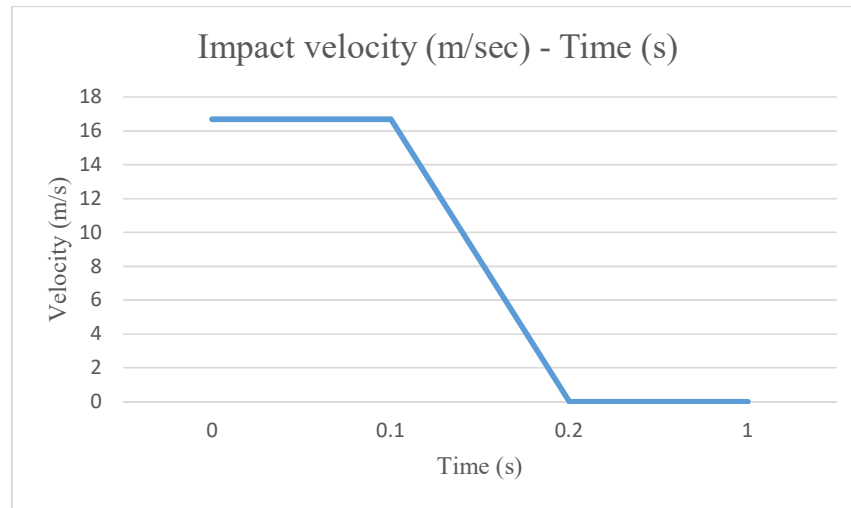


Figure 4.38: Velocity profile for side impact case

The followings are the results of the study:

- Battery pack acceleration response plot

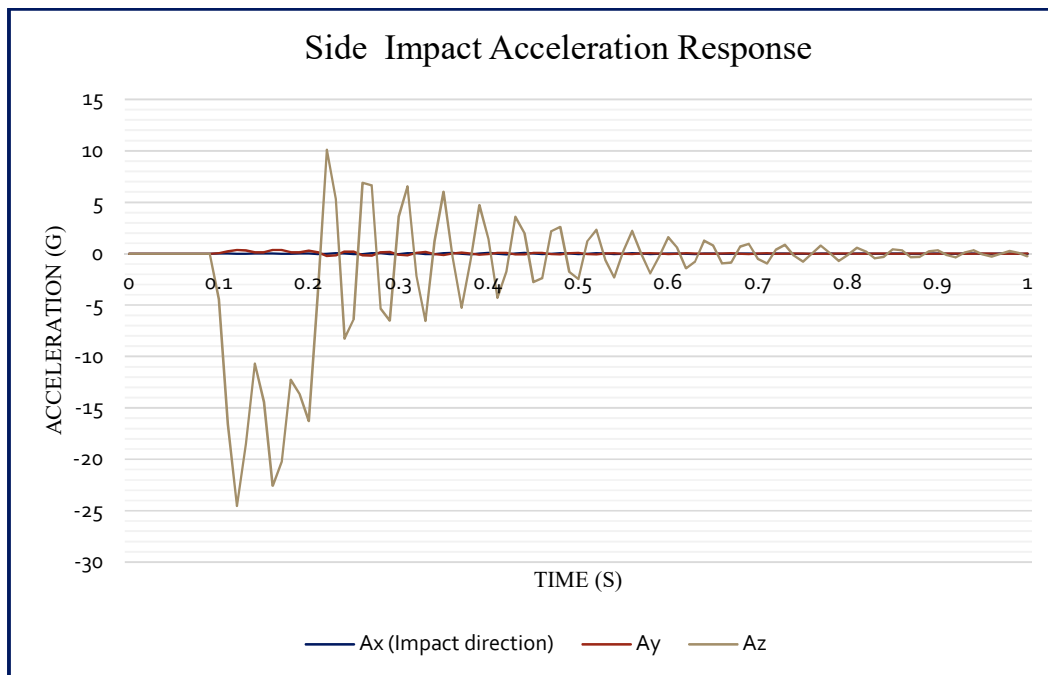


Figure 4.39: Side impact acceleration response plot

- The stress plot (at the maximum values)

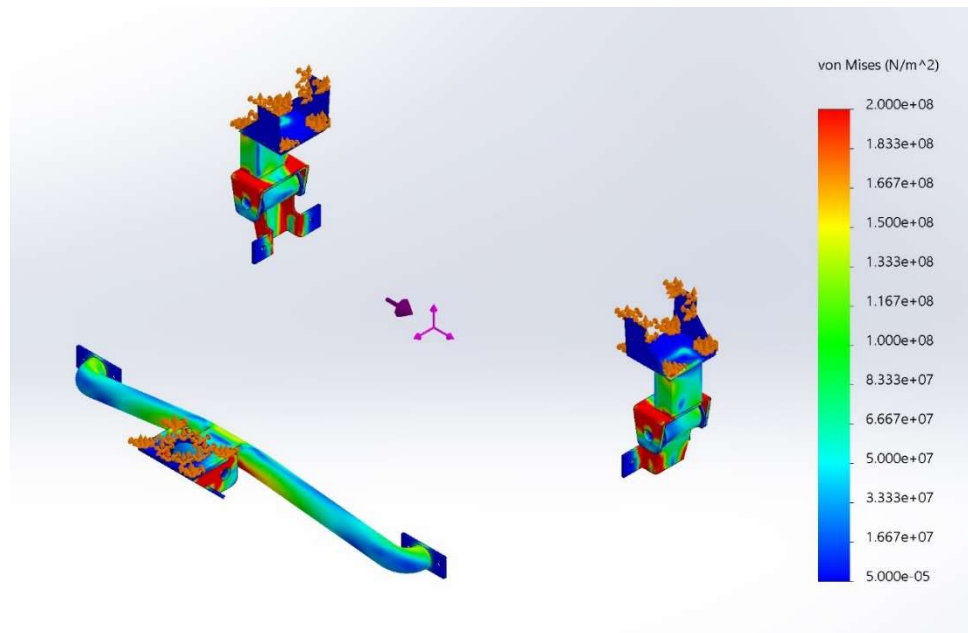


Figure 4.40: Side impact stress plot

- The residual displacement

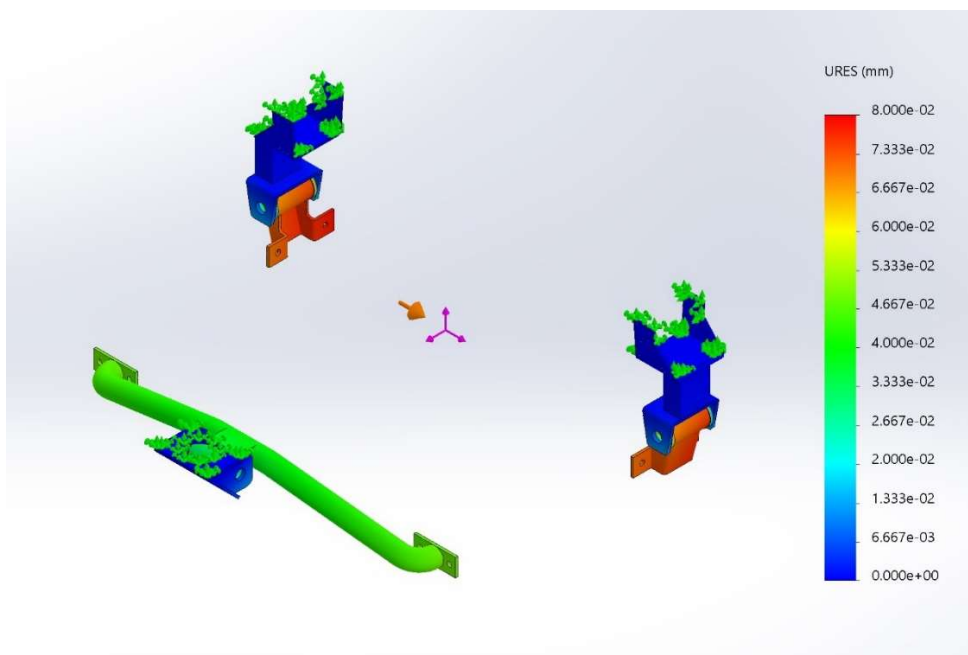


Figure 4.41: Side impact residual displacement plot

4.6.5. Dynamic case 3: Vertical road bump impact

In the event of a road bump impact, the mounts should be able to withstand the dynamic loads. Moreover, the peak loads might multiply in the when it's transmitted to the battery pack center of gravity. In this study, the mounts are examined in a case of extreme road bump impact, where the vehicle speed is at its highest (50 km/h).

In order to verify the examine the mounts in such scenario, based on the standard design for trapezoidal road bumps, the displacement input curve was defined.

For 50 km/h speed bump design:

- $L_1 = L_2 = 2 \text{ m}$
- $H = 0.1 \text{ m}$

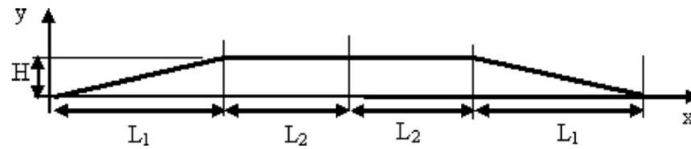


Figure 4.42: Standard trapezoidal speed bump profile [32]

The vehicle velocity is assumed constant at 50 km/h which equals 13.9 m/s. Thus the input displacement-time curve is based on speed bump geometry and vehicle speed. (

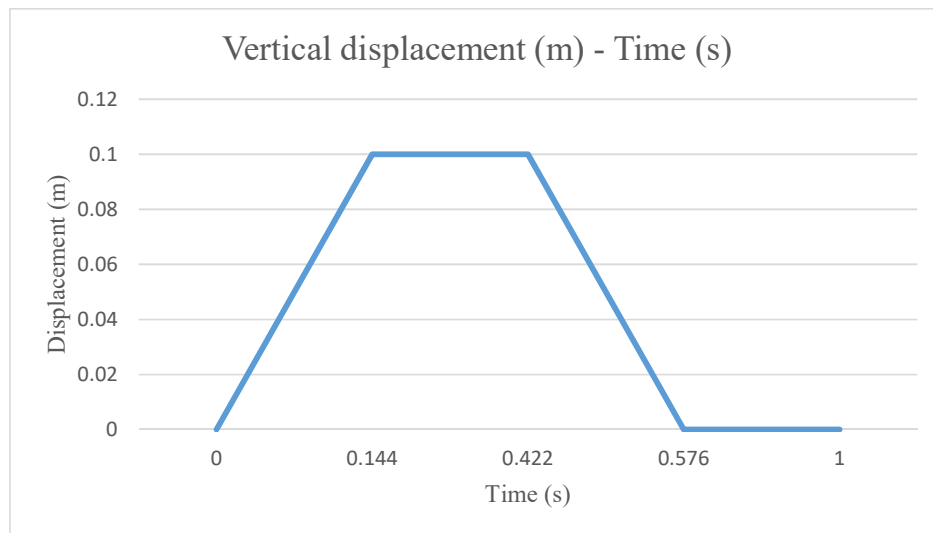


Figure 4.43: Displacement profile for vertical bump impact

The following are the results of the study:

- Battery pack acceleration response plot

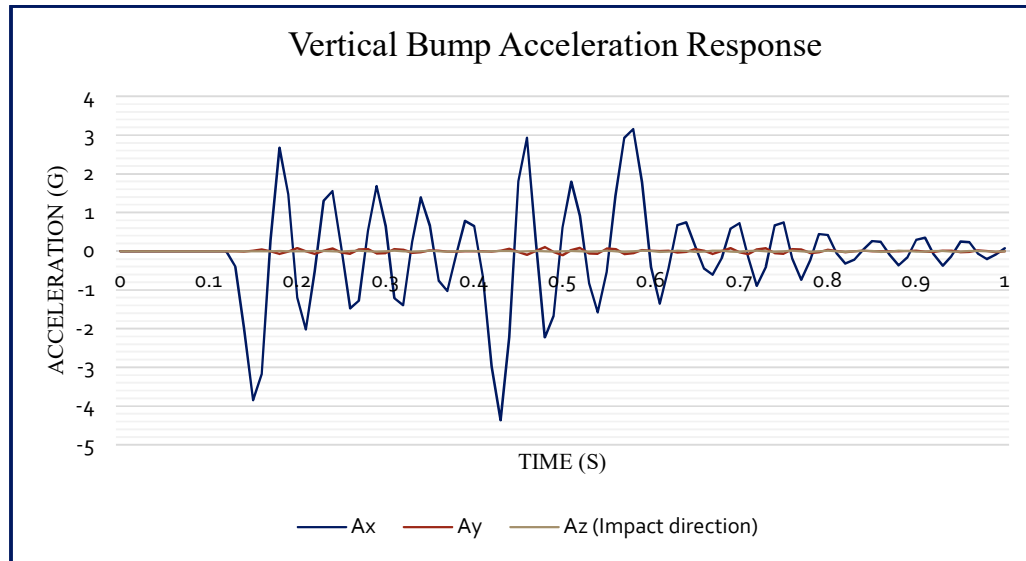


Figure 4.44: Vertical bump impact acceleration response plot

- The stress plot (at the maximum value)

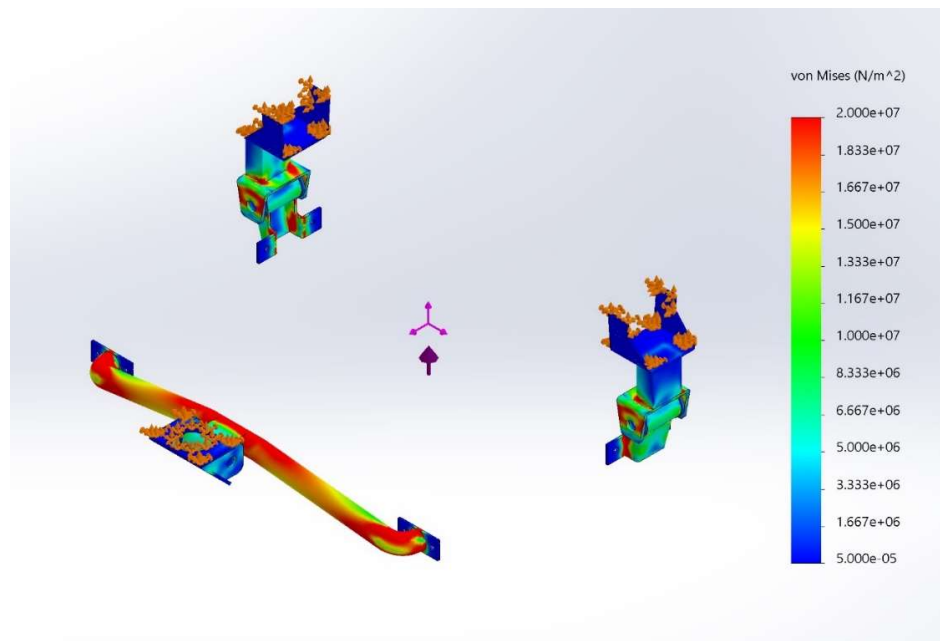


Figure 4.45: Vertical impact stress plot

- The residual displacement plot

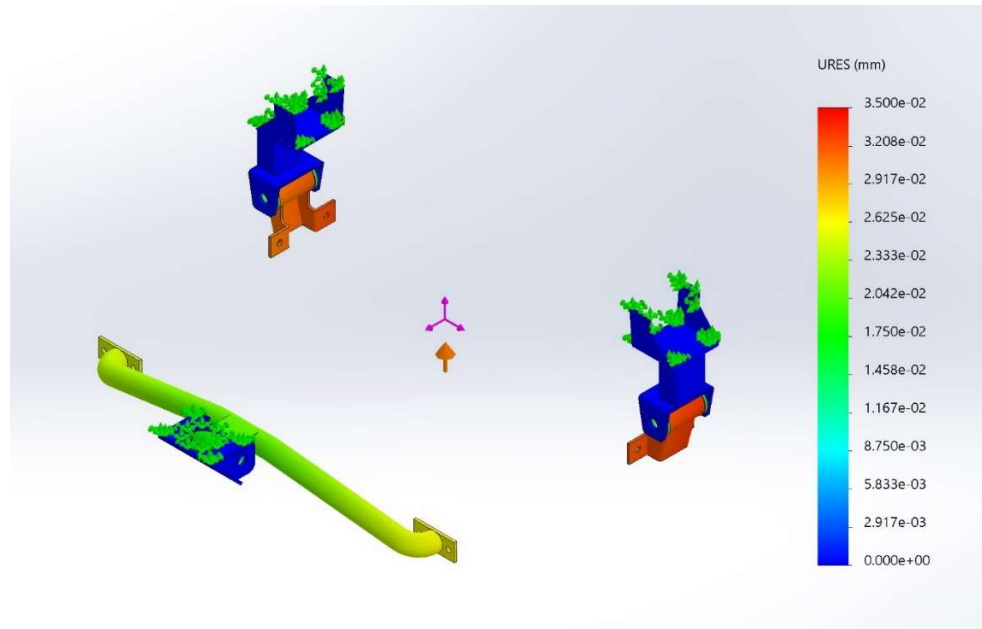


Figure 4.46: Vertical impact residual displacement plot

4.6.6. Results discussion

Regarding the frontal and side impact cases, in the stress analysis the side mount elements reach their yield stress threshold for the maximum stress level, which means the design might not be able to withstand the impact. It needs mentioning that such stress value only exerts on the model for a brief time frame.

However, such result demands that the surrounding suspension structure of the vehicle might need reinforcement, since there is a possibility that in the real impact scenario, the side mounts shear off or elongate, to the point that the battery pack surpasses the tolerances and hits the suspension elements.

In case of vertical bump impact however, the maximum values for the stress remains at least 10 times below the yield value for the mounting material and hence, despite the extreme simulation scenario, the battery pack mounts can withstand the vertical dynamic loads due to high speed road bumps.

4.7. Ground impact simulation

In the last section of design verification chapter, a comparison between the previous design and the proposed design was carried out. In this section, based on the studies carried out by Zhu et.al [33], a particular case of ground impact by road debris and rocks was devised. The study was particularly important because in order to guarantee the safety of the pack against cell damage and fire outbreak, the battery pack lower cover should be able to absorb the damage caused by an object hitting from the bottom of the pack.

4.7.1. Simulation setup

First a simplified version of the previous and present lower cover assembly plus the inner structural elements was modelled (Figure 4.47). Then an impact object in the shape of a sphere with 100mm diameter, representing the road debris was added. The impact object was then assembled and added to the battery pack models (Figure 4.48). The object is placed at a 10mm distance from the bottom side and is placed in a way to hit the center of the surface.

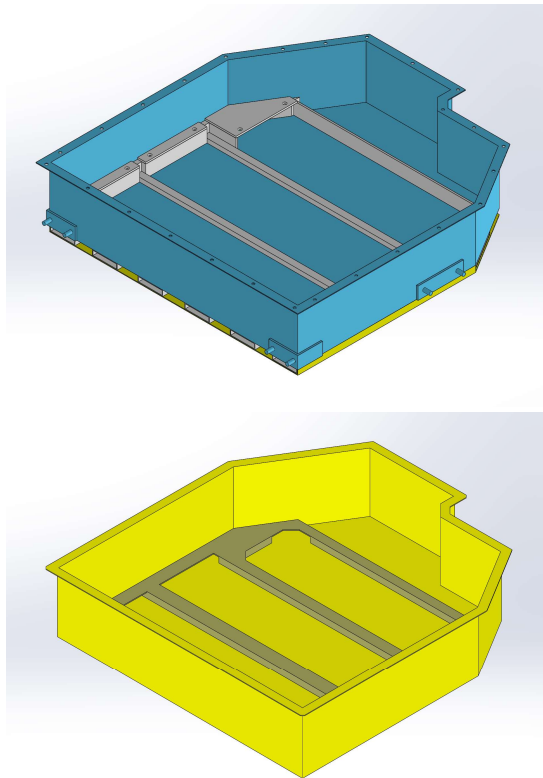


Figure 4.47: Ground impact mode for present (top) and previous (bottom) designs

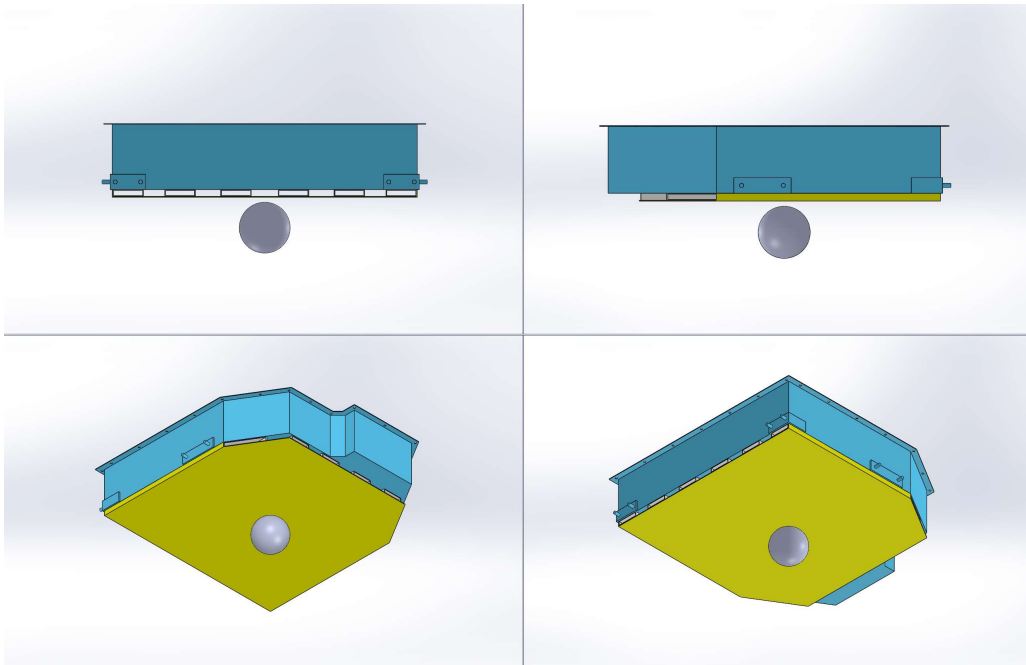


Figure 4.48: The ground impact full assembly

Then the assembled models were imported to Abaqus Explicit software for impact analysis. In the first step the steel materials were assigned to each part. There were 2 steel materials defined, one representing the battery pack model which should demonstrate the elastic and plastic behaviors, and another material for the impact object with only general and elastic properties, since the impact object does not deform during the impact. The values for the 2 set materials are listed in Table 4.9.

Table 4.9: Ground impact material properties

	Density	Elastic modulus	Poisson ratio	Plastic behavior
Impact object	7800 kg.m ⁻³	210 GPa	0.3	None
Simulation model	7800 kg.m ⁻³	210 GPa	0.3	Based on Figure 4.49

The plastic stress-strain data for the steel is demonstrated in Figure 4.49.

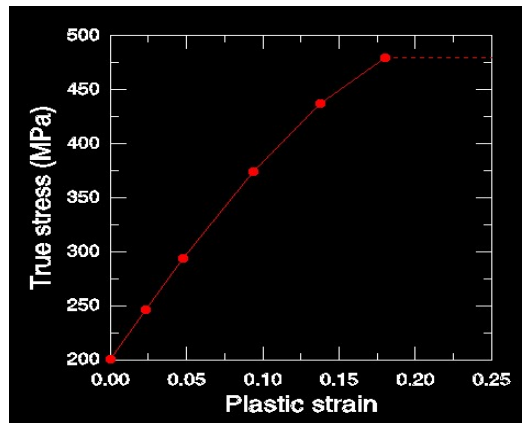


Figure 4.49: Plastic stress-stress curve for steel

In the next step the boundary conditions as well as the velocity field were defined (Figure 4.50 and Figure 4.51). The value for the initial velocity for the impact object was set at 10m/s or 36km/h, based on the normal driving speed of the vehicle.

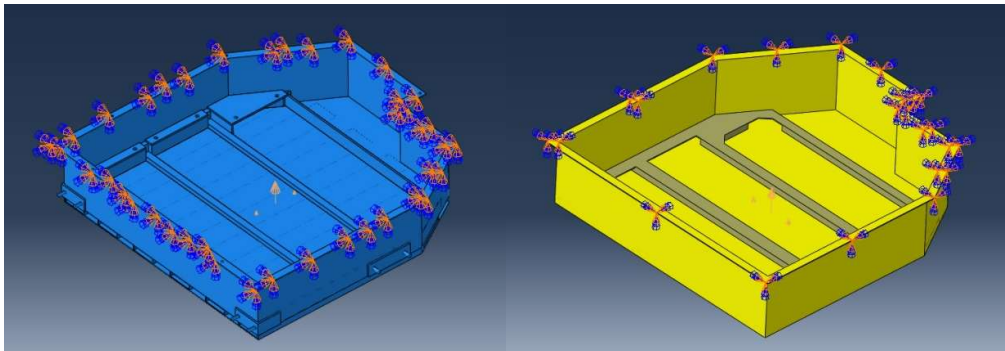


Figure 4.50: Boundary conditions on simulation models

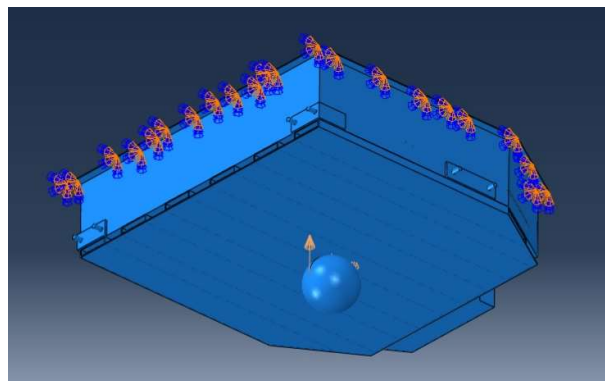


Figure 4.51: Velocity field assigned for the impact sphere

For model discretization, the tetrahedral mesh was chosen, since the frame and cover had a variety of sections and a number of bolt holes. The discretized assembly for the past design and the present one are shown in Figure 4.52 and Figure 4.53 respectively.

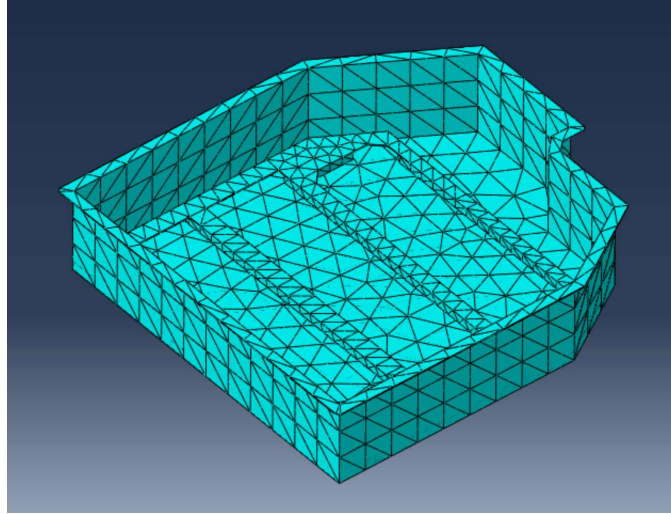


Figure 4.52: Mesh discretization on past model

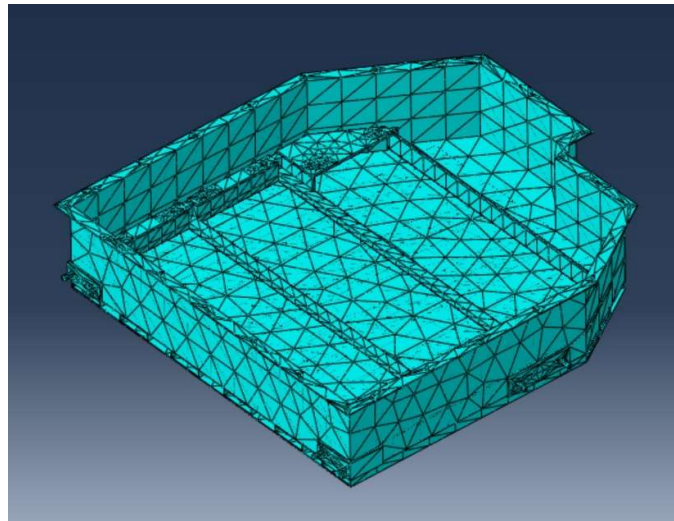


Figure 4.53: Mesh discretization on present model

In the last step before job submission, the analysis time step was created. Since the speed of the impact is relatively high and the initial response of the battery pack interests us more, the time step set for the analysis was 0.01 second, which was sufficient to demonstrate the behavior of the model against impact.

After setting up the simulation, the two simulation jobs were submitted. The results of the studies on the models are discussed in the next section.

4.7.2. Simulation results

- Stress and deformation plot for the past model

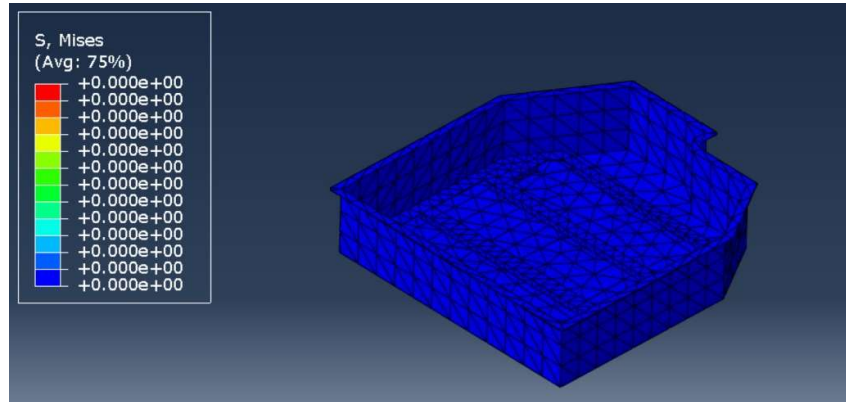


Figure 4.54: Past model at 0.0 s

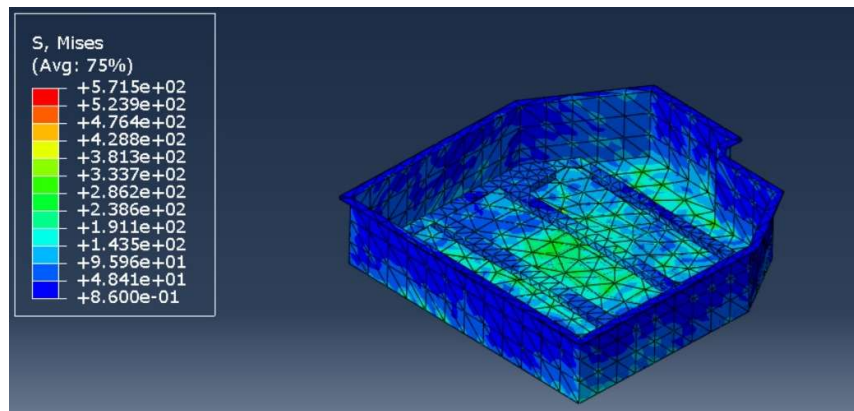


Figure 4.55: Past model at 0.002 s

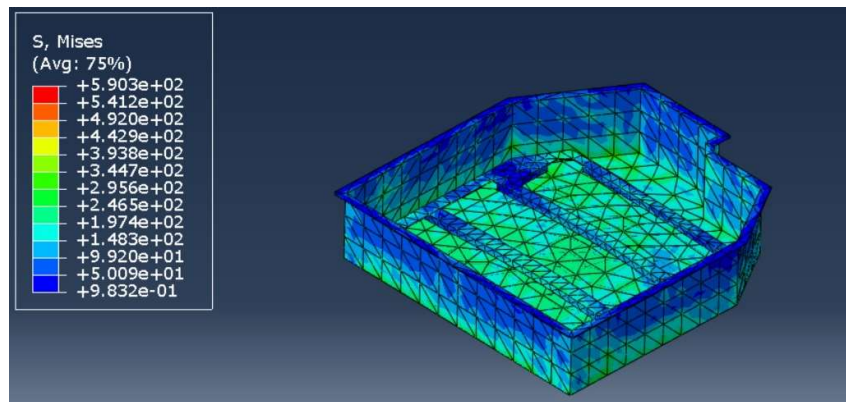


Figure 4.56: Past model at 0.004 s

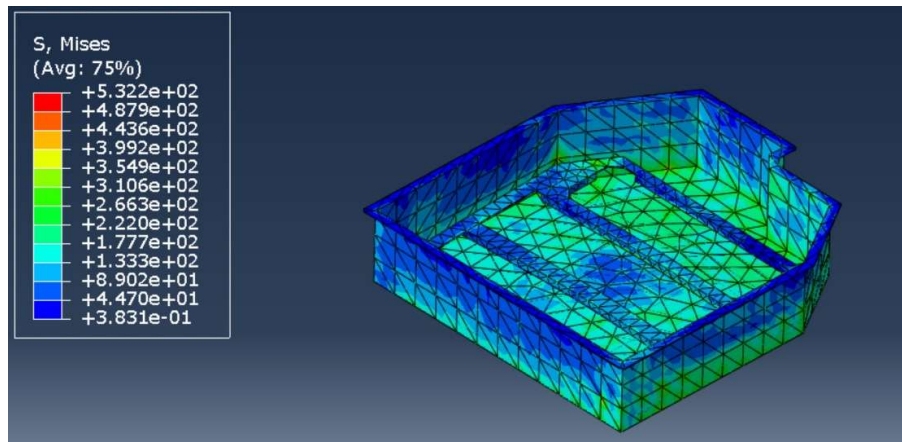


Figure 4.57: Past model at 0.006 s

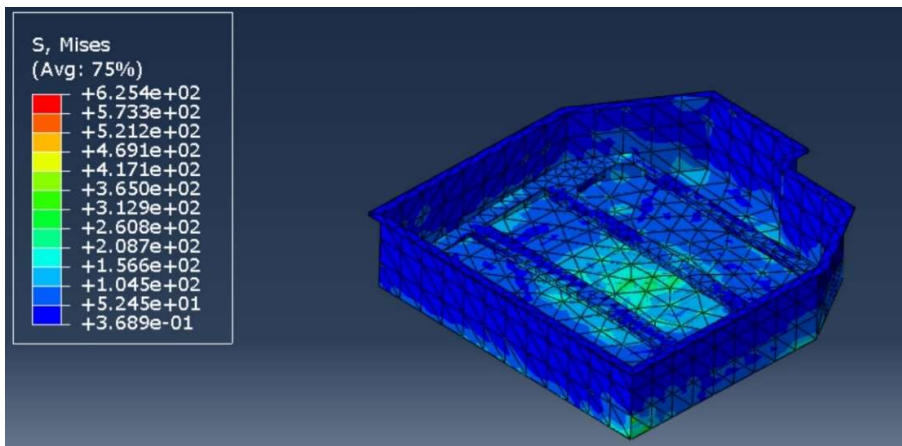


Figure 4.58: Past model at 0.008 s

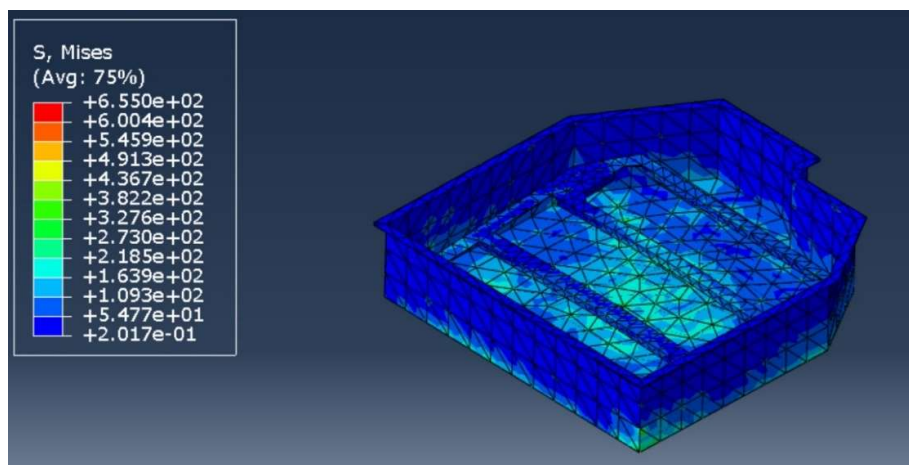


Figure 4.59: Past model at 0.01 s

- Stress and deformation plots for the present model

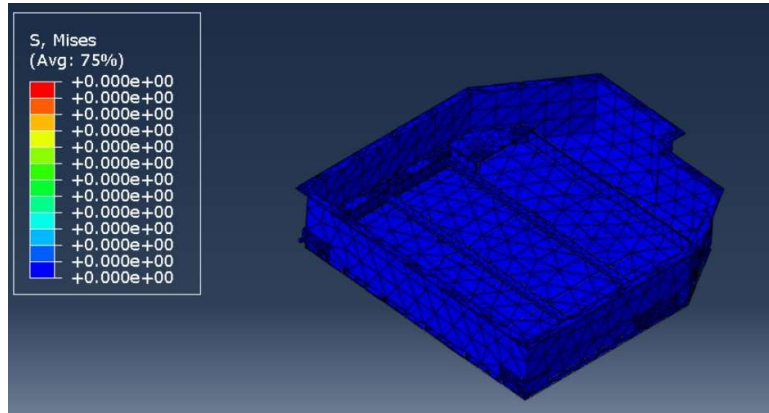


Figure 4.60: Present model at 0.0 s

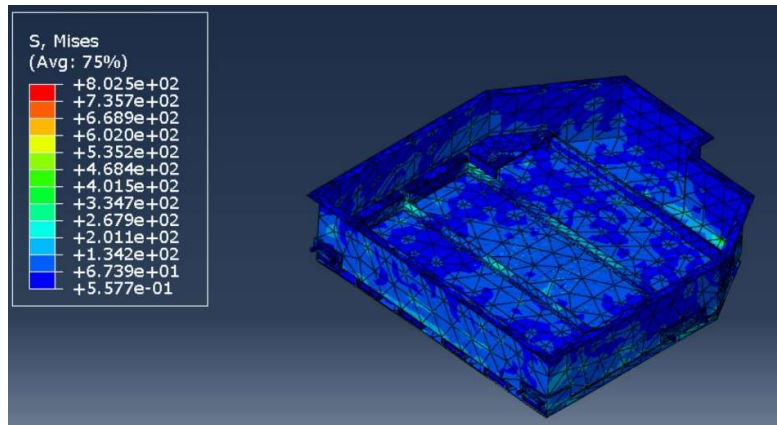


Figure 4.61: Present model at 0.002 s

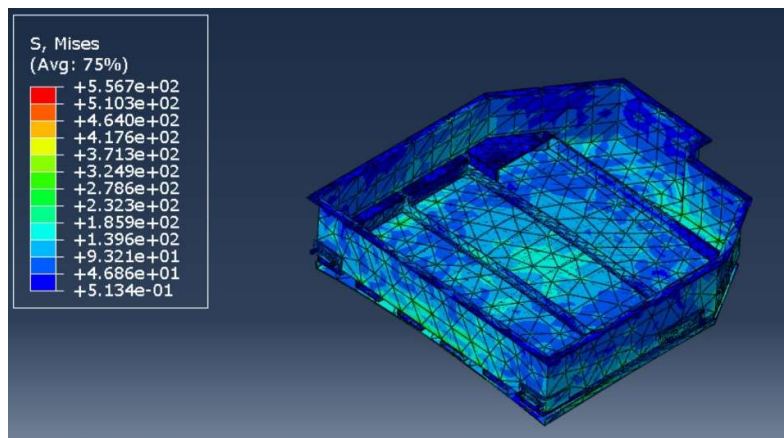


Figure 4.62: Present model at 0.004 s

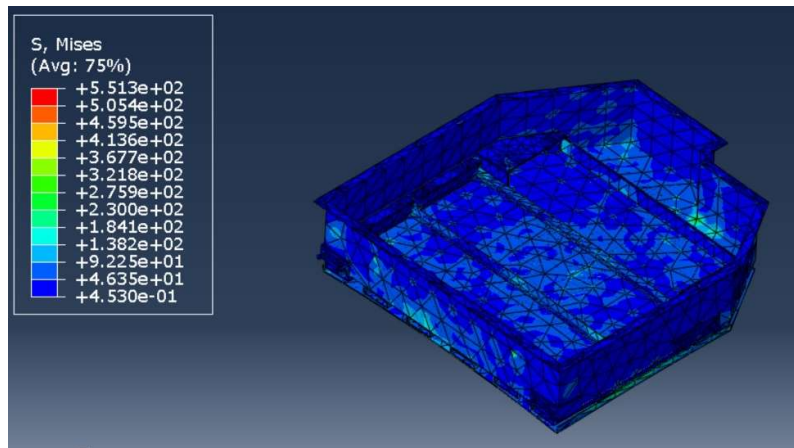


Figure 4.63: Present model at 0.006 s

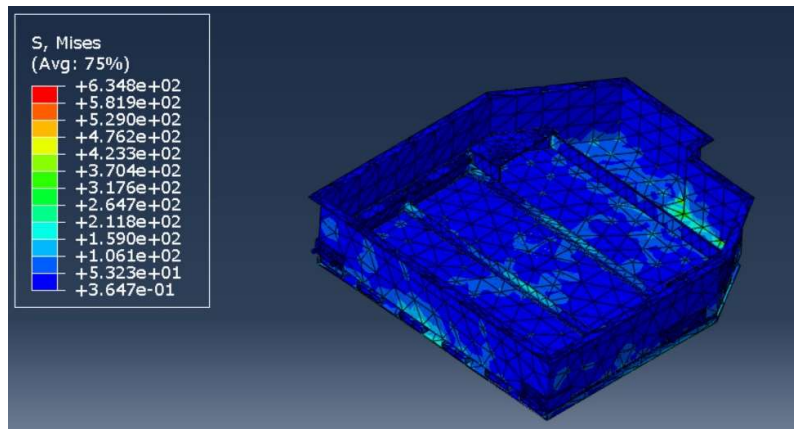


Figure 4.64: Present model at 0.008 s

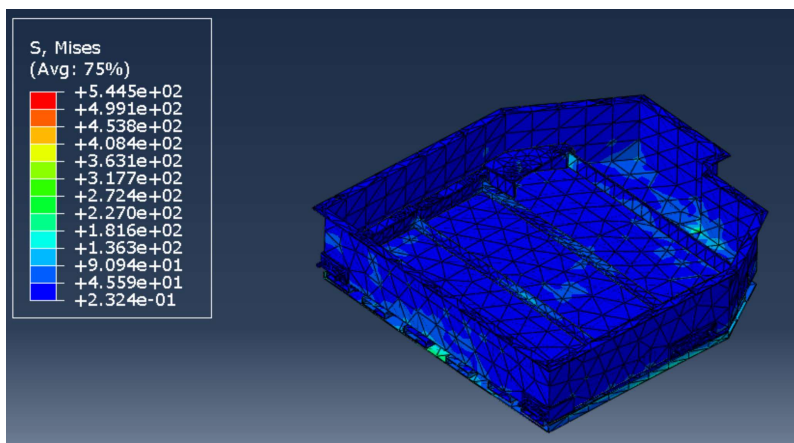


Figure 4.65: Present model at 0.01 s

4.7.3. Results discussion

Overall, it is apparent that the inner pack elements for the previous model experience higher deformation, while the deformation inside the proposed design is limited. At $t=0.002$ s when the impact element has already hit the bottom side, we can see the stress values at the new battery pack floor elements are at least 3 times lower than the ones in the previous designs model.

At 0.004 s, the stress values are only 30% higher than the new design, while at $t=0.006$ s, the maximum stress values for the older design has expanded from the center to the edges of the pack, in the new design the stress values at the floor remain well below half of the values in the older design.

At $t=0.008$ s, due the rebound motion of the impact ball, the stress and deformation values increase in the new design case, however the maximum stress value is still less than half of the maximum stress in the previous model.

At $t=0.01$ as the study time step reaches its end, the ducts and the protective shield in the proposed design model shows the signs of deflection, however the frame shows minor deformation. On the other hand, in the older design the inside frame, which actually acts as the foundation for he modules, is heavily distorted, proving that in the real impact case, the forces due to this distortion would be transmitted to the modules and hence the cells, which in turn cause rupture or even fire accident.

All in all, this comparison study confirms the protective feature of the new design and shows an improvement with respect to the previous design in the case of impacts from stones or other road elements.

5. Conclusion

In this thesis the design of the battery pack from cell level to the pack was developed and verified, with respect to the requirements, the dimension, cooling and structural integrity. First, the development background for battery pack design and architecture was discussed and application of each pack configuration in the industry was presented. Then, based on the previous efforts for designing a battery pack system for electric vehicle conversion, a new configuration for battery pack elements as well the mounting assembly was proposed. The design followed the most common approach in the industry regarding the configuration and assembly of the pack, while maintaining the simplicity and ease of assembly. Using a modular approach by defining each elements and building up the assembly from the cells up to the complete pack, the available space was used efficiently while the weight increase was avoided. This approach also allows for an easy maintenance (if needed) while guaranteeing the sufficient integrity in the 3 loading cases. The mounts were also designed in a way to allow a “bolt-on” mounting procedure, while satisfying the structural requirements as it was discussed in in simulation analysis.

In the table below, different aspects of the two designs are summarized and compared:

Table 5.1: Summary of design features and specification

	Previous design	Proposed design
Battery pack capacity	56 cells (10.2 kWh)	56 cells (10.2 kWh)
Cooling	--	Conductive air cooled
Structure type	Separated frame	Integrated frame
Protection	--	Bottom side protection
Ease of assembly	Complex	Simple
Weight	70 kg (Pack) + 30 kg (Mounting + Auxiliary)	93 kg (Pack) + 5 kg (Mounting)

In order to verify the design and based on variety of requirements and retrofitting regulations, the design was analyzed and in some cases compared to the previous works as well.

The verification criteria included:

- Maintaining the overall weight
- Respecting the vehicle geometry and dynamics
- Comply with the regulation enforced in the major markets
- Ability to withstand dynamic loads in extreme impact cases
- Protection against the environment during vehicle operation

First of all, the overall mass and the battery pack dimensions with respect to vehicle dynamics and geometry were assessed. It was verified that the battery pack and the mounting design not only respects the vehicle design and other sub-systems such as rear suspension, but also despite the addition of all the cooling and protective elements, the overall weight remains almost unchanged.

Secondly, the battery pack and the mounting assembly were analyzed through a number of structural static and dynamic simulation cases. These studies were based on electric vehicle conversion legislation and also the industry standard tests in order to verify vehicle safety, as well as battery system's integrity in the most common loading scenarios as well as extreme impact cases. Through SolidWorks™ simulation tool and based on the industry standard test protocols, the static and dynamic loads were simulated. Primarily, the modules and mounts were studied through the static cases in longitudinal, lateral and vertical directions, representing the 4 load cases stated in the legal documentation for EV conversion verification. Then for the dynamic analysis, the mounts were studied with velocity and displacement input loads, based on Euro NCAP latest rigid barrier frontal and side impact tests, as well as vertical impact in case of a high speed road bumps encounter. By plotting the stress and residual displacement for all the simulation cases as well as the response diagram for the battery pack center of gravity in dynamic cases, the results were discussed and the weak points in each loading case were obtained.

In the last step of the design verification, the bottom protection feature of the design was assessed with respect to the previous works. In this simulation study, using Abaqus™ Explicit FEM software, an example of ground impact on the bottom side of the vehicle was modelled, using an impact sphere and the two representative battery pack lower covers from the previous and the present design. The results of this study is discussed at the end and the battery pack protection claim was confirmed.

All in all, by assessing the results from the simulation cases, it is apparent that the proposed design has excelled in fulfilling the requirements set previously. It's safe to say that since the design followed a modular and a simplified approach towards battery pack configuration and assembly, this pack architecture can be applied on other retrofitting applications, given that battery sizing can be increased or decreased depending on the required battery capacity and number of modules.

References

1. *Hitting the EV inflection point*. 2021 May 10, 2021; Available from: <https://www.transportenvironment.org/publications/hitting-ev-inflection-point>.
2. Ukaew, A., *Model Based System Design for Electric Vehicle Conversion*. 2019, IntechOpen.
3. Burch, I. and J. Gilchrist, *Survey of global activity to phase out internal combustion engine vehicles*. Center of Climate Protection: Santa Rosa, CA, USA, 2018.
4. *Global EV Outlook 2020: Entering the Decade of Electric Drive?* 2020; Available from: <https://www.iea.org/reports/global-ev-outlook-2020>.
5. Muoio, D. *These countries are banning gas-powered vehicles by 2040*. 2017 Oct 23, 2017]; Available from: <https://www.businessinsider.com/countries-banning-gas-cars-2017-10>.
6. Cui, H. and S. Wappelhorst, *Growing momentum: Global overview of government targets for phasing out sales of new internal combustion engine vehicles*. The International Council on Clean Transportation, 2020. 11.
7. Buss, J. *Automakers Need A Global Timetable For Phasing Out Internal-Combustion Engines*. 2018 Mar 27, 2018]; Available from: <https://www.forbes.com/sites/oliverwyman/2018/03/27/automakers-need-a-global-timetable-for-phasing-out-internal-combustion-engines/>.
8. Eisenstein, P.A. *GM to go all-electric by 2035, phase out gas and diesel engines*. 2021 Jan. 29, 2021]; Available from: <https://www.nbcnews.com/business/autos/gm-go-all-electric-2035-phase-out-gas-diesel-engines-n1256055>.
9. Ewing, J. *Volvo Plans to Sell Only Electric Cars by 2030*. 2021 March 2, 2021]; Available from: <https://www.nytimes.com/2021/03/02/business/volvo-electric-cars.html>.
10. *Volkswagen says last generation of combustion engines to be launched in 2026*. 2018 DECEMBER 4, 2018]; Available from: <https://www.reuters.com/article/us-volkswagen-emissions-combustion-idUSKBN1O32O6>.
11. Rajashekara, K., *Present Status and Future Trends in Electric Vehicle Propulsion Technologies*. IEEE Journal of Emerging and Selected Topics in Power Electronics, 2013. 1(1): p. 3-10.
12. Pesaran, A.A., G.-H. Kim, and M. Keyser, *Integration issues of cells into battery packs for plug-in and hybrid electric vehicles*. 2009, National Renewable Energy Lab.(NREL), Golden, CO (United States).
13. Zwicker, M.F.R., et al., *Automotive battery pack manufacturing—a review of battery to tab joining*. Journal of Advanced Joining Processes, 2020. 1: p. 100017.
14. Löbbberding, H., et al., *From Cell to Battery System in BEVs: Analysis of System Packing Efficiency and Cell Types*. World Electric Vehicle Journal, 2020. 11(4): p. 77.
15. Kavanagh, L., et al., *Global lithium sources—industrial use and future in the electric vehicle industry: a review*. Resources, 2018. 7(3): p. 57.
16. Ding, Y., et al., *Automotive Li-Ion Batteries: Current Status and Future Perspectives*. Electrochemical Energy Reviews, 2019. 2(1): p. 1-28.
17. Antoine Chatelain, M.E., Pierre-Yves Moulière, and Philip Schäfer. *What a teardown of the latest electric vehicles reveals about the future of mass-market EVs*. 2018 March 21, 2018]; Available from: <https://www.mckinsey.com/industries/automotive-and-assembly/our->

[insights/what-a-teardown-of-the-latest-electric-vehicles-reveals-about-the-future-of-mass-market-evs.](#)

18. Su, J. *Elon Musk: Converting Lotus' Elise To Build The Tesla Roadster Was A Super Dumb Strategy*. 2018 Sep 18, 2018]; Available from: <https://www.forbes.com/sites/jeanbaptiste/2018/09/18/elon-musk-converting-lotus-elise-to-build-the-tesla-roadster-was-a-super-dumb-strategy/?sh=1dcb668f540f>.
19. Oliver, T. *The Invention of Tesla's Model S*. 2020 August 07, 2020]; Available from: <https://www.embeddedcomputing.com/application/automotive/electric-vehicles-powertrain/trial-error-the-road-to-the-invention-of-tesla-s-model-s>.
20. Griffiths, H. *Classic electric car conversions boom in popularity*. 2020 24 Jun 2020]; Available from: <https://www.autoexpress.co.uk/news/352597/ev-classic-car-conversions-see-boom-popularity>.
21. Kaleg, S., A. Hapid, and M.R. Kurnia, *Electric Vehicle Conversion Based on Distance, Speed and Cost Requirements*. Energy Procedia, 2015. **68**: p. 446-454.
22. *Electric vehicle conversion: optimisation of parameters in the design process*. Tehnicki vjesnik - Technical Gazette, 2017. **24**(4).
23. Pedrosa, D., et al. *A Case Study on the Conversion of an Internal Combustion Engine Vehicle into an Electric Vehicle*. IEEE.
24. *Modular electric drive matrix (MEB)*. 2021; Available from: <https://www.volkswagen-newsroom.com/en/modular-electric-drive-matrix-meb-3677>.
25. Thompson, D.L., et al., *The importance of design in lithium ion battery recycling – a critical review*. Green Chemistry, 2020. **22**(22): p. 7585-7603.
26. Snyder, J.F., et al., *Structural composite capacitors, supercapacitors, and batteries for US Army Applications*. Vol. 43314. 2008.
27. Asp, L.E. and E.S. Greenhalgh, *Structural power composites*. Composites Science and Technology, 2014. **101**: p. 41-61.
28. Udy, J. *Volvo S80 Prototype Uses Nano Battery Technology in Body Panels*. 2013 Oct 18, 2013]; Available from: <https://www.motortrend.com/news/volvo-s80-prototype-uses-nano-battery-technology-in-body-panels-417359/>.
29. SOLIDAIRE, M.D.L.T.É.E., *Arrêté du 13 mars 2020 relatif aux conditions de transformation des véhicules à motorisation thermique en motorisation électrique à batterie ou à pile à combustible*. JOURNAL OFFICIEL DE LA RÉPUBLIQUE FRANÇAISE, 2020.
30. B Munyazikwiye, B., et al., *Prediction of vehicle crashworthiness parameters using piecewise lumped parameters and finite element models*. Designs, 2018. **2**(4): p. 43.
31. Teng, T.L., et al. *Study of Crash Acceleration Curves on the Side-Impact Test*. Trans Tech Publ.
32. Başlamışli, S.C. and Y.S. Ünlüsoy, *Optimization of speed control hump profiles*. Journal of transportation engineering, 2009. **135**(5): p. 260-269.
33. Zhu, J., et al., *Structural Designs for Electric Vehicle Battery Pack against Ground Impact*. 2018, SAE Technical Paper.